Deutsches Zentrum für Neurodegenerative Erkrankungen und Technische Universität München

The global proteomic profiling of the BACE1 knockout mouse brain allows the identification of novel BACE1 candidate substrates in vivo

Bastian Dislich

Vollständiger Abdruck der von der Fakultät für Medizin der Technischen Universität München zur Erlangung des akademischen Grades eines

Doctor of Philosophy (Ph.D.)

genehmigten Dissertation.

Vorsitzende/r: Univ.-Prof. Dr. Arthur Konnerth

Betreuer: Univ.-Prof. Dr. Stefan Lichtenthaler

Prüfer der Dissertation:

1. Univ.-Prof. Dr. Günter Höglinger

2. Priv.-Doz. Dr. Klaus-Peter Janssen

Die Dissertation wurde am 01.07.2013 bei der Fakultät für Medizin der Technischen Universität München eingereicht und durch die Fakultät für Medizin am 23.08.2013 angenommen.

Contents

1 Introduction 5

1.1 Alzheimer's disease 5

1.1.1 Epidemiology 5

1.1.2 Pathology 5

1.1.3 Molecular pathology and the amyloid hypothesis 5

1.2 Regulated Intramembrane Proteolyis 6

1.2.1 RIP is a general cellular mechanism 6

1.2.2 RIP controls signaling pathways and the communication in between cells 8

1.2.3 RIP of APP 9

1.3 The β-secretase BACE1 9

1.3.1 BACE1 cell biology 9

1.3.2 Cellular localization, enzymatic activity and structure 11

1.3.3 Expression pattern 11

1.3.4 The physiological role of BACE1 11

1.3.5 Physiologically relevant substrates of BACE1: type III NRG1 and β-subunits of VGSCs 12

1.3.6 Therapeutic Inhibition of BACE1 12

1.4 Quantitative proteomics 13

1.4.1 Quantitative proteomics allows the accurate quantification of the proteome 13

1.4.2 Introduction to mass spectrometry and the orbitrap mass analyzer 13

1.4.3 Bottom up tandem mass spectrometry 15

1.4.4 LC-MS/MS workflow in bottom-up proteomics 16

1.4.5 Protein quantification in MS based proteomics 16

2 Aims of this work 18

3 Material and Methods 20

3.1 Cell culture 20

3.1.1 Cell lines 20

3.1.2 Cell culture conditions 21

3.1.3 SILAC labeling of HEK-293E cells 21

3.1.4 Transient liposomal transfection with plasmid DNA 21
3.1.5 Inhibitor treatment of primary cortical neurons 21
3.2 Animal related work 22
3.2.1 Mouse strains 22
3.2.2 Mouse brain extraction 22
3.2.3 Preparation of primary cortical neurons 22
3.2.4 Collection of CSF from the cisterna magna of adult mice 23
3.3 Biochemical methods 23
3.3.1 Concentration of conditioned media 23
3.3.2 Membrane preparation 24
3.3.3 DEA fractionation of brain tissue 25
3.3.4 Protein concentration measurements 26
3.3.5 Sodium dodecyl sulfate polyacrylamide gel electrophoresis (SDS-PAGE) 26
3.3.6 Coomassie and silver staining of polyacrylamide gels 28
3.3.7 Western Blotting 29
3.3.8 Immunofluorescence 30
3.4 Sample preparation methods for mass spectrometry 31
3.4.1 Filter-aided sample preparation (FASP) 31
3.4.2 In-solution digest 32
3.4.3 Peptide concentration measurements 33
3.4.4 Assembly of homemade STAGE-Tips 33
3.4.5 STAGE-Tip based desalting and clean-up 33
3.4.6 STAGE-Tip based strong anion exchange (SAX) of peptides 33
3.4.7 Preparation of peptides before injection into the LC autosampler 34
3.5 Mass spectrometry and high performance liquid chromatography 34
3.5.1 High performance liquid chromatography (HPLC) 34
3.5.2 Mass spectrometry measurements on the LTQ Velos Orbitrap Pro 36
3.5.3 Mass spectrometry measurements on the Q-Exactive 36
3.6 Analysis of mass spectrometry data 37
3.6.1 Search engine and quantitation 37

3.6.2 Statistical evaluation of the data 37
4 Results 37
4.1 Deep coverage of the membrane proteome by mass spectrometry 37
4.1.1 Efficient digestion of membrane proteins 37
4.1.2 Comparison of different membrane preparation protocols 39
4.1.3 Fractionation and technical replicates increase the proteomic coverage 41
4.2 Quantitative changes in the membrane proteome upon overexpression of BACE1 43
4.3 Identification and validation of BACE1-/- substrates in vivo using a spike-in SILAC mouse approach 48
4.3.1 A spike-in SILAC mouse based proteomic workflow to identify BACE1 substrates in vivo. 48
4.3.2 Analysis of the BACE1-/- brain membrane proteome identifies and validates BACE1 substrates 49
4.3.3 Validation of identified substrates in mouse brains by western blotting 56
4.3.4 Processing of EPHA4 by BACE1 from embryogenesis through adulthood 58
4.4 Analysis of the BACE1-/- brain soluble fraction reveals no major changes 61
4.5 Analysis of mouse CSF by quantitative proteomics 64
4.5.1 Identification of more than 1200 proteins in the CSF of adult mice 64
4.5.2 Analysis of the BACE1 -/- mouse CSF 66
4.5.3 Accurate quantification of the BACE1-/- CSF allows the validation and identification of novel BACE1 substrates 68
4.6 The QARIP webserver aids in the analysis of proteomic datasets targeted to RIP 72
5 Discussion 76
5.1 BACE1 and its therapeutic potential 76
5.2 Different approaches increase the number of BACE1 substrates 76
5.3 The physiological role of BACE1: lessons from the BACE1-/- mouse model and the BACE1 substratome 78
5.3.1 Defects in axonal guidance and outgrowth 78
5.3.2 Synaptic Plasticity 79
5.3.3 Reduced myelination 80
5.4 The quantitative analysis of murine CSF leads to the discovery of biomarkers 80

5.5 Outlook 82
6 Summary 84
7 Abbreviations 86
8 Index 88
9 Publication list 99

1 Introduction

1.1 Alzheimer's disease

1.1.1 Epidemiology

Alzheimer's disease (AD) is the most common neurodegenerative disease worldwide (Querfurth and LaFerla, 2010). Although the molecular mechanism of this disease is relatively well understood, no disease-modifying treatment is available (Lang, 2010). An international consensus study estimated in 2005 that there were 24 million people living with dementia in 2001, and predicts these numbers to roughly double every 20 years, leading to 42 million cases of dementia in 2020 and 81 million cases by 2040 (Ferri et al., 2005). Increasing age is the major risk factor for dementia and AD accounts for 60-80% of those cases. The observed cognitive decline occurs on average over a period of 9 years upon diagnosis and finally results in bedridden patients requiring intensive care (Citron, 2010). This posts a major challenge to the modern society, with estimated $200 billion spent alone in the US healthcare system on AD patients in 2012 (2012 Alzheimer's disease facts and figures, www.alz.org). The development of effective therapeutic approaches and tools to monitor their potential side effects is thus crucial.

1.1.2 Pathology

The brains of AD patients are atrophic, which is the result of neuronal death and the loss of functional and structural connectivity in between neurons. The atrophy, gliosis and the two histopathological hallmarks of AD, neurofibrillary tangles and amyloid plaques, were first described by Alois Alzheimer in 1907 (Alzheimer, 1907; Alzheimer et al., 1995). The extracellular amyloid plaques consist of the Aβ-peptide (Aβ), whereas abnormal filaments of the microtubule associated protein tau are the basis of the intracellular neurofibrillary tangles. Both proteinaceous lesions primarily localize to brain areas important for cognitive function and memory, such as the hippocampal area, the entorhinal cortex and the association cortices of the frontal, parietal and temporal lobe (Selkoe, 2011). More recently, it has become evident that the brain of AD patients is also subjected to neurovascular, inflammatory and immunological changes (Sagare et al., 2012; Wyss-Coray, 2006).

1.1.3 Molecular pathology and the amyloid hypothesis

Aβ represents the major constituent of amyloid plaques and is believed to be the main culprit of AD. According to the amyloid hypothesis, the accumulation of Aβ is thought to be a driving force in the disease process by initiating a neurotoxic cascade, which ultimately leads to neuronal death and dementia (Haass and Selkoe, 2007). Aβ is produced by the sequential endoproteolysis of the amyloid precursor protein (APP), a large type I transmembrane protein. Subsequent cleavage of APP by the β-secretase BACE1 (β-site APP cleaving enzyme 1) and γ-secretase liberates the hydrophobic Aβ peptide into the extracellular space (De Strooper et al., 2010). The stepwise cleavage of APP is a general biological process, that has been observed for many transmembrane

proteins and is known as regulated intramembrane proteolysis (RIP) (Lichtenthaler et al., 2011). In the case of APP, the increased proteolytic processing results in the increased production of Aβ over time. Increased Aβ production or decreased clearance leads to the formation of oligomeric Aβ species and plaques in the extracellular compartment of the brain. The toxic Aβ assemblies initially lead to alterations in synaptic function, followed by more severe defects such as spine loss, neuritic dystrophy, accompanying inflammatory processes and finally neuronal death as the disease progresses (Haass and Selkoe, 2007).

Evidence for the amyloid hypothesis in humans is based on three major findings in several genetic studies. First, patients with familial Alzheimer's disease harbor mutations in the genes coding for APP (Chromosome 21) or presenilin 1 or 2, which represent the catalytic subunit of γ-secretase. All these mutations result in an increase in Aβ production or a relative increase in the especially hydrophobic and neurotoxic Aβ species Aβ42. Second, patients with trisomy 21, that carry an additional APP allele, feature an increased Aβ load and a higher prevalence of AD (Bertram and Tanzi, 2005). Third, a protective mutation that is adjacent to the BACE1 cleavage site in APP, decreases Aβ by 40% in vitro and in vivo and protects the mutation carrier from developing AD (Jonsson et al., 2012). Interestingly, the main constituent of neurofibrillary tangles, tau, seems to be an integral part of the amyloid hypothesis, as tau-/- neurons are protected from Aβ toxicity in vitro and in vivo (Ittner et al., 2010; Rapoport et al., 2002).

1.2 Regulated Intramembrane Proteolysis

1.2.1 RIP is a general cellular mechanism

RIP is an evolutionarily conserved process that controls the communication between cells and is found from bacteria to humans. It results in the proteolytic release of protein fragments into the extracellular space and the cytosol, where the liberated peptides or proteins may exert signaling functions or a subjected to degradation (Brown et al., 2000; Lichtenthaler et al., 2011). RIP is a two-step process. The first proteolytic event, known as ectodomain shedding, is a prerequisite for the second proteolytic event, referred to as intramembrane proteolysis. The term RIP is somewhat misleading, as the tight regulation of this proteolytic cascade has been observed to be in general associated with the ectodomain shedding part, not the intramembrane proteolysis, as the term RIP suggests (Reiss and Saftig, 2009).

In the first step of RIP, the ectodomain of a transmembrane protein is removed by the proteolytic activity of a protease, that is itself membrane bound. These proteases are termed sheddases, and are amongst others members of the disintegrin and metalloproteinase (ADAM) family, the matrix metalloproteinases family or the unusual aspartyl proteases BACE1 and BACE2 (Hayashida et al., 2010; Lichtenthaler et al., 2011; Lichtenthaler and Steiner, 2007). Substrates subjected to RIP are usually single pass transmembrane proteins, with their N-terminus exposed to the

extracellular/luminal compartment (type I transmembrane protein) or towards the cytosol (type II transmembrane protein) (Lal and Caplan, 2011). However, some known shedding substrates are glycophosphatidylinositol (GPI)-anchored, and the shedding of proteins with several transmembrane domains has also been described (Altmeppen et al., 2011; Fleck et al., 2012; Hemming et al., 2009). The general principle of RIP is illustrated in Figure 1 A.

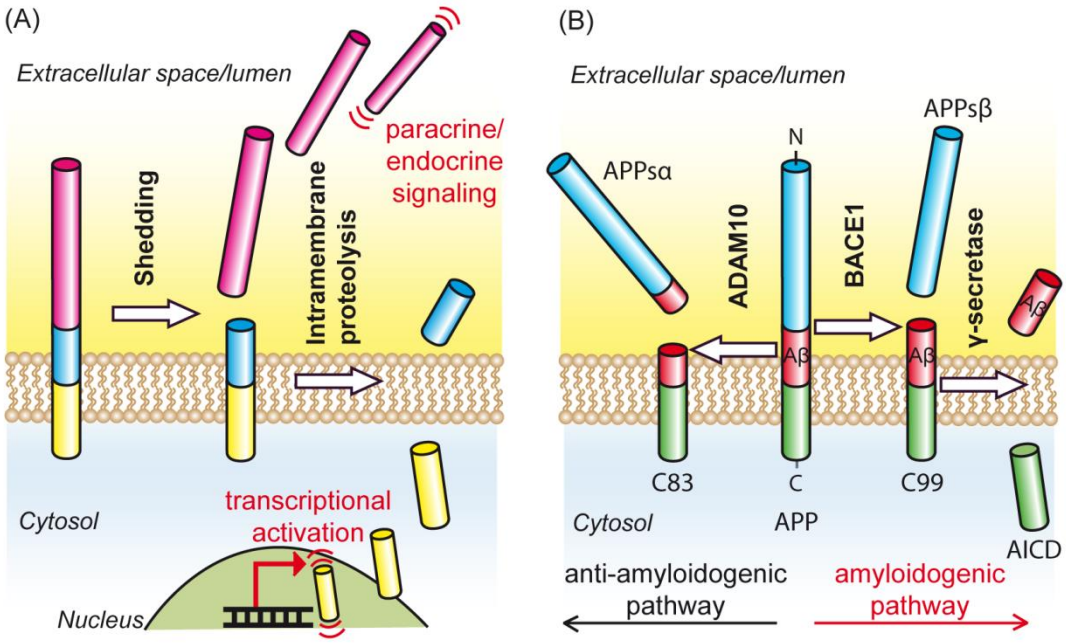

Figure 1: Regulated intramembrane proteolysis and the processing of APP. A) The general principle of RIP. RIP is a two-step process. The first step is referred to as ectodomain shedding and liberates the extracellular domains of transmembrane proteins into extracellular space, where they may act as signaling molecules. In the second step, the membrane bound fragment is processed by a family member of the intramembrane proteases, which results in the release of the cytosolic domain (also known as intracellular domain) into the cytosol, where it may translocate to the nucleus to directly or indirectly regulate transcription. **B)** Processing of APP. RIP of APP occurs by two mutually exclusive pathways. Ectodomain shedding by BACE1 leads to the disease-relevant amyloidogenic pathway. It releases the soluble APP ectodomain (APPsβ) and generates the N-terminus of the Aβ peptide. The membrane bound C-terminal fragment (CTF, C99) is then processed by γ-secretase. This releases the Aβ peptide into the extracellular space and the APP intracellular domain (AICD) into the cytosol, where it is subjected to rapid degradation. In the alternative, anti-amyloidogenic pathway, the first cleavage event is carried out by ADAM10. This cleavage occurs in the middle of the Aβ domain, thus preventing the formation of this toxic peptide, and releases the APP extracellular domain (APPsα). The remaining CTF (C83) is further processed by γ-secretase, which generates the secreted p3 peptide (not shown). The figure was modified from Dislich and Lichtenthaler (Dislich and Lichtenthaler, 2012).

After the ectodomain has been removed by a sheddase, the remaining membrane bound fragment is then subjected to intramembrane proteolysis, the second step of RIP. This releases a

short fragment into the extracellular compartment, and liberates the intracellular domain into the cytosol. Four protease families are capable of cleaving the transmembrane domain of proteins within the hydrophobic environment of the lipid bilayer. Type I transmembrane proteins are processed by γ-secretase and rhomboid proteases, while type II transmembrane proteins are cleaved by signal-peptide peptidase and site-2 protease (Urban and Freeman, 2002). These proteases all share a similar layout, with the active site being formed by multiple transmembrane domains each donating residues to the active site that resides in the lipid bilayer. The multiple domains form a pore like structure, which allows the essential catalytic water molecules to enter the catalytic site and thereby to bypass the hydrophobicity of the lipid bilayer (Lazarov et al., 2006; Li et al., 2013; Wu et al., 2006).

1.2.2 RIP controls signaling pathways and the communication in between cells

RIP in general controls the amount of transmembrane proteins at the cell surface, but also regulates the production of functional protein ectodomains such as cytokines as well as functional intracellular domains that act directly or indirectly as transcriptional modulators (Brown et al., 2000). In order to illustrate the mechanisms and diversity by which RIP controls signaling within and in between cells, the fate of two well-studied proteins and their proteolytic fragments is described in the following.

The type I transmembrane protein Notch is a cell surface receptor in control of cell fate decisions. The binding of Notch ligands at the neighboring cell to the Notch ectodomain causes a conformational change of the latter, which facilitates the ectodomain shedding of Notch by ADAM10 (Bozkulak and Weinmaster, 2009; Hartmann et al., 2002; Lal and Caplan, 2011). The remaining Notch fragment is then further processed by γ-secretase. This releases the Notch intracellular domain into the cytosol, where it translocates to the nucleus to transcriptionally activate Notch target genes via interactions with CSL and MAML proteins (Guruharsha et al., 2012; Lal and Caplan, 2011).

Another prominent RIP substrate is the tumor necrosis factor α (TNFα), where in contrast to Notch the shed extracellular domain acts as a signaling molecule. The type II transmembrane protein TNFα is a proinflammatory cytokine and in control of cell growth, cell differentiation and cell death. Pro-TNFα is shed by ADAM17 to generate the soluble and highly active ectodomain TNFα, which enhances TNF signaling, for example under conditions of septic shock (Murphy et al., 2008; Saftig and Reiss, 2011). Mice lacking ADAM17 are protected from endotoxic shock lethality due to the absence of high levels of TNFα in the blood (Horiuchi et al., 2007). In addition, the intramembrane proteolysis of TNFα by signal peptide peptidase-like 2 A and B proteases release the TNFα intracellular domain into the cytosol, which drives the expression of the pro-inflammatory cytokine interleukin-12 (Fluhrer et al., 2006; Friedmann et al., 2006).

1.2.3 RIP of APP

AD is one of the best studied examples were RIP of a protein is not only a physiological process, but also a disease mechanism, as the proteolytic processing of APP gives rise to the neurotoxic Aβ peptide. Two alternative protease activities compete for the ectodomain shedding of APP, and are generally referred to as α- and β-secretase (Figure 1 B). In the α-secretase mediated pathway, APP is cleaved by ADAM10, which is the constitutively active α-secretase in neurons in vitro and in vivo (Kuhn et al., 2010; Lammich et al., 1999; Postina et al., 2004). The cleavage site is within the Aβ domain, thus precluding the formation of Aβ but giving rise to an extracellular APP fragment termed APPsα (Esch et al., 1990). The remaining C-terminal fragment (CTF) C83 is then processed by γ-secretase and yields the APP intracellular domain (AICD) and the small extracellular peptide p3. As this pathway counteracts Aβ production, it is referred to as the non-amyloidogenic pathway (Lichtenthaler and Haass, 2004).

In the amyloidogenic pathway, APP is processed by the β-secretase BACE1 (Hussain et al., 1999; Lin et al., 2000; Sinha et al., 1999; Vassar et al., 1999; Yan et al., 1999). This cleavage liberates the soluble APP ectodomain APPsβ into the extracellular space and generates the N-terminus of the Aβ peptide, which makes up the first 40 to 42 amino acids of the remaining membrane bound CTF C99. C99 is further processed by γ-secretase, which leads to the liberation of Aβ into extracellular space and also releases the APP intracellular domain. γ-secretase itself consists of four different subunits (APH-1, PEN-2, nicastrin, presenilin 1 or 2) with either presenilin 1 or 2 harboring the enzymatic activity. The remainder of the subunits are necessary for proper maturation, stabilization and substrate recognition of the complex (Steiner et al., 2008). As γ-secretase cleavage is somewhat imprecise, multiple Aβ species of different length are generated, amongst them the highly neurotoxic Aβ42 (O'Brien and Wong, 2011). The RIP of APP is illustrated in Figure 1 B.

1.3 The β-secretase BACE1

1.3.1 BACE1 cell biology

BACE1 and its homologue BACE2 are type I transmembrane proteins, which makes them unique amongst the aspartyl proteases. They belong to the family of pepsin and retroviral aspartic proteases, are 501 and 518 amino acids long, feature an extracellular/luminal orientated active site and a relatively short cytoplasmic domains (21 and 26 amino acids respectively). The two aspartic residues that are critical for the enzymatic activity are located in the typical D-T/S-G-T/S motifs, and it is currently unclear whether the two aspartates of the active site are contributed by the same BACE1 molecule or shared between two BACE1 molecules forming a dimer (Bennett et al., 2000; Hussain et al., 1999; Schmechel et al., 2004; Vassar et al., 1999). After synthesis of BACE1 in the endoplasmic reticulum, its prodomain is removed by furin prohormone convertases

in the Golgi compartment, which results in a twofold increase in enzymatic activity (Benjannet et al., 2004; Benjannet et al., 2001; Bennett et al., 2000; Capell et al., 2000). The enzyme than travels to the plasma membrane and is subsequently internalized into early endosomal compartments, a trafficking fate that is directed by a dileucine motif in the cytoplasmic domain (Huse et al., 2000). BACE1 has a relatively slow turnover rate, which is due to its constant recycling between the endosomal compartments and trans-Golgi network and the plasma membrane (Wahle et al., 2005; Walter et al., 2001). Monoubiquitination at lysine 501 tags the protein for lysosomal degradation (Kang et al., 2010). A schematic diagram of the BACE1 protease is shown in Figure 2.

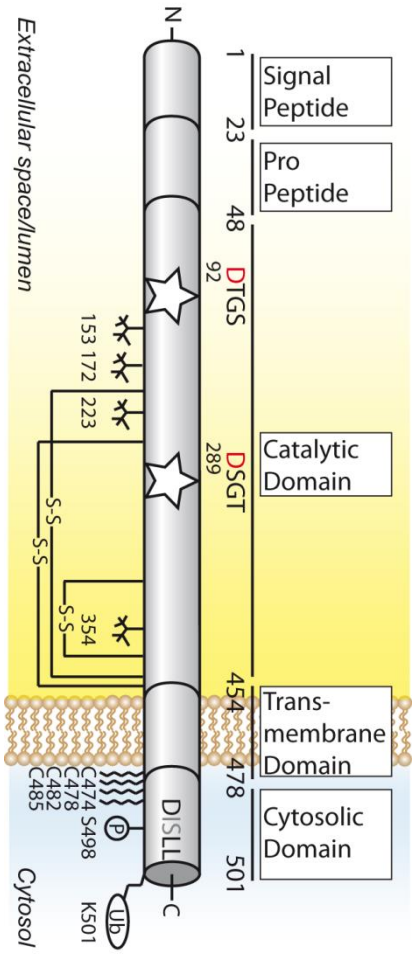

Figure 2. Schematic diagram of BACE1 structure and postranslational modifications. The active isoform (501 amino acids) is shown. The white stars represent the active site motifs DTGS and DSGT at position 92-95 and 289-292. The critical aspartic acid residues are shown in red. The DISLL motif at the cytosolic domain is recognized by adaptor proteins, thus targeting BACE1 to early endosomal compartments. Glycosylation sites are depicted as sugar “trees”, palmitoylation sites as fatty acid chains. S-S: disulfide bond (connecting amino acids 216-420, 278-443, 330-380); P: phosphorylation site; Ub: ubiquitination site. This figure was modified from Dislich and Lichtenthaler (Dislich and Lichtenthaler, 2012).

1.3.2 Cellular localization, enzymatic activity and structure

Mature BACE1 localizes to the acidic environment of the trans-Golgi network and the early endosomal compartments, where also the majority of Aβ is generated. This environment fits to the pH optimum of the enzyme, which is at pH 4.5 (Gruninger-Leitch et al., 2002; Haass et al., 1993; Vassar et al., 1999). A secreted form of BACE1 is capable of processing substrates in vitro (Gruninger-Leitch et al., 2002; Yan et al., 2001). However, the efficient processing of APP depends on the correct spatial interaction between the protease and its substrate, which is only given for the full length transmembrane form of BACE1. The structure of BACE1 is known from X-ray diffraction crystallography and shares the bilobal fold of the active cleft with BACE2 and the aspartyl protease pepsin. An antiparallel hairpin loop shields the large active cleft and controls specificity and access of substrates. In comparison to other aspartyl proteases, the active cleft is unusually large and open, which makes the design of specific inhibitors especially challenging (Hong et al., 2000; Ostermann et al., 2006; Turner et al., 2005).

1.3.3 Expression pattern

BACE1 is expressed in many different tissues and cell lines, but the expression as determined by the mRNA level is the highest in brain and pancreas (Sinha et al., 1999; Vassar et al., 1999; Yan et al., 1999). Within the brain, BACE1 activity is almost exclusively restricted to neurons, as expression levels in glia cells is very low (Harada et al., 2006; Laird et al., 2005; Zhao et al., 2007). Whether BACE1 primarily localizes to pre- or postsynaptic compartments in neurons is currently under debate, as results from different studies using immunofluorescence labeling of BACE1 or the retrieval of sAPPβ and Aβ from axonal and somatodendritic compartments is contradictory (Lazarov et al., 2002; Sannerud et al., 2011; Sheng et al., 2003). During development of mice, the highest levels in the brain are found in the first postnatal days, and especially prominent in the hippocampus, cortex and cerebellum (Irizarry et al., 2001; Willem et al., 2006).

1.3.4 The physiological role of BACE1

Up to date most of the insights into the biological importance of BACE1 have been gained from the various strains of BACE1-/- mice generated by several independent research groups (Cai et al., 2001; Dominguez et al., 2005; Luo et al., 2001; Roberds et al., 2001). The knockout of the BACE1 gene generates mice that weigh ~30% less than their wild type littermates, suffer from premature lethality, reduced myelination in the peripheral nervous system, increased anxiety, schizophrenia-like behavior, altered synaptic function, impaired memory and alterations in locomotion (Dominguez et al., 2005; Wang et al., 2013). As the function of a protease is defined by its substrates, a deeper understanding of substrate processing and its biological relevance allowed mechanistic insights into the function of BACE1 and could partially be linked to the observed phenotypes in BACE1-/- mice. The BACE1 substrates type III neuregulin 1 (NRG1), APP, the β-subunits 2 and 4 of voltage-gated sodium channels and the β-galactoside α2, 6-sialyltransferase are processed by BACE1 in vivo. In addition, their cleavage has been shown to be

functionally relevant. Two of these substrates, type III NRG1 and the β-subunits 2 and 4 of voltage-gated sodium channels will be discussed in further detail.

1.3.5 Physiologically relevant substrates of BACE1: type III NRG1 and β-subunits of VGSCs

In 2006, two independent research groups could link the altered processing of type III NRG1 to the reduced peripheral myelination observed in BACE1-/- mice, thus indicating for the first time the biological importance of this protease (Hu et al., 2006; Willem et al., 2006). The growth factor NRG1 acts as a ligand for members of the epidermal growth factor (EGF) receptor family and initiates the myelination of nerve fibers during development. The isoform type III NRG1 harbors two transmembrane domains, that are connected by a luminal EGF domain. BACE1 cleaves C-terminal to this EGF like domain, exposing the domain for juxtacrine signaling with neighboring cells (Mei and Xiong, 2008). A second cleavage by BACE1 or alternatively ADAM17 N-terminal to this domains finally releases the EGF domain from the membrane, which than acts as a signaling molecule in a paracrine fashion (Fleck et al., 2013). BACE1-/- mice phenocopy the reduced peripheral myelination of NRG1+/- mice (the complete NRG1 knockout is lethal) and show increased levels of the full length form of type III NRG1, while the levels of the cleavage product are decreased (Hu et al., 2006; Willem et al., 2006). It is noteworthy to mention that NRG1 is one of the few shedding substrates known that feature more than one transmembrane domain.

The (Navβ2, Navβ4) of voltage-gated sodium channels (VGSCs) are type I transmembrane proteins and also processed by BACE1 in vivo. The cleavage of these subunits by BACE1 alters the surface levels of VGSC, by initiating a signaling cascade, which is similar to that of Notch as described above (Kovacs et al., 2010). After ectodomain shedding by BACE1, the CTFs are processed by γ-secretase, which releases the intracellular domain into the cytosol. They enter the nucleus and transcriptionally activate expression of the VGSC α-subunits, which increases the total level of VGSCs at the cell surface (Kim et al., 2007; Wong et al., 2005). In AD patients, that feature increased expression of BACE1, surface levels of VGSC α-subunits are increased accordingly, while reduced surface levels are found in BACE1-/- mice. It is currently under debate whether the spontaneous seizures monitored in a subset of BACE1-/-, as conflicting results from different labs using different biochemical extraction methods (Hu et al., 2010; Kim et al., 2007; Kim et al., 2011; Wong et al., 2005).

To conclude, these substrates illustrate the functional diversity of BACE1 in the cellular context and show the versatility of the RIP process, that generates a functional ectodomain in the case of type III NRG1 and a functional intracellular domain in the case of the β-subunits 2 and 4 of VGSCs.

1.3.6 Therapeutic Inhibition of BACE1

BACE1 is the rate-limiting enzyme of Aβ generation, and the main if not only β-secretase, as Aβ and its precursor C99 are no longer detectable in the brain of BACE1-/- mice (Cai et al., 2001;

Dominguez et al., 2005; Luo et al., 2001; Roberds et al., 2001). Its inhibition is currently one of the most promising strategies to prevent AD or alter the disease progression, next to immunization against the Aβ peptide itself. Numerous BACE1 inhibitors have been developed since the crystal structure of BACE1 bound to a transition state inhibitor has been published (Ghosh et al., 2001; Gruninger-Leitch et al., 2002; Hong et al., 2000). Several of them have the required specificity and are small enough to cross the blood-brain-barrier, while still being able to successfully block the large active site of BACE1. Their effectiveness is measured by the efficient reduction of Aβ levels in the brain, cerebrospinal fluid (CSF) and plasma of different animal models (Fukumoto et al., 2010; Sankaranarayanan et al., 2009). One proof of principle study reported the efficient inhibition of Aβ generation in man using an orally available BACE1 inhibitor, but had to be stopped due to non-mechanism based adverse effects (May et al., 2011). The development of BACE1 inhibitors and clinical trials testing their efficacy will continue in the future, but concerns have been raised about the possible side effects, given the complex phenotype of BACE1-/- mice and the diverse biological functions of this protease. This has to be kept in mind and could be addressed by only partially inhibiting BACE1, possibly in conjunction with the parallel administration of other Aβ lowering drugs. Further research on BACE1 and it substrates will provide additional insights into the specificity, substratome and physiological relevance of this protease, providing essential knowledge to screen for possible side effects during therapeutic inhibition and to develop novel biomarkers that aid in diagnosis and treatment.

1.4 Quantitative proteomics

1.4.1 Quantitative proteomics allows the accurate quantification of the proteome

As most of this work is based on modern quantitative mass spectrometry (MS), the general principle of MS as well as state of the art technology and experimental strategies are introduced in the following sections. Quantitative proteomics allows the relative or even absolute quantification of entire proteomes, with the proteome being defined as “the total complement of all proteins expressed in a given cellular or tissue state” (Cox and Mann, 2011). This increasingly powerful technique is now capable of analyzing up to 10.000 proteins in a single cell line in a quantitative manner. This for example allows the investigation of complex signaling networks, the identification of novel protein-protein interactions or the monitoring of the proteome wide response to the inhibition or knockout of a given protein or gene (Cox and Mann, 2011; Mann et al., 2013). MS based proteomics has finally reached the same system-wide scale as DNA-based methods and continues to revolutionize systems biology (Sabido et al., 2012).

1.4.2 Introduction to mass spectrometry and the orbitrap mass analyzer

A mass spectrometer allows the precise determination of the masses of molecules and the visualization of the resulting mass spectra. Charged molecules show a characteristic behavior

when subjected to an electrical field, which is directly correlated to their mass to charge ratio (m/z). The analysis of this behavior or “movement” is used by the mass analyzer of a mass spectrometer to determine the m/z of a given molecule. In general, a mass spectrometer consist of three parts: An ion source, a mass analyzer and a mass detector. The ion source provides the ions to be analyzed, the mass analyzer separates them by their mass and charge, while the detector allows the detection of the ions of interest. The mass analyzer used for this work is known as an orbitrap and uses only electrostatic fields to analyze the ion of choice. It consists of a negatively charged spindle-shaped inner and a barrel shaped outer electrode. Ions (which are positively charged due to prior acidification) are injected into the orbitrap, which results in a stable trajectory of the ion around the central spindle. Ions are orbiting in a circular fashion around the spindle, but also oscillate back and forth on the z-axis, which is in parallel to the orientation of the spindle (axial oscillation). The harmonic axial oscillation is only dependent on the m/z of the ion and independent of any other properties. This independence is responsible for the high mass accuracy and resolution of orbitrap mass analyzers. As the ion oscillates back and forth along the z-axis, it induces a current, which is detected by the outer electrode that serves as the mass detector. The signal is subsequently amplified and Fourier-transformed to a frequency spectrum, from which the m/z is finally calculated (Makarov, 2000; Perry et al., 2008). Figure 3 shows a picture and a schematic overview of the orbitrap mass analyzer.

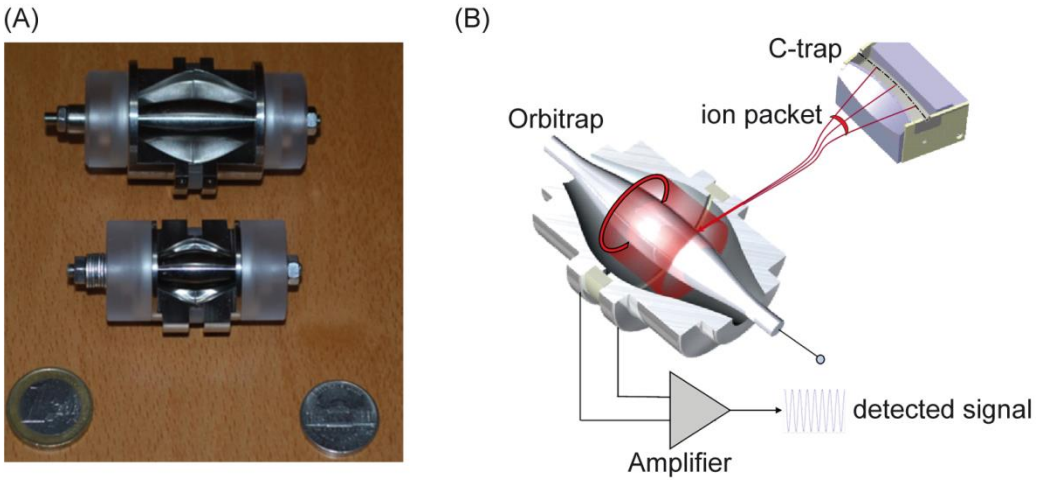

Figure 3: The orbitrap mass analyzer. A) Above: the standard orbitrap mass analyzer. Below: The improved high-field orbitrap, featuring a higher resolution. The orbitrap has been cut along its longitudinal axis in order to allow the inner cavity to be visualized. **B)** Ions are ejected in packages corresponding to a certain m/z from the C-trap. They enter the orbitrap through a narrow slit, which results in the stable oscillation of the injected ions around the inner spindle. The oscillation of the orbiting ions is dependent on their m/z and induces a current, that is amplified, detected and finally converted using Fourier transformation. The figure was modified from Zubarev et al. (Zubarev and Makarov, 2013).

To deduce the mass of the m/z of a detected molecule, one takes advantage of naturally occurring isotopes such as ^{13}C atoms. Two molecules that differ only by the presence of one ^{13}C in one of the molecules have a mass difference of exactly one Dalton (Da, u), as the additional neutron of C13 weighs almost precisely one Da. If these two molecules show a difference in their m/z of exactly one Dalton, the charge state is "one". If the difference of their m/z is 0.5, the charge state is "two", and so forth (0.33 for charge state "three", 0.25 for charge state "four"). Therefore the isotope pattern allows the deduction of the charge state and the determination of the precise mass of the molecule.

1.4.3 Bottom up tandem mass spectrometry

In modern, discovery-based proteomic workflows, bottom-up tandem MS is employed. Instead of analyzing entire proteins, short peptide fragments created from complex protein mixtures are analyzed. The detected peptides are then mapped to their proteins of origin in silico, by using databases containing all protein sequences of a given organism. This is known as bottom-up proteomics, as the identity of a proteins is deduced from the observed peptides. Peptides are generated by digesting the proteins of interest using sequence specific enzymes such as trypsin, that cleaves carboxyterminal of lysine and arginine residues and creates peptides with an average length of nine amino acids. The researcher has thus not to deal with intact proteins, which are difficult to work with, due to poor signal intensity during MS measurements, differences in solubility during sample preparation and extremely complex fragmentation patterns. Instead, tryptic peptides are analyzed, that are easy to handle, show high signal intensities and give rise to fragmentation spectra that can be analyzed automatically by various software algorithms (Ahrens et al., 2010; Steen and Mann, 2004).

In order to identify a peptide from a complex mixture, it is not sufficient to determine its mass alone (MS signal), as two peptides sharing the same amino acids, but in different order, have the same mass and are therefore not distinguishable from each other. This is why sequence specific information has to be obtained for each peptide. The principle of determining the mass of a peptide in a first step and its sequence in a second step is known as tandem mass spectrometry (MS/MS or MS^2). After the m/z of a peptide has been determined, the same peptide (also termed the precursor ion) is isolated and fragmented with the use of an inert gas such as helium. This leads to the disruption of the peptide along its peptide backbone, as the breakage of the amid bonds represents the lowest energy pathway. A series of product ions is generated, that are

subjected to the mass analyzer (MS/MS signal). Their precise masses provide the necessary information to then determine the peptide sequence (Glish and Vachet, 2003; Steen and Mann, 2004).

1.4.4 LC-MS/MS workflow in bottom-up proteomics

The following section describes the typical workflow of a bottom-up discovery based proteomics, that has first been described as a powerful application with high proteome coverage in 2001 (Washburn et al., 2001). The biological sample of interest (cells, tissue, body fluids) is lysed and subjected to enzymatic digestion, usually by trypsin. The generated peptide mixture is fractionated off line using e.g. anion exchange chromatography or isoelectric focusing and then further fractionated online using high-performance liquid chromatography (HPLC). HPLC separates the peptide species according to their hydrophobicity, by eluting them from a highly hydrophobic material with increasing percentages of an organic solvent. Peptides are then ionized using nano-electrospray and enter the mass spectrometer, being guided by electrical fields and a decrease in atmospheric pressure. The obtained mass spectra are then matched with protein databases using different search algorithms (Gilmore and Washburn, 2010; Liao et al., 2009). Figure 4 summarizes the LC-MS/MS workflow in modern bottom-up proteomics.

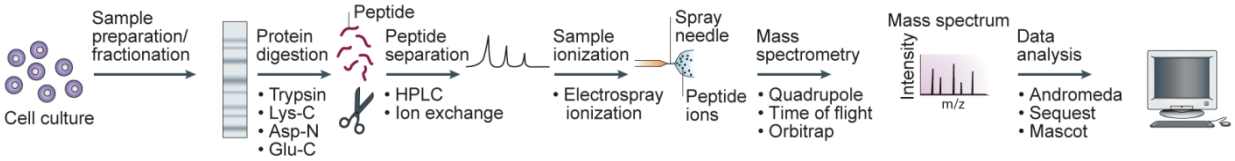

Figure 4: Worflow in bottom-up proteomics. The biological material of interest is solubilzed and fractionated. Proteins are digested using sequence-specific proteases. The resulting peptides are further fractionated by HPLC or pipet tip based fractionation methods. Peptides are finally separated by HPLC according to their hydrophobicity, ionized using electrospray ionization and injected into the mass spectrometer. The obtained mass spectra are then analyzed using different search engines, such as Andromeda, Mascot or Sequest. The figure was modified from Steen et al. (Steen and Mann, 2004)

1.4.5 Protein quantification in MS based proteomics

The proteomic workflow described above explains how complex proteomes are analyzed in a qualitative manner in order to identify as many proteins as possible with high confidence in an acceptable time period. In order to differentiate in between two biological states, for example

between inhibitor treated versus control treated cells, a quantitative dimension must be integrated into the workflow. It is currently not possible to directly correlate the signal intensity of a measured peptide to its absolute quantity, as differences in ionization, solubility and accession of the sequence-specific protease create a bias for each individual peptide. In other words, MS is not inherently quantitative, which is why different techniques have been invented to bypass this shortcoming (Sjödin et al., 2013; Steen and Mann, 2004). In general, absolute and relative quantification is possible and two different strategies are employed: label-free versus label-based quantification.

As mentioned above, the peak intensity of a peptide cannot be directly correlated to its absolute amount, but can be used for the relative quantification in between different measurements. This holds true if certain prerequisites are met, most importantly high reproducibility during liquid chromatography (LC), which reassures that the same peptide elutes at the same time in between different runs. Current label-free quantification algorithms rely on the integration of the complete MS signal of every eluting peptide. In order to do this, the absolute intensity within a predefined mass tolerance window of a peptides m/z is displayed over time (extracted ion chromatogram), and the area under the peak is integrated and compared in between runs (Cox and Mann, 2011; Luber et al., 2010). Label-free quantification can be applied to any sample, even to already existing data sets, and is not limited to a certain dynamic range. It is however time consuming, as each sample has to be measured separately and does not reach the accuracy of label-based quantification methods (Merl et al., 2012).

In comparison to label-free approaches, label-based methods are more accurate, but rely on the introduction of an artificial label either on the protein level in vivo (metabolic labeling) or the peptide level in vitro (chemical or enzymatic labeling). Measurement time is reduced compared to label-free approaches as the differentially labeled samples can be mixed and analyzed in the same run. The labeled proteins or peptides elute as pairs during LC and show up as pairs in the mass spectra, where they can be directly compared to each other. If a peptide pair features a 1:2 ratio, it means that the abundance of those peptides in between the original samples is precisely 1:2. Similar to label-free approaches, it is actually the integrated area of the extracted ion chromatogram of the peptide pairs that is used for quantification (Mann, 2006). The most accurate form of metabolic labeling is stable isotope labeling with amino acids in cell culture (SILAC). It relies on the introduction of amino acids containing stable non-radioactive isotopes into newly synthesized proteins. By incorporating the naturally occurring amino acid (“light” label) into one and the isotope-labeled amino acid (“heavy” label, containing e.g. ^{13}C instead of ^{12}C) into the other cell population, a light and a heavy proteome is generated. This leads to a light and a heavy spectrum for each measured peptide, and the intensities of the spectra are compared relatively to each other. The advantage of SILAC is the labeling on the level of proteins, which allows mixing of the samples during the earliest stages of sample processing and keeps

quantitative errors to an absolute minimum (Ong et al., 2002; Ong and Mann, 2006). Since its invention in 2002, SILAC has made a major step forward, as it is no longer restricted to cell culture. Meanwhile complete organisms such as the nematode *C. elegans*, the fruit fly *Drosophila melanogaster* or even the laboratory mouse have been successfully labeled (Kruger et al., 2008; Larance et al., 2011; Sury et al., 2010).

2 Aims of this work

BACE1 is the rate limiting enzyme of Aβ generation and its inhibition leads to a nearly complete block in Aβ production in vitro and in vivo (Cai et al., 2001; Luo et al., 2001; Roberds et al., 2001; Stachel et al., 2004). It is thus a prime target for therapeutic inhibition and the development and characterization of specific and safe inhibitors is currently addressed by academia and the pharmaceutical industry (Klaver et al., 2010; Vassar and Kandalepas, 2011; Wang et al., 2013). Keeping in mind the emerging data about the physiological role of BACE1, increased awareness for mechanism-based side effects upon inhibition of the enzyme has emerged in the community of BACE1 researchers. A minority of the phenotypes observed in BACE1-/- mice could be linked to BACE1 substrates, the molecular mechanism for the majority of the phenotypes is still unknown. Therefore a more thorough understanding of BACE1, its physiological role and its substrates is needed to aid in the future developments of BACE1 inhibitors, to monitor for adverse effects during therapy and to develop diagnostic and prognostic biomarkers for AD.

As BACE1 lacks a sequence specific cleavage motif, the prediction of novel substrates by bioinformatic analysis of the amino acid sequence of putative proteins is not feasible. In the past,

2 Aims of this work

BACE1 substrates have been identified using candidate based approaches, by taking an educated guess on proteins that were homologues to previously known substrates or had been described as substrates by other sheddases. This led to the identification of 13 BACE1 substrates (Dislich and Lichtenthaler, 2012). More recently, an unbiased screen for novel BACE1 substrates lead to the identification of 64 type I transmembrane proteins, 1 type II transmembrane proteins and three GPI-anchored proteins (Hemming et al., 2009). Although this work provided an interesting insight into the possibly large substratome of this protease, it was limited due to the fact that it was carried out under overexpressing conditions of BACE1 and in non-neuronal cell lines. Overexpression of a protease can lead to the processing of substrates that would not be processed under endogenous conditions (for example proteins localized in the endoplasmic reticulum) and important neuronal substrates may have been missed in the peripheral cell lines analyzed.

The work presented here aims to address three major goals:

1. To overcome the limitations of previous studies and to enhance the knowledge about BACE1 and its substrates, the main goal of this work is the identification of novel BACE1 substrates under physiologic conditions in vivo. The BACE1-/- mouse is viable and fertile and represents an excellent tool to address the function of this protease in vivo. As candidate based approaches are biased and cumbersome, a powerful discovery based quantitative proteomics workflow will be used.

2. In addition, the entire proteome of the BACE1-/- brain will be analyzed, to observe if the deletion of BACE1 leads to drastic changes associated to the reduced or missing processing of substrates and to gain a systems level understanding of this protease.

3. Last but not least, the BACE1-/- mouse CSF will be investigated by quantitative mass spectrometry. As CSF is the only compartment of the brain that can be routinely accessed in living humans, the confirmation and discovery of BACE1 substrates in CSF could be a valuable tool for the development of diagnostic and prognostic biomarkers and could be used to monitor for adverse effects during therapeutic inhibition.

3 Material and Methods

3.1 Cell culture

3.1.1 Cell lines

HEK-293 EBNA (HEK-293E) cells were cultivated in Dulbecco's Modified Eagles Medium (DMEM, Gibco), supplemented with 10% fetal calf serum (FCS, Gibco) and 1% penicillin/streptomycin (Gibco). Cells stably expressing BACE1 (HEK-293E_BACE1) or the empty control vector (HEK-293E_control) were additionally grown in the presence of 1.0 µg/ml puromycin (Sigma) in order to maintain selection pressure for the plasmid of interest. Plasmids (p12-BACE1, encoding cDNA

of human BACE1 and p12-linker, empty control vector) were generated by Stefan F. Lichtenthaler (DZNE, TUM, Munich)

3.1.2 Cell culture conditions

Cells were grown in 10 cm dishes (Nunc) in an incubator (Hera Cell, Heraeus) at 37 °C and 5% CO_2. Cells were handled under a sterile work bench (Hera Safe, Heraeus) with the help of single-use plastic pipettes (Sarstedt) and a battery powered pipetting device (Accu Jet Pro, Brand). Cells were passaged twice a week. To do so, the conditioned medium was removed, cells were washed once with phosphate buffered saline (14 mM NaCl, 10 mM Na_2HPO_4, KCl, 1,75 mM KH_2PO_4, pH 7,4) and incubated for 5 minutes at 37 °C with 1 ml tissue culture grade trypsin (Gibco). Cells were then detached from the dish by gently rocking the dish back and forth. 3 ml of fresh DMEM were added the cell suspension, which was then transferred to new 10 cm dishes (usually 10% of the original cell suspension per dish). For long term storage, the cell pellet of a 50% confluent 10 cm dish was cryoconserved in 1 ml FCS supplemented with 10% cell culture grade DMSO (Dimethyl sulfoxide, Sigma) and stored at -80 °C for a few months or in liquid nitrogen for several years.

3.1.3 SILAC labeling of HEK-293E cells

SILAC media were purchased from SILANTES (www.silantes.com). DMEM (without arginine or lysine) was supplemented with 0.398 mM arginine, 10% of dialyzed FCS and 2 mM glutamine. 0.798 mM of lysine were added for the “light” SILAC medium, whereas 0.798 mM Lysine $^{13}C^{15}N$ were added for the “heavy” SILAC medium. HEK-293E_p12BACE and HEK-293E_p12linker cells were grown in “heavy” and “light” SILAC media for at least 7 doublings, in order to achieve an isotope labeling above 95%. SILAC media did not have any observable effect on cell growth or viability when compared to our regular growth media.

3.1.4 Transient liposomal transfection with plasmid DNA

Cells were plated at a density of $3.5x10^5$ /ml in 6 cm dishes (5 ml/dish). After 16 hours, cells were transfected using lipofectamin 2000 (Invitrogen) according to the manufacturer’s protocol. Briefly, 500 ng of plasmid DNA was mixed with 250 µl of Opti-MEM medium (Invitrogen). 15 µl of lipofectamin 200 were mixed with 250 µl of Opti-MEM in a second tube and briefly vortexed for 10 s. After incubation for 5 minutes at room temperature, the tubes containing plasmid DNA and lipofectamin were mixed and incubated for another 20 minutes at room temperature. The transfection mix was then carefully added to the cells in the 6 cm dish. Medium was replaced after 24 h. To obtain cell lines that stably express the plasmid of interest, the medium was supplemented with increasing concentrations of Puromycin (1.0 µg/ml) in order to select for cells where the plasmid had stably integrated into the genome.

3.1.5 Inhibitor treatment of primary cortical neurons

Table 1: Inhibitor treatment of primary cortical neurons

TAPI-1	25 µM in DMSO, Peptides International
C3 (β-secretase inhibitor IV)	2 µm in DMSO, Merck Millipore
DMSO	Sigma

Neurons were treated with inhibitors over night. Control cells were treated with equal amounts of pure DMSO.

3.2 Animal related work

3.2.1 Mouse strains

Wild type and BACE1-/- mice used for preparation of mouse brains and primary cortical neurons tissues were maintained according to the European community council directive (86/609/ECC). BACE1-/- mice were kindly provided by Michael Willem (Adolf Butenandt Institute, LMU, Munich) and were originally created by Phil Wong (Johns Hopkins University, Baltimore, USA) and can be imported from the Jackson Laboratory (B6.129-Bace1tm1Pcw/J). C57BL/6 wild type mice were obtained from the common colony of the Adolf Butenandt Institute (LMU, Munich). Heavy labeled SILAC mouse brains (Lys ^{13}C, 97%) were purchased from SILANTES (www.silantes.com)

3.2.2 Mouse brain extraction

P3 mice were decapitated and the skull was opened by dorsal incision along the median axis of the head with curved scissors. The lateral parts of the skull were removed using a small pair of forceps. The brains (including the cerebellum, without the brain stem) were carefully liberated from the base of the skull using a spatula. All surgical tools were purchased from Fine Surgical Tools (FST). The brains were washed once in cold PBS (140 mM NaCl, 10mM $Na_2HPO_4*2H_2O$, 1,4 mM KH_2PO_4, 2,7 mM KCL), flash frozen in 1.5 ml tubes in liquid nitrogen and stored at -80 °C.

3.2.3 Preparation of primary cortical neurons

Primary cortical neurons were prepared in house by Dr. Alessio Colombo.

Table 2: Isolation and culture of primary cortical neurons

Culture medium	Neurobasal medium (Invitrogen), supplemented with 2% (v/v) B27 DMEM (Invitrogen), 0.5 mM glutamine, 1% Penicillin/Streptomycin (v/v)
Plating medium	DMEM, High Glucose, Glutamax (Invitrogen), supplemented with 10% (v/v) FCS, 1% Penicillin/Streptomycin (v/v)
Digestion medium	9.7 ml DMEM, High Glucose, Glutamax, 0.01 g cysteine neutralized with 27 µl 1 M NaOH (Sigma), 200U Papain (Sigma)

Preparation medium	Hank's balanced salt solution (HBSS) with Calcium and Magnesium (Invitrogen)
Dissociation medium	DMEM, High Glucose, Glutamax, supplement with 10% FCS (v/v)
Coating medium	25 µg/ml Poly-D-Lysine (Sigma)

The pregnant female mouse containing embryos aged 15-16 days post fertilization was killed by cervical dislocation. Access to the abdominal cavity was gained after displacing fur, skin and subcutaneous fat tissue and cutting along the midline through the peritoneum. The embryos along with the surrounding uterus were disconnected carefully from their blood supply and placed into the 15 cm dish containing ice cold HBSS. Embryos were carefully extracted from the uterus and the brains were exposed by removing the skin and the underlying dura mater, beginning at the lambda. The brains were freed from the head and the pia mater was removed carefully. The brain hemispheres were then placed into prewarmed digestion medium and incubated at 37 °C for 15 minutes in an incubator (Heraeus). In order to singularize individual cells, the hemispheres were carefully grated with a 2 ml syringe attached to a Peleus ball. The dissociated neurons were transferred to a new falcon tube. Neurons were pelleted at 800 rpm for 5 minutes, dissociated in plating medium and seeded according to the desired density. 4 h after plating, the plating medium was exchanged for the culture medium. All necessary surgical instruments were purchased from Fine Surgical Tools (FST).

3.2.4 Collection of CSF from the cisterna magna of adult mice

The CSF use in this work was collected by Teresa Bachhuber (Adolf Butenandt Institute, LMU, Munich). The protocol for CSF isolation was adopted from DeMattos et al. (DeMattos et al., 2002). CSF was isolated from the cistern magna. Mice were anesthetized with a mixture containing Ketamine (Bayer, 100mg/kg body weight) and Rompun (Ratiopharm, 20 mg/kg body weight). A dorsal excision along the base of the skull to the dorsal thorax up to Th1 was made. The musculature was displaced and the meninges on top of the cisterna magna were exposed. The area was cleaned using cotton swabs, and the cisterna magna was punctuated using a micro needle. The CSF was collected using glass micropipettes (Stoelting, #50614). CSF samples were visually inspected for the presence of blood and subjected to centrifugation on a benchtop centrifuge in order to remove any residual erythrocytes. Samples were blood contamination was seen were excluded from the analysis. A total volume of 5-20 µl of blood free CSF were collected from each animal. The animals were sacrificed afterwards.

3.3 Biochemical methods

3.3.1 Concentration of conditioned media

Cells were grown in 10 cm dishes (2 dishes/condition) up to a confluency of ~95%. The conditioned medium was then exchanged for serum free medium. After 24 h the conditioned

serum free medium was carefully collected. Free floating cells and debris were pelleted in 15 ml falcon tubes at 4000 rpm for 5 minutes. The conditioned media were not transferred into a new falcon tube in order to keep protein loss to a minimum. The falcon tube was stored on ice and 12 ml of HEK-293E_p12BACE ("heavy") and HEK-293E_p12linker ("light") conditioned media each were gradually concentrated together in a Amicon Ultra centrifugal filter unit (4ml, 3 kDa NMWCO, Millipore) to a final volume of 100 µl. Centrifugation was carried out at 4000 rpm for about 3h in a benchtop centrifuge (MegaFuge 40R, Thermo Fisher Scientific). The concentrate was mixed with 100 µl of 2-fold SDT buffer (2%(w/v) SDS, 100mM Tris/HCl pH 7.6, 0.1M DTT) and incubated for 5 minutes at 95 C° in an 1.5 ml low protein binding tube (Eppendorf).

3.3.2 Membrane preparation

Protocol 1: The protocol was adopted from Regina Fluhrer (Adolf-Butenandt Institute, LMU, Munich). 200 mg of mouse brain were homogenized in 4 ml hypotonic buffer (10 mM TRIS pH 7.4, 1 mM EDTA, 1 mM EGTA) supplemented with protease inhibitor mix (1:100, Roche) using a tissue homogenizer (Omni International) at maximum speed for 20 s. The homogenate was further homogenized by sonication with 10 pulses and 30% of the maximum intensity (Branson Sonicator) in 1.5 ml tubes. The homogenate was incubated 10 min on ice, pipetted up and down 15 times with a 1 ml syringe (Terumo) and a 0.6 mm syringe tip (Terumo) and centrifuged at 6000 rpm for 5 minutes at 4 °C to pellet nuclei and cytoskeleton. The supernatant was transferred to a new 1.5 ml tube and centrifuged at 13000 rpm for 1 h at 4 °C. The obtained pellet represented the membrane fraction and was solubilized in 200 µl SDT-lysis buffer (see below) and boiled for 5 minutes at 95 °C at 900 rpm in a heated benchtop mixer (Eppendorf).

Protocol 2: The protocol was adapted from Nielsen and Wisniewski et al. (Nielsen et al., 2005; Wisniewski et al., 2009a).

Table 3: Membrane preparation

High salt buffer	2 M NaCl, 10 mM HEPES/NaOH, pH 7.4, 1 mM EDTA, in ddH_2O
Carbonate buffer	0.1 M Na2CO3, pH 11.3, 1 mM EDTA, in ddH_2O
Urea buffer	5 M urea, 100 mM NaCl, 10 mM HEPES, pH 7.4, 1 mM EDTA, in ddH_2O
TRIS HCl	0.1M TRIS/HCL, pH 7.6, in ddH_2O
SDT-lysis buffer	2%(w/v) SDS, 100mM TRIS/HCl pH 7.6, 0.1M DTT, in ddH_2O
Tissue blender	Omni TH, Omni International

HEK-293E cells, 200 mg of mouse liver and whole mouse brains were homogenized in 1 ml of high salt buffer supplemented 1:100 with protease inhibitor mix (Roche) using a tissue blender at maximum speed for 60 s. The homogenate was centrifuged at 4 °C at 13.000 rpm in a benchtop centrifuge for 15 minutes. The supernatant was discarded and the cell pellet was washed twice with carbonate buffer, once with urea buffer and two more times with TRIS-HCl. A 15 minutes

centrifugation at 13.000 rpm at 4 °C was carried out after each washing step. After the final washing step, the membrane pellet was resuspended in 50 µl of SDT buffer and incubated for 5 minutes at 95 C°.

3.3.3 DEA fractionation of brain tissue

To obtain the soluble and insoluble fractions of mouse brain tissue, a method based on diethylamine (DEA) fractionation was applied.

Table 4: DEA fractionation of brain tissue

DEA lysis buffer	0,2% diethylamine (v/v), 50 mM NaCl, 2 mM EDTA + 1:100 protease inhibitor mix (Roche)
Neutralisation buffer	0.5 M TRIS pH 7.5
Triton lysis buffer	150 mM NaCl, 50 mM TRIS, 2 mM EDTA pH 7.5, 1% Triton-X100 (v/v)+ 1:100 protease inhibitor mix (Roche)
Tissue blender	Omni TH, Omni International
4-fold protein sample buffer	0.25 M TRIS/HCl pH 6,8, 8% SDS (v/v), 40% glycerol (v/v), 1 1% bromophenol blue (SIGMA), in ddH_2O
2 ml and 1.5 ml tubes	Sarstedt
1.5 ml ultracentrifugation tubes	Beckman Coulter
TLA-55 Rotor	Beckman Coulter
Ultracentrifuge	Optima Max-XP, Beckman Coulter

2 ml tubes were filled with 220 µl of TRIS buffer and stored on ice. The frozen mouse brain was placed into a 15 ml falcon, 2 ml of DEA lysis buffer were added and the tissue was homogenized using the tissue blender at maximum speed for 60 s. The homogenate were transferred to the 2 ml tubes that had been prefilled with TRIS buffer, mixed carefully and centrifuged for 10 minutes at 4 °C and 5000 rpm in a benchtop centrifuge. The supernatant was then carefully collected, split into two 1.5 ml ultracentrifugation tubes and subjected to ultracentrifugation at 100.000 g for 30 minutes at 4 °C. The supernatant of the ultracentrifugation step represents the DEA fraction (extracellular fraction) and was mixed with 4-fold protein sample buffer, incubated for 5 minutes at 95 °C and stored at -20°C.

The remaining pellet was carefully washed with 1 ml PBS and again subjected to centrifugation for 10 minutes at 5000 rpm at 4 °C on a benchtop centrifuge. The pellet was then carefully sucked dry, followed by the immediate addition of 1 ml Triton lysis buffer and an incubation for 1 hour on ice. Afterwards, the solubilized pellet was centrifuged at 15000 rpm for 10 minutes at 4 °C to remove any insoluble material. The supernatant represents the membrane fraction and was mixed with 4-fold protein sample buffer, incubated for 5 minutes at 95 °C and stored at -20°C.

3.3.4 Protein concentration measurements

Solution A and B of the BC Assay kit (Uptima) were mixed in a 1:50 ratio. 10 µl of protein lysate was loaded in duplicates into 96 well plates (Nunc) and mixed with 200 µl of the 1:50 mixed solution. After incubation for 20 minutes at 37 °C in an incubator (Heraeus), absorbance at 562 nm was measured on a plate reader (Powerwave XS, Biotek) according to the manufacturer's protocol. Measured values were corrected for the blank solution (lysis buffer).

3.3.5 Sodium dodecyl sulfate polyacrylamide gel electrophoresis (SDS-PAGE)

Table 5: SDS PAGE

4-fold protein sample buffer	0.25 M TRIS/HCl pH 6.8, 8% SDS (v/v), 40% glycerol (v/v), 1% bromophenol blue (SIGMA), in ddH_2O
4-fold lower TRIS buffer	1.5 M TRIS pH 8.8, 0.4% SDS (v/v) in d dH2O
4-fold upper TRIS buffer	0.5 M TRIS pH 8.8, 0.4% SDS (v/v) in d dH2O
Schägger Gel Buffer	3 M TRIS/HCl pH 8.45, 0.3 % SDS (v/v)
Glycerol	32 % (v/v)
Acrylamide	40%, Serva
TEMED	N,N,N',N'-Tetramethylethylendiamine, Roth
APS	10% (w/v), Ammoniumpersulfate, SIGMA
10-fold TRIS-Glycine	0.24 M TRIS Base, 0.2 M Glycine (v/v), Roth, dH2O ad 5 l (for 10x TRIS-Glycine/SDS, add 0.1% SDS (v/v) to 1x-buffer)
Protein ladder See blue plus 2	Invitrogen
Mini-Protean Minigel system	Biorad
Power pack: Power Pac 300	Biorad
Gelcombs, glassware	Biorad

Proteins were separated in one-dimension using the Biorad Minigel system. Gels were made in-house according to the manufacturer's protocol. Gels were 1.5 mm in thickness and were equipped with up to 15 wells per gel.

Table 6: Pipetting scheme for home-made 8% TRIS-glycine-polyacrylamide gels

substance:	**amount:**
Resolving gel:	
Acrylamide 40%	7.8 ml
ddH_2O	4.2 ml
4-fold lower TRIS buffer	4 ml
APS	30 µl
TEMED	30 µl

∑=	**16 ml**

substance:	**amount:**
Stacking gel:	
Acrylamide 40%	1.3 ml
ddH_2O	6.5 ml
4-fold upper TRIS buffer	2.5 ml
APS	30 µl
TEMED	30 µl
∑=	**10.3 ml**

Table 7: Pipetting scheme for home-made 16.5% TRIS-trycineSchägger gels

substance:	**amount:**	
Resolving gel:	16.5%	10%
Acrylamide 49.5%	3.5 ml	1.5 ml
ddH_2O	-	3.5 ml
Gel buffer	3.5 ml	2.5 ml
32% glycerol (v/v)	3.5 ml	-
APS	30 µl	30 µl
TEMED	4 µl	4 µl
for one gel	**5 ml**	**2.5 ml**

substance:	**amount:**
Stacking gel:	
Acrylamide 49.5%	0.5 ml
ddH_2O	4.2 ml
Gel buffer	1.55 ml
APS	25 µl
TEMED	5 µl
for one gel	**2 ml**

Gels were mixed at room temperature using a benchtop mixer (Vortex Genie 2, Scientific Industries). In the case of Schägger gels, the 16.5% and 10% solutions were prepared at the same

time, and the 5 ml of the 16.5% solution were carefully overlaid with 2.5 ml of the 10% solution. 0.5 ml of isopropanol (Sigma) were overlaid during the polymerization of the gels in order to prevent the upper end of the gel to dry out. Gels were loaded at room temperature and ran initially at 90 V. After the first proteins entered the resolving gel, voltage was increased to 120 V. TRIS-Glycine buffer supplemented with 0.1% SDS was used as the running buffer. All proteins lysates were mixed with 4-fold protein sample buffer and incubated for 5 minutes at 95 °C before being loaded onto the gels. In order to run the gels under reducing conditions, 10% of ß-mercapto-ethanol were added to the 4-fold protein sample buffer.

3.3.6 Coomassie and silver staining of polyacrylamide gels

Table 8: Coomassie stain

Staining solution	50% (v/v) isopropanol, 10% (v/v) acetic acid, 1% (v/v) Coomassie blue brilliant G, in ddH_2O
Destaining solution	5% (v/v) isopropanol, 7% (v/v) acetic acid, in dH_2O
Benchtop shaker	Duomax 1030, Heidolph

SDS-gels were washed several times with ddH_2O and incubated with the staining solution for 1 h at room temperature on a benchtop shaker. Afterwards, the staining solution was discarded and the gel was incubated for multiple rounds in the destaining solution, until the protein bands were easily distinguishable from the background.

Table 9: Silver stain

Fixing solution	40% (v/v) ethanol, 10% (v/v) acetic acid, in ddH_2O
Washing solution	30% (v/v) ethanol, in ddH_2O
Thiosulfate solution	0.02% (w/v) sodium thiosulfate, in ddH_2O
Silver nitrate solution	0.2% (w/v) silver nitrate, in ddH_2O
Developing solution	3% (w/v) Na_2CO_3, 0.05% H_2CO, in ddH_2O
Stop solution	0.5% glycine
Benchtop shaker	Duomax 1030, Heidolph

SDS-gels were subjected to silver staining if the expected band pattern was not visible by Coomassie staining, as silver staining is more sensitive. All steps were carried out at room temperature. Gels were incubated with the fixing solution for 2 h on a benchtop shaker. Gels were washed three times with ddH2O (20 minutes each), treated for 1 minute with the thiosulfate solution, washed again three times with ddH2O, treated for 1 h with the silver nitrate solution. After washing for three times with ddH2O, they were developed using the developing solution until the protein bands were easily distinguishable from the background. The gels were then washed for 1 minute with ddH2O, treated with the stop solution for 5 minutes and finally washed for 30 minutes with ddH2O.

3.3.7 Western Blotting

Table 10: Western Blot

PBS-Tween	140 mM NaCl, 10mM Na_2HPO_4*$2H_2O$, 1.4 mM KH_2PO_4, 2.7 mM KCL, 1% Tween-20 (Merck), in dH_2O
i-Block	Tropix, prepared according to manufacturer's protocol
10-fold transfer buffer	0.24 M TRIS, 0.2 M glycine (Roth), in dH_2O
Mini-Protean Blotting System	Biorad
Power pack: Power Pac 300	Biorad
Filterpaper Whatman	Schleicher&Schuell
PVDF membrane	Millipore
ECL-System	GE Healthcare
X-ray film	Super RX, Fujifilm
Developing solution	Developer 153, AGFA
Fixing solution	Rapid Fixer G354, AGFA
Developer	Cawomat 2000 IR, Cawo
Chemoluminescence camera and software	LAS-4000 Fujifilm
Imaging processing software	Multi Gauge, Fujifilm; Adobe Photoshop
Primary antibodies:	in PBS-Tween supplemented with 5% BSA
EPHA4-4C8H5	anti-EPHA4-receptor, Invitrogen, clone: 4C8H5,1:1000, mouse
EPHA4-SEK	anti-EPHA4-receptor, BD Transduction Lab., 1:1000, mouse
EPHA4-AF641	anti-EPHA4-receptor, R&D Systems, 1:1000, mouse
MDGA1	anti-MDGA1, Santa Cruz, clone: G15, 1:1000, goat
CNTN2	anti-CNTN2, R&D Systems, clone: AF4439, 1:1000, goat
CHL1	anti-CHL1, R&D Systems, clone: AF2147, 1:1000, goat
ALPL2	anti-APLP2, Calbiochem, clone: 2D11, 1:5000
APP	anti-APP, Millipore, clone: 22C11, 1:1000, mouse
BACE1	anti-BACE1, Robert Vassar (Northwestern University, Chicago, USA), clone: 3D5, 1:2000
Actin	anti-Actin, Sigma, clone: A5316, 1:5000, mouse
Tubulin	Anti-Tubulin, Sigma, clone: B512, 1:2000, mouse
Secondary antibodies:	in PBS-Tween supplemented with 5% BSA
α-mouse-HRP	anti-mouse IgG, Promega, 1:10000, goat

α-rabbit-HRP	anti-rabbit IgG, Promega, 1:10000, goat
α-goat-HRP	anti-goat IgG, Santa Cruz, 1:5000, donkey

After proteins were separated by SDS-PAGE, they were transferred onto PVDF membranes for subsequent immunostaining with antibodies. All steps were carried out at room temperature. The PVDF membranes were incubated for 30 seconds in isopropanol to increase their protein binding capacity and subsequently washed in dH_2O. The transfer sandwich was then built in the following manner: anode plate, sponge, 2 layers of filter paper, PVDF membrane, SDS gel, 2 layers of filter paper, sponge, cathode plate. The sandwich was placed into the transfer chamber, which was filled up with transfer buffer. Finally a cooling element was added to avoid the build-up of excessive heat during transfer. Transfer was performed at 400 mA for 1 h. Afterwards, the PVDF membrane was incubated in i-Block for 30 minutes, washed twice with PBS-Tween, and was incubated twice for 5 minutes on benchtop shaker in PBS-Tween. The primary antibody solution was added and incubated over night at 4 °C on a benchtop shaker. On the next morning, the membrane was washed twice with PBS-Tween, and was incubated twice for 5 minutes on benchtop shaker in PBS-Tween. Secondary antibody solution was added for 45 minutes at room temperature and the membrane was washed four times for 5 minutes (all at room temperature). Finally 1 ml of the ECL developing solution was added to the membrane for 3 minutes. The membrane was transferred to the dark room, where X-ray films were exposed to the membrane and developed according to the manufacturer's protocol. The developed membranes were quantified using the LAS-4000 (GE Healthcare) imaging system.

3.3.8 Immunofluorescence

Table 11: Immunofluorescence

Fixation medium	4% (w/v) paraformaldehyde, 5% sucrose (both), in ddH_2O
Permeabilization buffer	0.3% (v/v) Triton-X100 (Sigma) in PBS
Blocking medium 1	5% normal goat serum (Gibco) in PBS
Antibody medium	2% normal goat serum (Gibco) in PBS
PBS	140 mM NaCl, 10mM $Na_2HPO_4*2H_2O$, 1,4 mM KH_2PO_4, 2,7 mM KCL
Primary antibody	anti-EphA4 (S-20), Santa Cruz Biotechnology, 1:200, rabbit
	anti- β -Tubulin, Sigma (T8535), mouse
Secondary antibody	anti-mouse Alexa-488, Invitrogen, 1:1000, goat
	anti-rabbit Alexa-555, Invitrogen, 1:1000, goat
8-well imaging chambers	15 µ slide, 8 well, Ibidi
Inverted confocal microscope	TCS SP5 II/DM6000 CFS (Leica)
Imaging Software	ImageJ/FIJI, Photoshop 8.0 (Adobe)

For immunofluorescence analysis, 30.000 neurons/well were plated on poly-L-lysine (1:100 in ddH_2O, Gibco) coated Ibidi imaging chambers. All steps except where indicated were carried out at room temperature. The supernatant was carefully sucked off and the cells were incubated for 10 minutes in fixation medium, followed by three washes with PBS (5 minute incubation period each time). Afterwards cells were permeabilized by treating them 5 minutes with Permeabilization buffer, followed by three washes with PBS (5 minute incubation period each time). Cells were treated for 1 h with blocking medium. The primary antibody was diluted in antibody medium and the neurons were incubated in this antibody solution at 4 °C over night, followed by three washes with PBS (5 minute incubation period each time). Afterwards, the secondary antibody was diluted in the antibody medium and the neurons were incubated for 1 h at room temperature, followed by three washes with PBS (5 minute incubation period each time). Images were acquired on an inverted confocal microscope (Leica). Contrast and brightness were adjusted using the open-source software ImageJ and the final pictures were assembled in Photoshop (Adobe).

3.4 Sample preparation methods for mass spectrometry

3.4.1 Filter-aided sample preparation (FASP)

Table 12: FASP

SDT-lysis buffer	2%(w/v) SDS, 100mM TRIS/HCl pH 7.6, 0.1M DTT, in ddH_2O
UA buffer	8 M urea (Sigma, U5128) in 0.1 M Tris/HCl pH 8.5, in ddH_2O
UB buffer	8 M urea (Sigma, U5128) in 0.1 M Tris/HCl pH 8.0, in ddH_2O
UC buffer	2 M urea, 25 mM Tris/HCl pH 8.0, in ddH_2O
IAA solution	0.05 M iodoacetamide in UA buffer
Ammonium bicarbonate	0.05M NH_4HCO_3, in ddH_2O
Trypsin	Promega
Lys-C	Promega
Filter units	Vivacon 500, 0.5 ml, 30.000 NMWCO, Sartorius Stedim

Filter aided sample preparation was adopted from Wisniewski et al. (Wisniewski et al., 2009b). All steps were carried out at room temperature. Protein lysates in SDT buffer were subjected to Amicon centrifugation units. A maximum of 200 µg protein was subjected to each filter unit in order to avoid clogging of the filter membrane. In addition UA buffer was always added in an excess amount (10-fold volume) to the SDT buffer before the filters were loaded. This was done in order to avoid damaging the filter due to the relatively high SDS concentration of the SDT buffer. Filter units were centrifuged for 10 minutes at 12.000 rpm in a benchtop centrifuge. 200

µl of UA buffer were added, followed by centrifugation. 100 µl of the iodoacetamide solution was then added to the filter units, which were then incubate for 20 minutes in complete darkness. This step ensured the alkylation of all reduced cysteines, in order to avoid intra- and interpetide disulfide bond formation. Iodoacetamide was then removed by centrifugation and the filter units were washed three times with UA buffer, followed by three washes with ammonium bicarbonate. 40 µl of trypsin in ammonium bicarbonate were added (enzyme to protein ratio 1:100), and the filter units were gently rocked back and forth for 1 minute. Afterwards, filter units were placed in a wet chamber and incubated for 16 h at 37 °C in an incubator (Heraeus). Filter units were then transferred to new collection tubes, and the peptides were collected by centrifugation. Another centrifugation step with 40 µl of MilliQ water was used to collect any remaining peptides.

If digestion was carried out with Lys-C instead of trypsin, the protocol was adjusted in the following manner: After the removal of iodoacetamide, filter units were washed three times with UB buffer, followed by three washes with UC buffer. 40 µl of Lys-C in UC buffer (enzyme to protein ratio 1:50), and the filter units were gently rocked back and forth for 1 minute and subsequently incubated for 16 hours at room temperature. The rest of the protocol was carried out as described above.

3.4.2 In-solution digest

The in-solution digest was performed for small sample amounts (below 5 µg of total protein).

Table 13: In-solution digest

Denaturation buffer	6 M urea (Sigma, U5128) in 10 mM HEPES pH 8.0, in ddH_2O
Ammonium bicarbonate	0.05M NH_4HCO_3, in ddH_2O
Reduction buffer	10 mM dithiothreitol in 0.05 M ammonium bicarbonate
Alkylation buffer	55 mM iodoacetamide in 0.05 M ammonium bicarbonate
Lys-C solution	0.5 µg/µL Lys-C (Promega) in 0.05 M ABC
Trypsin	Promega
Lys-C	Promega
Trifluoroacetic acid	Sigma

All steps were performed at room temperature. Proteins were solubilized in denaturation buffer (sample to buffer ratio 1:10) in low protein binding tubes (Eppendorf). 1 µl of reduction buffer was added for 10 µl of digestion buffer, followed by an incubation for 30 minutes. Then, 1 µl of iodoacetamide solution for 10 µl of digestion buffer was added, followed by an incubation for 20 minutes. Lys-C solution (enzyme to protein ratio 1:50) was added and incubated for 4 h. The sample was the diluted 4-fold with ammonium bicarbonate, trypsin solution was added (enzyme to protein ratio 1:50) and incubated for 16 h. The digestion reaction was stopped using 100% trifluoroacetic acid (as a general rule of thumb, 1 µl of trifluoroacetic acid brings the pH to 2-2.5 if an initial sample volume of 50 µl (~5 µg of protein) is used).

3.4.3 Peptide concentration measurements

After digesting proteins using the FASP method, the peptide yield was determined using UV spectroscopy. The peptide yield was usually around 50% of the total protein input. A small aliquot of the peptides were dissolved in PBS in order to reach a final concentration of 0.2-2 mg/ml. The absorbance of tryptophan at 280 nm was measured on a cuvette spectrophotometer to estimate the peptide concentration. A BSA standard (Uptima) was used to derive the absolute concentration by setting up a linear calibration curve.

3.4.4 Assembly of homemade STAGE-Tips

Homemade STAGE-Tips (STAGE is an acronym for "Stop And Go Extraction") were used for the concentration, desalting, clean-up and offline fractionation of peptides in a pipet-based format. An excellent introduction on how to use STAGE Tips has been published by Juri Rappsilber (Rappsilber et al., 2007). Briefly, STAGE-Tips are pipet tips (typical size: 100 µl) that have been equipped with a disk-shaped piece of C18 (octadecyl carbon chain bonded to porous silica) embedded into a PTFE (polytetrafluoroethylene) matrix. Peptides bind to the hydrophobic C18 material if passed through the pipet tip in an aqueous solution and can be retrieved using non-polar organic solvents, such as acetonitrile. This allows the efficient clean-up of peptides, buffer exchange or desalting. The C18 material was stamped out from larger disks (Empore) by the use of a blunt Hamilton syringe needle and inserted into the pipet tips using an appropriate plunger. For desalting and clean-up of peptides, two C18 disk were stacked on top of each other, whereas 6 ASR disks were used for the peptide fractionation by strong anion exchange (see below). Sample and buffer were passed through the STAGE Tips either by using the single-use syringe of a multidispenser pipet (Eppendorf) or by centrifuging the STAGE Tips in 1.5 ml tubes at 2000-4000 rpm in a benchtop centrifuge. STAGE Tips were fixed in the 1.5 ml tubes by passing them through a small hole that had been introduced into the tube lid with a surgical scalpel.

3.4.5 STAGE-Tip based desalting and clean-up

All samples were subjected to a STAGE-Tip based cleanup before being subjected to LC-MS/MS. C18 STAGE-Tips were conditioned with 100 µl methanol (HPLC grade, SIGMA), washed twice with 100 µl 0.5% acetic acid in HPLC grade H_2O (both SIGMA) and eluted into 0.5 ml tubes with 20 µl of a buffer containing 0.5 % formic acid and 60% acetonitrile (HPLC grade, Sigma) in HPLC grade water. Alternatively, peptides were stored on C18 STAGE-Tips in washing buffer at -20°C.

3.4.6 STAGE-Tip based strong anion exchange (SAX) of peptides

STAGE-Tip based offline fractionation of peptides with SAX was adopted from Geiger et al. (Geiger et al., 2011).

Table 14: STAGE-Tip based SAX fractionation of peptides

C18 STAGE-Tip	Homemade STAGE-Tip containing 2 discs of C18 material (3M)

SAX STAGE-Tip (1 per fraction)	Homemade STAGE-Tip containing 6 discs of Anion-SR (ASR) material (3M). Anion-SR is a poly-styrenedivinylbenzene-copolymer that is used for anion exchange.
Methanol	HPLC grade, SIGMA
Washing buffer	0.5% acetic acid in HPLC grade H_2O (both SIGMA)
Elution buffer	0.5 % formic acid and 60% acetonitrile in HPLC grade water (all Sigma)
Britton and Robinson (B&R) buffer	5-fold stock solution: 0.1 M acetic acid (Sigma), 0.1 M phosphoric acid (Sigma) and 0.1 M boric acid (Serva) in MilliQ H_2O, titrated to pH 11, 8, 6, 5, 4, 3 with NaOH. Before use, dilute buffers 5-fold and ad 5 M NaCl to buffer pH3 for a final concentration of 0.25 M
NaOH	1 M in MilliQ H_2O, Merck

C18 STAGE-Tips were conditioned with 100 µl of methanol, 100 µl of elution buffer and 100 µl of MilliQ H_2O. SAX STAGE-Tips were conditioned with 100 µl methanol, 100 µ NaOH and 100 µl of B&R buffer pH 11. For each pH fraction and sample, one C18 STAGE-Tip was prepared. Up to 50 µg of peptides were diluted in B&R buffer pH 11 and titrated with 1 M NaOH to a pH of ~11.5. Peptides were loaded onto the SAX STAGE-Tip, which was placed inside a C18 STAGE-Tip. Peptides were directly eluted onto C18 STAGE Tips using B&R buffer pH 11, pH 8, pH 6, pH 5, pH 4 and pH 3. Each buffer was used for two rounds of elution, and the C18 STAGE-Tip was swapped for a new one after each pH step. The C18 STAGE-Tips (containing the individual peptide fractions) were then washed once with 100 µl washing buffer and peptides were retrieved into 0.5 ml tubes using 20 µl of the elution buffer. Alternatively, peptides were stored on C18 STAGE-Tips in washing buffer at -20°C.

3.4.7 Preparation of peptides before injection into the LC autosampler

After elution from STAGE-Tips, peptides were dried by in a speed vac (Scanvac) for 30 minutes at room temperature. The dried peptides were solubilized in 10 µl of HPLC grade water containing 0.1 % formic acid (Fluka analytical, Sigma), sonicated for 5 minutes in a sonication bath (Sonorex, Bandelin) and pipetted into the 96 well plates of the LC autosampler (Thermo Fisher Scientific).

3.5 Mass spectrometry and high performance liquid chromatography

3.5.1 High performance liquid chromatography (HPLC)

All experiments were either carried out on an easy nLC II (Proxeon) or easy nLC 1000 (Thermo Fisher Scientific) nano-HPLC setup.

A one-column setup was used with the easy nLC II, together with in-house-packed 15 cm columns. The empty nano-capillary-emitter columns (75 µm inner diameter) were purchased from New Objective (FS360-75-8-N-S-C15) and filled with C18 beads with a 2.4 µM diameter (ReproSil-Pur 120 C18-AQ, Dr. Maisch GmbH). Briefly, beads were washed three times with HPLC grade methanol (Sigma) and finally sonicated in methanol for 5 minutes. The bead slurry was transferred into a 1.5 ml glass vial and equipped with a small, PTFE coated magnetic stir bar. The glass vial was then placed into the packing unit (SP-400 packing unit, coupled to the CE-005 high pressure adapter kit, Nanobaume). The packing unit was placed on a heated magnetic stirrer (Heidolph) set to 40 °C and 650 rpm. The actual packaging procedure was performed using technical nitrogen and pressures of up to 45 bar. Columns were allowed to air dry after packaging and stored until used. The columns were connected to the easy nLC II systems and equilibrated for 20 minutes with a constant flow rate of 0.4 µl/minute at 95% acetonitrile (HPLC grade, Sigma). The actual sample run was performed at 20 °C on a Thermo Fisher Scientific flex ion source, using a maximum pressure of 280 bar.

In terms of the easy nLC 1000, a two-column setup was used. The pre-column (Acclaim Pep Map 100, 75 µm x 2 cm, nano Viper C18, 3 µm, Thermo Fisher Scientific), waste line and the analytical column (Pep Map RSLC, C18, 2 µm, 75 µm x 50 cm, Thermo Fisher Scientific) were interconnected using a three way mixing tee. The analytical column was equilibrated as described above. The actual sample run was performed at 50 °C at a maximum pressure of 800 bar on a Thermo Fisher Scientific Easy Spray ion source.

HPLC runs where performed using bi- or trilinear gradients. The aqueous solvent (solvent A) always consisted of HPLC grade 0.1% formic acid in water, whereas the organic solvent was pure HPLC grade acetonitrile (solvent B) (both solvents purchased from Sigma).

A bilinear gradient was used for measurements on the easy nLC II / LTQ Velos Orbitrap Pro setup: The column was equilibrated with at least ten column volumes solvent A, followed by loading of the sample a maximum pressure of 280 bar (in solvent A). The bilinear gradient consisted of linear increase in solvent B from 8-25% in the first 145 minutes, and 25-45% in the following 82 minutes at a flow rate of 0.4 µl/minute. At the end of the gradient, the column was washed with at least 10 column volumes of 95% solvent B.

A trilinear gradient was used for measurements on the easy nLC 1000 / Q-Exactive. The layout of the gradient was provided by Dr. Nagarjuna Nagaraj (Max Planck Institute of Biochemistry, Martinsried). The column was equilibrated with at least ten column volumes of solvent A, followed by loading of the sample a maximum pressure of 800 bar (in solvent A). The trilinear gradient consisted of the following linear increases in solvent B: 5-25% 175 minutes, 25-35% 45 minutes, 35-60% 20 minutes. At the end of the gradient, the column was washed with at least 10 column volumes of 95% solvent B.

3.5.2 Mass spectrometry measurements on the LTQ Velos Orbitrap Pro

The LTQ Velos Orbitrap is a hybrid ion trap mass spectrometer from Thermo Fisher Scientific, featuring an Orbitrap and a dual-pressure linear ion trap. In general, MS spectra were recorded in the orbitrap, whereas MS/MS spectra were recorded in the linear ion trap. MS spectra were acquired using a data-dependent top 14 method at a resolution of 60.000. The automatic gain control target value was set to 1.000.000. Top 14 implies that the fourteen most intense ions detected during the MS scan in the orbitrap were subsequently isolated, fragmented and analyzed in the linear ion trap (MS/MS spectra acquisition). The fragmentation method used was collision-induced dissociation fragmentation (set to 35%), and the isolation width for the precursor ion was set to 2 Da (wideband activation was applied). In order to avoid the unnecessary fragmentation of already fragmented precursor ions, a dynamic exclusion list was enabled. Precursor ions that had been fragmented in the past 50 seconds were thus not reselected for MS/MS fragmentation, if their mass window was within 1.5 Da of the detected mass. The automatic gain control target value for MS/MS acquisition was set to 10.000. Singly charged molecules were not selected for fragmentation, as they usually do not represent peptides, but common contaminants (derived from the tubing of the LC system, impurities during sample preparation, ambient air, etc.). In addition, the monoisotopic precursor selection was enabled, thus subjecting only those ions to fragmentation, where the isotopic pattern had the typical pattern of a peptide and therefore allowing to deduce the charge state of the measured m/z (as explained in 1.4.2).

3.5.3 Mass spectrometry measurements on the Q-Exactive

The Q-Exactive is an orbitrap only benchtop mass spectrometer from Thermo Fisher Scientific. This implicates that MS and MS/MS spectra are recorded in the orbitrap mass analyzer, whereas a linear quadrupole serves as a mass filter. For the work presented here, a top 10 method at a resolution of 70.000 at the MS level was used. The automatic gain control target was set to 3.000.000 and a maximum injection time of 50 ms was allowed. The MS/MS spectra were recorded at a resolution of 17.500 with the automatic gain control target set to 100.000 and a maximum injection time of 50 ms. Precursor selection was done in a mass window of 2.0 m/z. And the normalized collisional energy for the higher-energy C-trap dissociation fragmentation was set to 25. A dynamic exclusion list with a time window of 40 seconds was used, singly charged molecules were not selected for fragmentation, and the monoisotopic precursor selection was enabled. The underfill ratio (minimum percentage of the estimated target value at maximum fill time) was set to 0.1%.

3.6 Analysis of mass spectrometry data

3.6.1 Search engine and quantitation

The freely available MaxQuant software (version 1.3.0.5, www.maxquant.org) and the implemented Andromeda search engine were used for matching of the data against the UniProt database and SILAC and label-free quantitation. The following settings were chosen for the MaxQuant software environment: Oxidation of methionines and N-terminal acetylation were set as variable modifications. Mass deviation was set to 20 ppm for the first and 6 ppm for the main search. The maximum number of peptide modifications was set to 5, the maximum number of missed cleavages was set to 2. Peptide and site false discovery rate were set to 0.1. The search for co-fragmented peptides in the MS/MS spectra was enabled ("second peptides" option).

3.6.2 Statistical evaluation of the data

Statistical evaluation of the data was performed with the freely available Perseus statistics software (version 1.2.0.17, www.maxquant.org) and Microsoft Excel as described in the results section. For the false discovery rate based multiple hypothesis testing, the default parameters of Perseus were applied.

4 Results

4.1 Deep coverage of the membrane proteome by mass spectrometry

4.1.1 Efficient digestion of membrane proteins

All known BACE1 substrates are integral membrane proteins and their quantity is expected to change within the membrane after BACE1 overexpression or inhibition/knockout, as it has been shown in vivo for type III NRG1 (Willem et al., 2006). As biological membranes can be retrieved from cell lines and tissues with relatively little effort, their qualitative and quantitative analysis by proteomics should in principle allow to monitor for changes in the membrane proteome in the presence or absence of BACE1. This approach should therefore lead to the discovery of putative novel substrates and of associated secondary changes. To investigate the membrane proteome in as much depth as possible, the efficient retrieval and digestion of membrane proteins is a

prerequisite. However, membrane proteins were underrepresented in proteomic datasets in the past, as the efficient retrieval and digestion of these proteins require strong detergents such as SDS (Babu et al., 2012). SDS however dominates mass spectra and the removal of this detergent is necessary before the proteomic analysis. Gel-based sample preparation methods partially solve this issue, as most of the SDS is lost in the workflow, but the gel reduces peptide recovery and therefore limits the proteomic coverage.

In 2009, a novel sample preparation method known as Filter Aided Sample Preparation (FASP) was introduced to circumvent these issues (Wisniewski et al., 2009b). FASP makes use of a filter device, that efficiently retains denatured proteins but allows the retrieval of small peptides. Proteins are digested using SDS and captured on the filter device. This is followed by several washes with urea that efficiently removes the SDS from retained proteins. Alkylation of cysteine-residues and the enzymatic digestion into peptides amenable for mass spectrometry are than carried out directly on the filter unit. Finally, the obtained peptides can be retrieved from the filter unit by centrifugation. The nominal molecular weight cut off (NMWCO, 10-30 kDa) of the filter units is small enough to retain denatured proteins, but large enough to allow the passage of e.g. tryptic peptides. It must be noted that even proteins smaller than the given NMWCO are retained, as their stokes radii increase upon denaturation.

In order to test the FASP protocol, the membrane pellet of a wild type mouse liver was split into four equal aliquots (~200 µg of total protein). Each aliquot was solubilized in 2% SDS subjected to the FASP protocol using a filter unit with a 30 kDa NMWCO and trypsin for digestion of the proteins. The FASP protocol was then stopped at different stages for the individual aliquots in order to monitor the efficient processing of the proteins on the filter unit. The input (SDS lysate), the SDS-depleted retenate (SDS lysate on the filter unit after several washes of urea), the tryptic digest (material on the filter unit after digestion) and the final eluate (peptides eluted from the filter unit by centrifugation after digestion) were then loaded onto a 16.5% Schägger gel and stained with Coomassie blue and silver nitrate (Figure 5). Proteins down to a molecular weight of 5 kDa where detectable in the input (before loading onto the filter) and SDS-depleted retenate (retrieved by centrifugation of the upside-down oriented filter unit) in a qualitative and quantitatively similar manner. This shows that even small proteins are retained efficiently by the filter unit, even after several washings with urea. The tryptic digest (obtained by centrifugation of the upside-down oriented filter unit after digestion of the proteins with trypsin) did not show any remaining proteins, but a smear of protein fragments and larger peptides between the 4 kDa and 6 kDa reference proteins of the molecular weight marker. This demonstrated the efficient digestion of proteins on the filter unit.

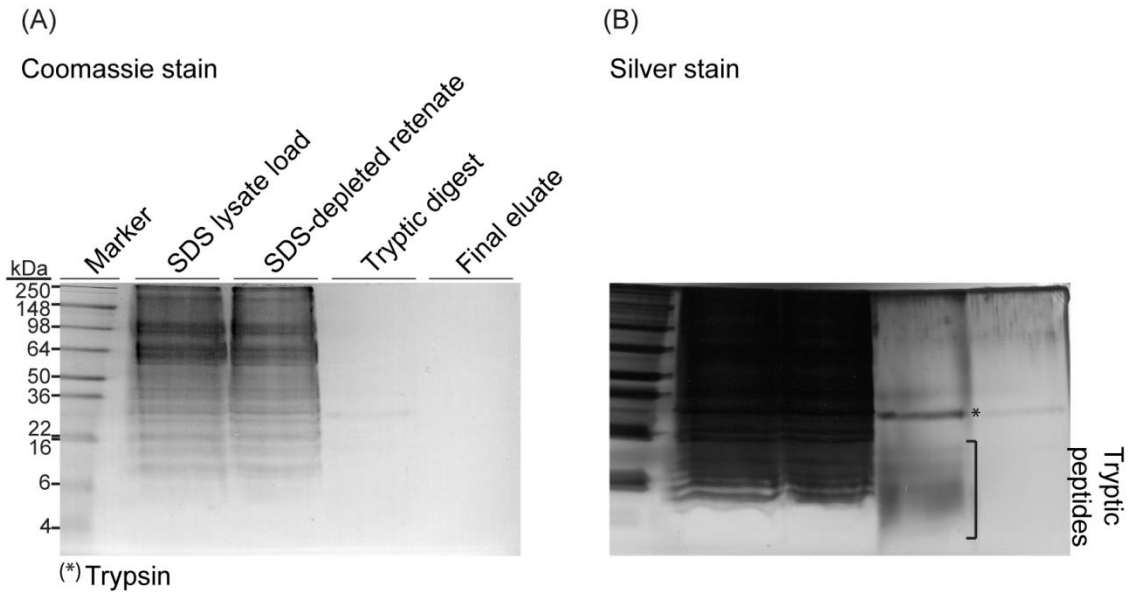

Figure 5. Filter aided sample preparation (FASP) for the effcient digestion of membrane proteins. The efficient on-filter digestion of mouse liver membrane pellets (200 µg of protein) solubilized in SDS is shown. Proteins or peptides were loaded onto a 16.5% Schägger gel and subjected to SDS-PAGE. **A)** shows the Coomassie staining of the gel, whereas **B)** shows the same gel with the more sensitive silver nitrate staining. SDS lysate load: This lane represents membrane proteins lysed in 2% SDS and thus the input for the FASP protocol. SDS-depleted retenate: SDS lysate on the filter unit that had been subjected to several washes with 8 M urea. Tryptic digest: SDS-free proteins that were digested by trypsin over night. Final eluate: Eluate retrieved from the filter unit by centrifugation after digestion with trypsin. The average tryptic peptide is 9 amino acids long and too small to be visualized on a Schägger gel. This is why only larger tryptic peptides are observed in the tryptic digest, that do not pass through the filter unit in the final eluate. * trypsin: full length trypsin is seen in the tryptic digest. This is due to the fact that the porcine trypsin used for these experiments is chemically modified by reductive methylation, which renders it resistant to autocatalytic proteolytic digestion. Trypsin is also seen in trace amount in the final eluate, as it has a molecular weight of 23 kDa and is not denatured, thus being small enough to pass the filter unit partially.

4.1.2 Comparison of different membrane preparation protocols

In order to enrich effectively for integral membrane proteins, membranes have to be isolated from the tissue of interest and biochemically purified from contaminating proteins stemming from the diverse cellular compartments. In addition, an efficient removal of peripheral membrane proteins, that are unlikely to be BACE1 substrates, is beneficial. However, as the number of purification steps increases the total yield of the protein fraction of interest also decreases, as cellular fractionation and purification is not perfectly specific. Two different membrane preparation protocols were compared against each other in terms of effectiveness of purifying integral membrane proteins. In addition, a PBS soluble preparation was carried out, in order to obtain a reference of how strong integral membrane proteins were enriched by the membrane preparation protocols. A schematic overview of the membrane protocols that were compared to each other is shown in Figure 6.

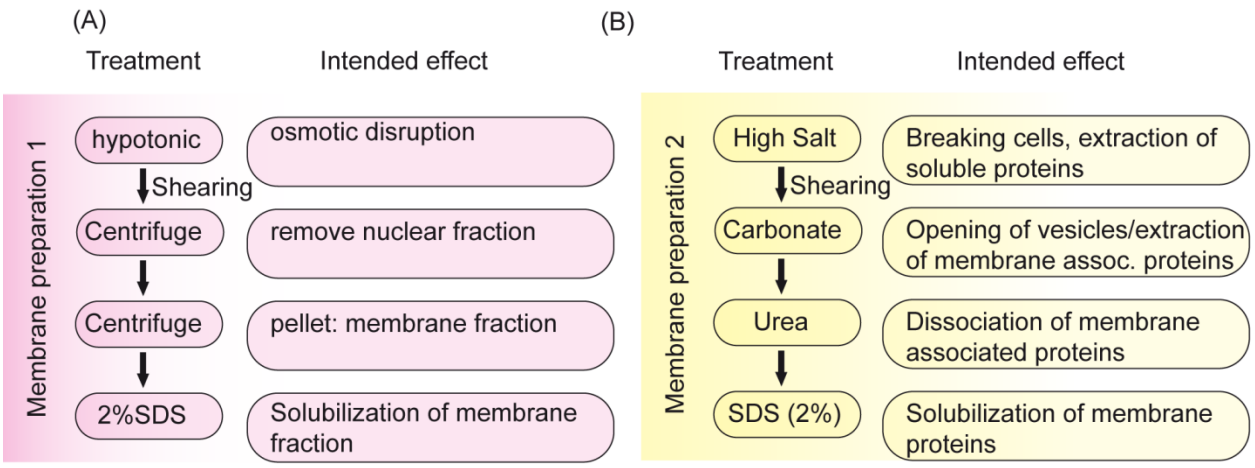

Figure 6. Schematic workflow of two membrane preparation protocols for the enrichment of integral membrane proteins. A) A simple and straightforward protocol, that is based on two centrifugation steps. In the first step, the nuclear fraction is removed by centrifugation. In the second step, the remaining post-nuclear fraction is then centrifuged to pellet the membrane fraction. Cells are initially broken up using a hypotonic buffer and shear stress induced by forcing the sample through a narrow syringe needle. **B)** A more sophisticated protocol that uses several washes with carbonate and urea to extract and remove peripheral membrane proteins from the membrane pellet. Cells are initially broken up by placing them in a hypertonic environment and subjecting them to shear stress with a tissue homogenizer.

Adult mouse brains were subjected to membrane preparation 1, membrane preparation 2 or solubilized in PBS and analyzed on the LTQ Velos Orbitrap mass spectrometer using 4 h gradients and a 15 cm column. The identified proteins were then annotated using the Gene Ontology (GO) database, that represents a bioinformatic initiative to standardize the descriptions of protein function and cellular localization (www.geneontology.org). Proteins were classified according to a preselected number of GO terms, amongst them the term “intrinsic to membrane” which is defined as “located in a membrane such that some covalently attached portion of the gene product, for example part of a peptide sequence or some other covalently attached group such as a GPI anchor, spans or is embedded in one or both leaflets of the membrane”. This specific term was chosen as it described the known properties of a BACE1 substrate. Membrane preparation 2 enriched most selectively for proteins tagged with the GO term “intrinsic to membrane” (~50%), whereas the enrichment for the membrane preparation 1 was only around ~35%. In contrast, only ~10% of integral membrane proteins were found in the PBS soluble fraction. Despite a more stringent purification process when compared to membrane preparation 1, the membrane preparation 2 yielded enough material for the LC-MS/MS workflow and was thus chosen for the analysis of the membrane proteome in the following experiments. Figure 7 shows the comparison of the two membrane preparations with regard to the enrichment of proteins with the preselected GO terms.

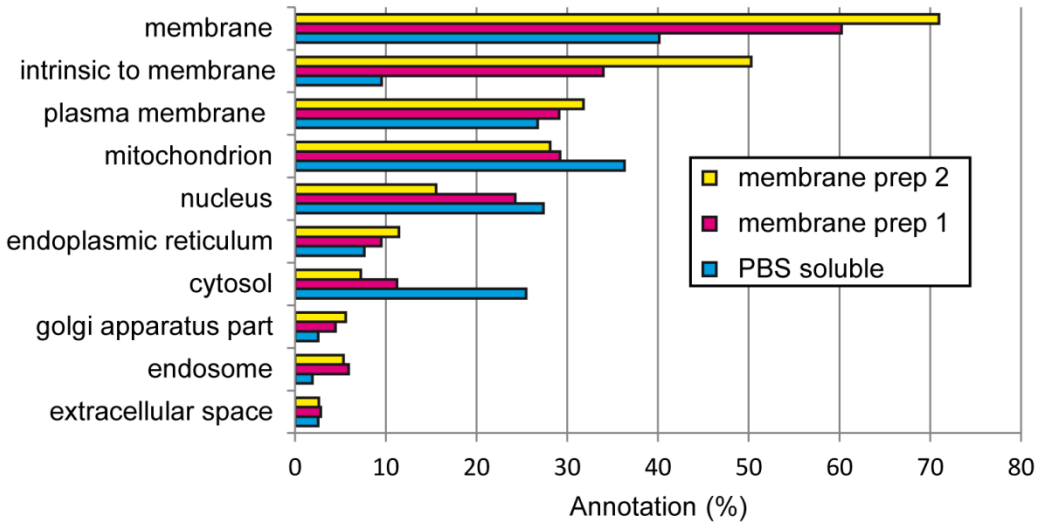

Figure 7. Comparison of membrane preparation protocols in terms of the enrichment for integral membrane proteins. Mouse brains were subjected to two different membrane preparation protocols or solubilized in PBS. The individual preparations were than analyzed by LC-MS/MS. The identified proteins were classified according to the GO database. The percentage of proteins tagged with 10 preselected GO terms is plotted on the x-axis. Prep: preparation.

4.1.3 Fractionation and technical replicates increase the proteomic coverage

In order to increase the proteomic coverage, multiple strategies can be employed during the proteomic workflow. One of them is to decrease the complexity of the sample by fractionation. This avoids the parallel elution of too many peptides at the same during liquid chromatography, which would outreach the detection speed of the mass spectrometer. The downside is that expensive measurement time on the mass spectrometer is increased with every fraction. To investigate if the fractionation of the membrane proteome would increase the number of identified proteins in a justifiable manner, mouse brain membrane preparations were either analyzed in a single run or prefractionated into six fraction using strong anion exchange chromatography (SAX). The fractionation of peptides by SAX in a pipet tip based format is illustrated in Figure 8.

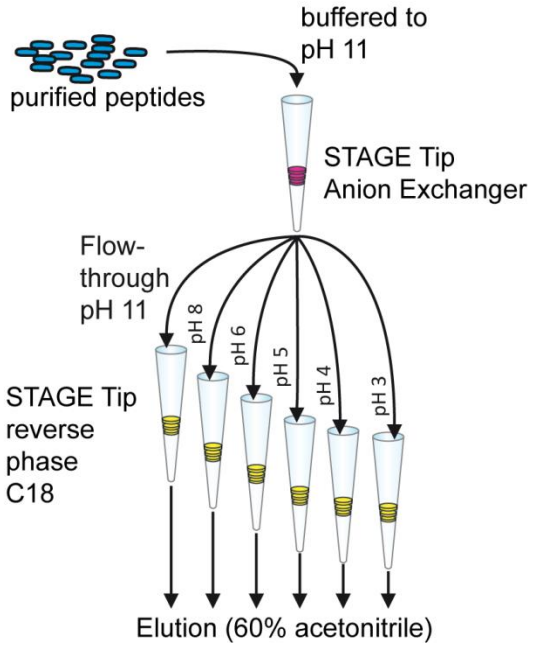

Figure 8. STAGE Tip based SAX fractionation of peptides. The complex peptide mixture is brought to pH 11 and loaded onto a pipet tip containing an anion exchanger embedded in an inert matrix. The individual peptide fractions are eluted using a buffer with decreasing pH. Peptides are collected on pipet tips equipped with hydrophobic C18 discs, desalted and finally eluted with an organic solvent. STAGE Tip: STop And Go Extraction Tip. The STAGE Tip procedure was adopted from Rappsilber et al. (Rappsilber et al., 2007).

In addition, technical replicates increase the number of protein identifications, as low abundance proteins that are close the detection limit of the given instrument may be missed in one but not the next technical replicate. For this reason the sample was run twice under the same settings in order to investigate whether the gain in protein identification could be justified with the increase in measurement time. The samples were run on 15 cm columns using 4 h gradients on the LTQ Velos Orbitrap. Figure 9 summarizes the results of a single run analyses compared to a six fraction SAX analysis and a six fraction SAX analysis with two technical replicates.

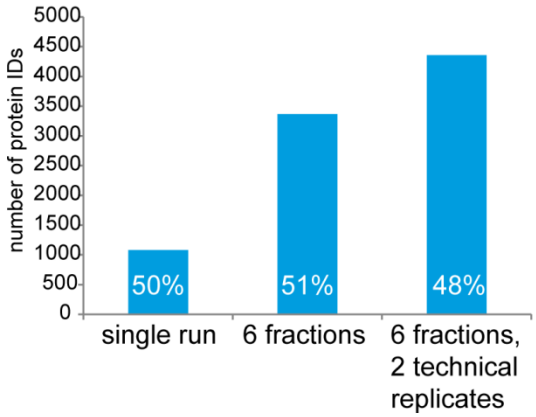

Figure 9. Comparison of a single run analysis with SAX fractionation and SAX fractionation with technical replicates. Mouse brain membrane preparations were either analyzed in a single run or prefractionated into six fractions using SAX chromatography. Percentages shown in white represent the percentage of annotated proteins with the GO term “intrinsic to membrane”. ID: Protein identification.

In summary, membrane preparation 2 followed by FASP and SAX based peptide fractionation emerged as the preferred workflow for the detailed investigation of the membrane proteome. Technical replicates increased the protein identifications by ~20% and were therefore included in the following experiments.

4.2 Quantitative changes in the membrane proteome upon overexpression of BACE1

The main goal of this work was to elucidate novel BACE1 substrates in vivo. Before analyzing the membrane proteome of mouse brains, a proof of principle study was carried out in HEK-293E cells. The aim of this preliminary study was to investigate whether changes of the membrane proteome induced by the presence or relative absence of BACE1 could be monitored by quantitative mass spectrometry. The term “relative absence” indicates that endogenous BACE1 is expressed in HEK-293E cells, albeit at a very low level and several orders of magnitude lower than in the cells overexpressing BACE1. The conditioned media were analyzed in parallel, as the decrease of a BACE1 substrate in the membrane upon BACE1 overexpression should lead to an increase of the shed ectodomain in the conditioned media, thus validating the results obtained from the membrane fraction. As the expected changes in the membrane fraction were estimated to be rather small (1.2-3 fold, based on previous experiments in our laboratory using antibody dependent techniques such as western blotting or immunofluorescence) SILAC was chosen in order to accurately monitor these changes. SILAC is currently the most accurate form of relative quantification in mass spectrometry, but requires the labeling of the cell lines of interest using stably isotope labeled amino acids (Mann, 2006). Two cell lines were generated, that either stably expressed BACE1 or the empty control vector. Figure 10 shows a western blot that demonstrates the expression levels of BACE1 in the cell lysates of the generated cell lines.

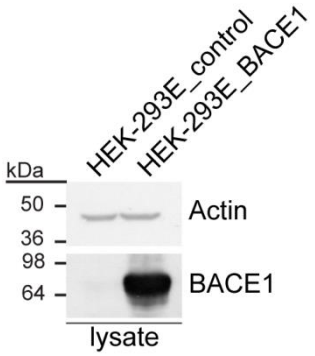

Figure 10. Western blotting analysis of the cell lines stably expressing BACE1 or the empty control vector. HEK-293E_control and HEK-293E_BACE1 cell lines were cultured for several weeks in the appropriate selection medium and then analysed by western blotting using antibodies directed against BACE1 and actin (actin serving as a loading control).

The cells were cultured for 8 passages in either "light" or "heavy" SILAC medium in order to achieve a labeling efficiency greater than 95%. After the last passage, the conditioned media were replaced with serum free medium buffered with HEPES. Serum free medium was chosen as the fetal calf serum protein concentration ranges between 0.3-0.5 mg/ml (Invitrogen), primarily due to the presence of BSA and other highly abundant serum proteins. Serum proteins thus exceed the abundance of the proteins of interest (shed ectodomains) by several orders of magnitude and therefore limit the detection of low abundance proteins by mass spectrometry, as the peptides of the high abundance proteins dominate the mass spectra. After 20 h, the conditioned media were collected, "light" and "heavy" media were mixed and concentrated. The adherent cells were harvested in parallel, washed with PBS and pelleted by centrifugation. "Light" and "heavy" cells were mixed and subjected to membrane preparation 2. The membrane fraction and the concentrated media were than digested by FASP. Afterwards, the digested concentrated media were directly analyzed by LC-MS/MS, whereas the digested membranes were further fractionated by SAX. Two biological replicates with two technical replicates each were carried out for the membrane fraction. No technical replicates were performed for the analysis of the conditioned media, as the total amount of proteins was low. The samples were analyzed on the LTQ Velos Orbitrap using 4 h gradients and a 15 cm column. Figure 11 illustrates the workflow of this experiment.

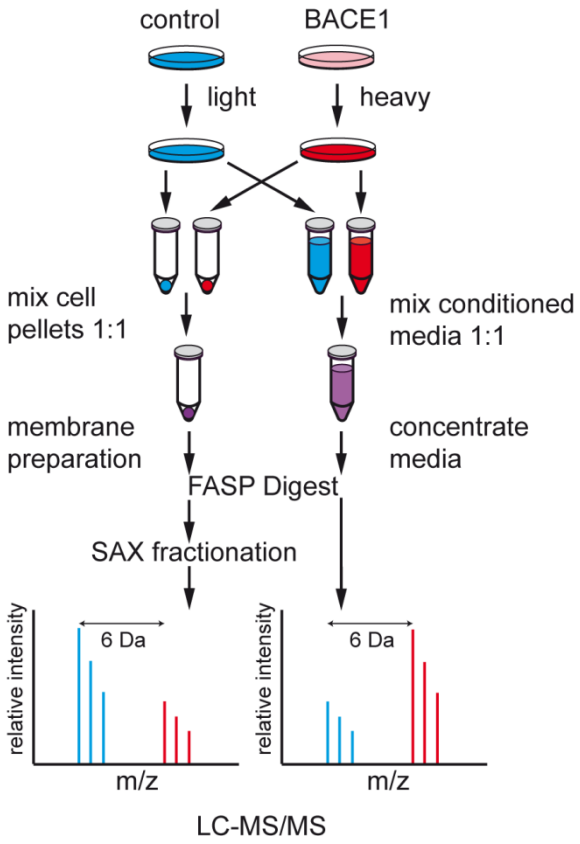

Figure 11. Workflow for the analyis of the membrane fraction and conditioned media upon overexpression of BACE1 in HEK-293E cells. Cells stably expressing BACE1 or an empty control vector were labeled with "heavy" or "light" amino acids (SILAC) respectively. The conditioned media of "heavy" and "light" labeled cells was collected, mixed, concentrated, digested and analyzed by LC-MS/MS. In parallel, "heavy" and "light" cells were harvested, mixed, the membrane fraction was isolated, digested and analyzed by LC-MS/MS. The bottom panels show a schematic of two high resolution MS spectra. Two different peptides are depicted in the plot, the "heavy" peptide in red, the "light" peptide in blue. The difference in peptide mass is 6 Da and is introduced by the incorporated heavy lysine $^{13}C^{15}N$ (see introduction). Both peptides are shown as a series of isotopic peaks, which is the result of the natural abundance of heavy isotopes.The relative abundance of the peptides is reflected by their relative intensity. The "heavy" peptide is twice as abundant as the "light" peptide in the conditioned media, whereas the "light" peptide is twice as abundant as the "heavy" peptide in the membrane fraction.

Only proteins where the "heavy" and matching "light" peptide were found are included in the analysis. In addition, only proteins identified by at least two unique peptides (matching unambiguously to only one protein) that were identified in both biological and both technical replicates were included. Finally, only proteins tagged with the GO term "intrinsic to membrane" were included in the analysis. A total of 789 proteins in the membrane fraction matched these criteria. A total of 80 proteins in the conditioned media were quantifiable accordingly, with the

exception that no technical replicates were performed. Figure 12 shows the qualitative and quantitative outcome of this experiment in a scatter plot.

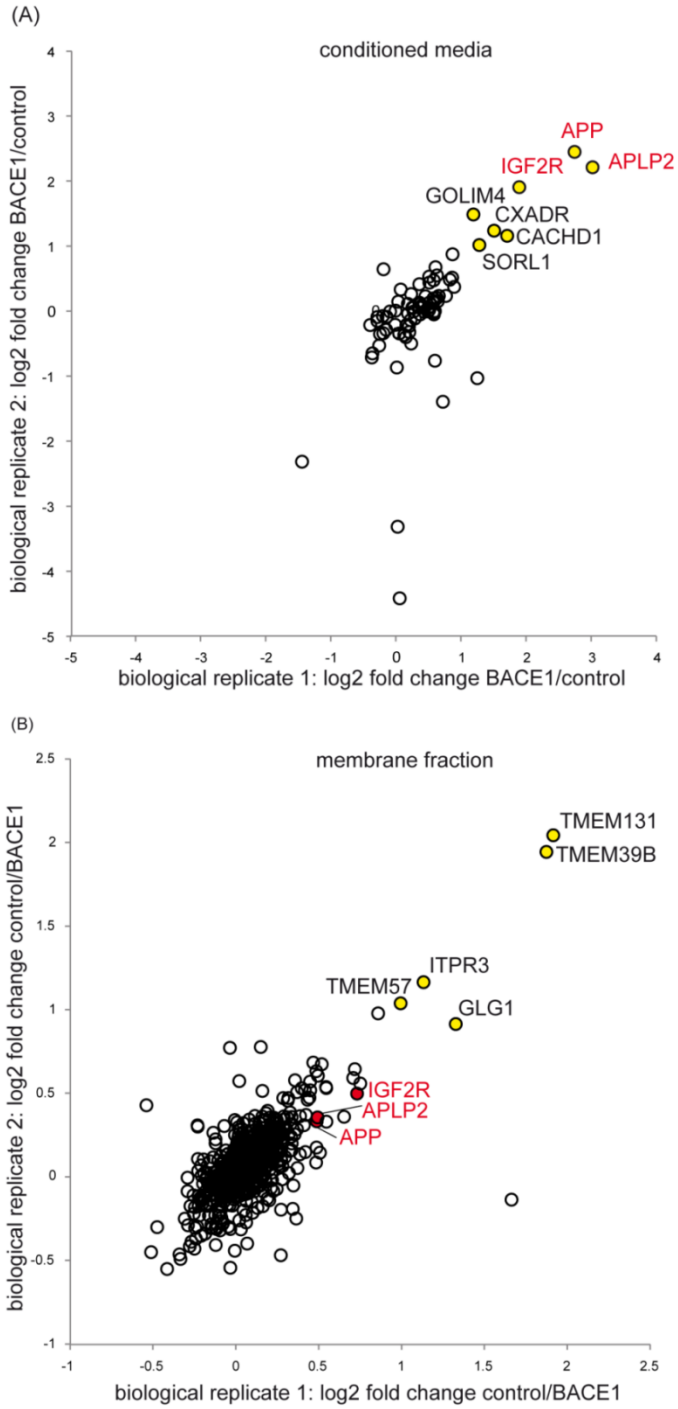

Figure 12. Analysis of the membrane fraction and conditioned media in HEK-293E cells overexpressing BACE1 by LC-MS/MS. Each black circle represents a protein that was quantifiable in each biological replicate. **A)** Conditioned media**:** The scatter plots shows the log2 fold change obtained from the SILAC ratios for each identified protein in the biological replicate 1 and 2. The SILAC ratios are derived by dividing the average relative intensity of the "heavy" peptides in the BACE1 expressing cells by the average relative intensity of the "light" peptides in the control cells for a given protein. Proteins displayed with a yellow circle are enriched at least 2-fold in the conditioned media upon overexpression of BACE1. Gene names in "red" mark previously known BACE1 substrates **B)** Membrane fraction: data are displayed in the same manner as in A), but with an inverted SILAC ratio (light/heavy), in order to show the increase in proteins in the membrane fraction in the relative absence of BACE1. Proteins shown with a yellow circle are enriched at least 2-fold in the membrane fraction of the control cells. The top three proteins that were accumulating in the conditioned media and were also found in the membrane fraction are highlited by a red circle.

The great majority of identified proteins did not change (SILAC ratio close to 1), but a minor fraction of proteins was increasing in the conditioned media and decreasing in the membrane fraction of BACE1 overexpressing cells compared to the control. The previously known BACE1 substrates APP and APLP2 (Amyloid like protein 2) showed the strongest accumulation (APP 6.1-fold; APLP2 6.4 fold) in the conditioned media. In addition, the type I transmembrane protein cation-independent mannose-6-phosphate receptor (IGF2R) showed a strong accumulation (3.7-fold). This was reassuring, as this type I transmembrane protein had been identified as a putative BACE1 substrate in a previous study (Hemming et al., 2009), thus further validating the outcome of this experiment. All three proteins were also detected in the membrane fraction, where they showed a concomitant decrease in the BACE1 overexpressing cells. APP and APLP2 showed a 24% decrease, IGFR2 a 34% decrease (which can also be expressed as a 1.3 and 1.5 fold accumulation in the control cells respectively, see Figure 12). Although not being the proteins with the strongest fold-change in the membrane fraction, these three BACE1 substrates separated nicely from the great majority of the detected proteins. In conclusion, the changes in abundance of BACE1 substrates in the membrane fraction induced by the absence or presence of this protease can be quantified using a SILAC based proteomics workflow. The absence of BACE1 leads to a decrease in ectodomain shedding and a resulting increase in full length proteins in this compartment. A similar workflow should thus be applicable to investigate the membrane proteome of the brains of BACE1-/- mice and their wild type littermates as controls and lead to the identification and validation of BACE1 substrates in vivo.

4.3 Identification and validation of BACE1-/- substrates in vivo using a spike-in SILAC mouse approach

4.3.1 A spike-in SILAC mouse based proteomic workflow to identify BACE1 substrates in vivo.

The changes in the brain membrane fraction of BACE1-/- mice and their wild type littermates were expected to be rather subtle. This assumption was based on the results of the previous experiment in HEK-293E cells, for example as seen in Figure 12 B for APP, APLP2 and IGF2R. SILAC was thus chosen to accurately monitor these changes. The SILAC labeling of mice has been first achieved in 2009 and the fully labeled mice do not show any observable anatomic, physiologic or behavioral phenotype (Kruger et al., 2008). However, SILAC labeling of mice is cost intensive and time consuming, as mice have to be fed with a diet that contains ^{13}C lysine as the only source of lysine for at least three generations in order to achieve complete labeling (Zanivan et al., 2012). In addition, it is recommended not to you use the SILAC mice as the direct experimental setup, as the SILAC mouse diet may have a metabolic effect (communicated by Matthias Mann, Max Planck Institute of Biochemistry, Martinsried). In order to save time, money and to avoid this possible metabolic effect, a spike-in SILAC mouse approach was used, where heavy SILAC reference tissue is spiked into the 2 tissues of interest (e.g. knockout and wild type). This leads to two ratios, wild type:reference and knockout:reference, and the ratio of ratios allows the comparison of wild type to knockout tissue, as the reference in the denominator is cancelled out. The major disadvantage in the spike-in SILAC mouse approach is the 2-fold increase in measurement time.

To identify and validate BACE1 substrates directly in the brain of BACE1-/- mice, the spike-in SILAC mouse technique was combined with the existing quantitative proteomic workflow used for the analysis of the membrane proteome of HEK-293E cells. This approach is depicted in Figure 13.

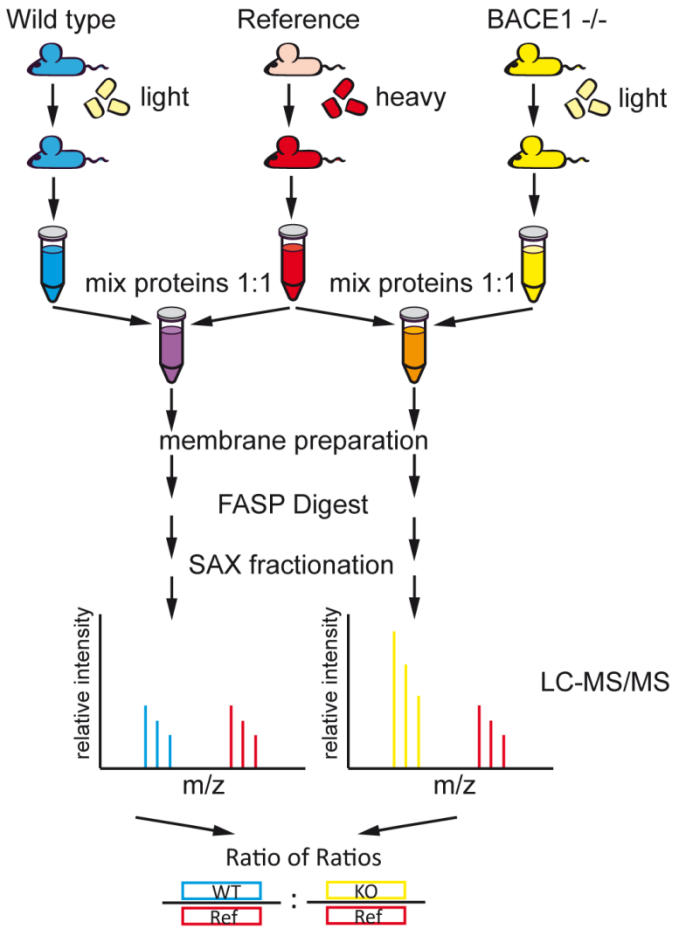

Figure 13. A spike-in SILAC mouse based proteomic workflow to identify BACE1 substrates in vivo. Reference mice are labeled with ^{13}C lysine for at least three generations using "heavy" mouse food that contains the essential amino acid ^{13}C lysine as the only lysine source. Wild type and BACE1-/- are maintained using regular ("light") mouse food. The brains of these mice are extracted and lysed. Brain lysates of wild type and knockout mice are than mixed with the brain lysate of the reference mouse in a 1:1 ratio. The membrane fraction is then isolated from these mixed brain lysates and digested. The resulting peptides are further frationated using SAX and subjected to LC-MS/MS. The obtained SILAC ratios are then compared against each other by building the ratio of ratios. This eliminates the reference in the denominator and allows the comparison of the relative protein abundances of wild type with knockout mice. BACE1 substrates are assumed to accumulate in the membrane fraction of the BACE1-/- mice, which is illustrated in the diagramm by the 2-fold abundance of the yellow peptide over the red reference and the blue wild type peptide.

4.3.2 Analysis of the BACE1-/- brain membrane proteome identifies and validates BACE1 substrates

The highest BACE1 expression levels in the brain are found in the first few days after birth (P3-P5) (Willem et al., 2006). The measurable changes in the membrane proteome of BACE1-/- and wild type mice should therefore be most easily detectable around this time period. Therefore the brains of BACE1-/- mice and their wild type littermates at day three after birth (P3) were chosen

for analysis. In order to do allow a p-value based statistical analysis of the data, three knockout and three wild type mice were analyzed, all from the same litter that resulted from the mating of a BACE+/- male with a BACE1+/- female. Heavy SILAC labeled P3 mouse brains were obtained from the SILAC mouse colony of SILANTES and served as the spike-in reference standard. A total of four technical replicates were measured from each biological replicate, except for one biological replicate, where the peptide yield (6 µg) was very low due to sample loss during sample preparation. The average peptide yield for one biological replicate was 60 µg, which resulted in 2.5 µg of peptides that there were used for a single run (60 µg total, 15 µg per technical replicate, 2.5 µg per SAX fraction; 6 SAX fractions in total). Samples were measured using 4h gradients and a 15 cm column on a LTQ Velos Orbitrap.

The quality of the heavy SILAC reference brains was excellent, as the majority of proteins showed similar expression levels between the wild type and reference animals as well as between the knockout and reference animals. The correlation of protein expression levels between the wild type and knockout mice (obtained by the ratio of ratios) were even stronger (Figure 14). Although the reference mice were of the same strain, they were from a different colony and might have been slightly younger than the mice under investigation, as their brains were slightly smaller and weighed less. This could explain the observed difference, but does not influence the actual comparison of BACE1-/- mice and their wild type littermates, as these difference are cancelled out by building the ratio of ratios. To conclude, the vast majority of the quantifiable proteins did not change significantly between BACE1-/- mice and their wild type littermates, which is expected for a viable knockout.

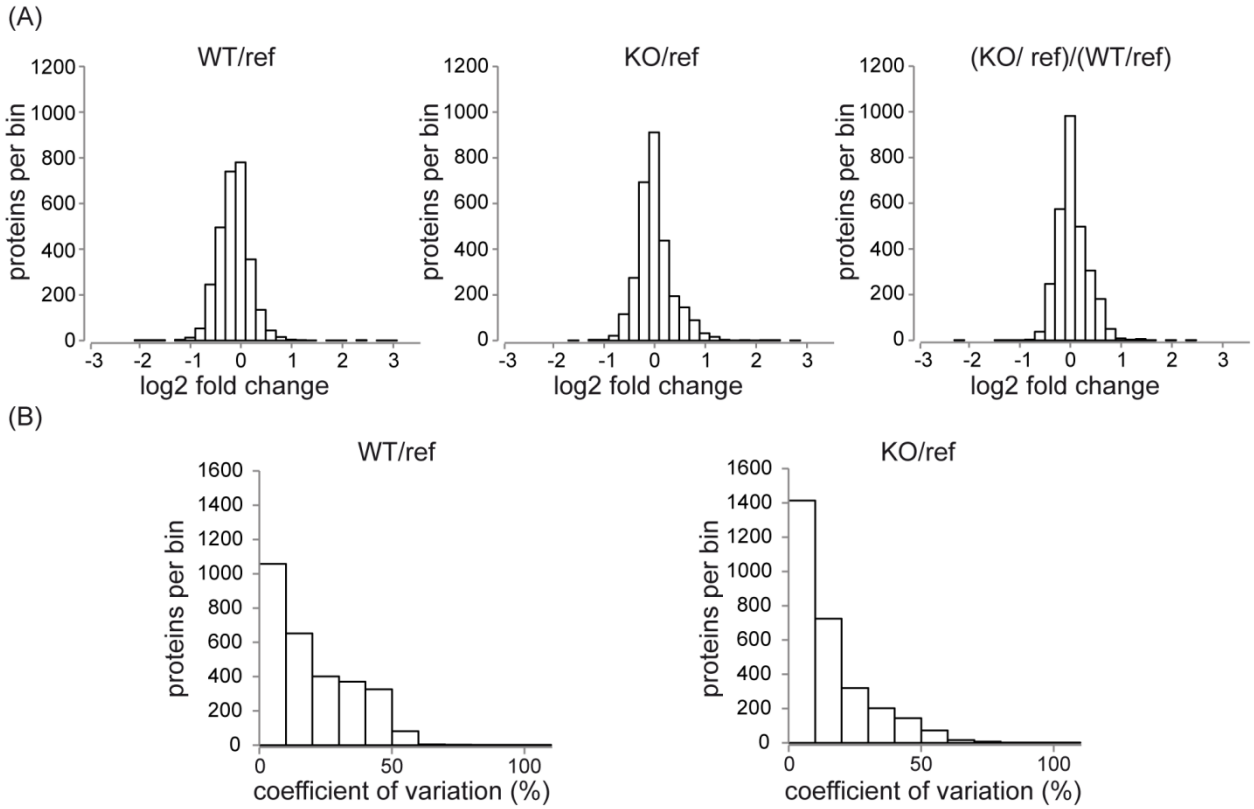

Figure 14. Quality control of the mouse brain reference standard and the experimental setup. A) Histogramms display fold changes in protein expression between wild type (WT), reference (ref) and BACE1-/- (KO) brain membrane proteomes. Each bin represents the indicated number of proteins for a given range of fold changes. Fold changes are derived by building the indicated ratio or ratio of ratios. **B)** The coefficient of variation is defined as the standard deviation divided by the mean.

Only proteins where the “heavy” and matching “light” peptide was found were included in the analysis. In addition, only proteins identified by at least two unique peptides that were identified in at least one technical in all three biological replicates were included. This lead to the identification of 2903 proteins that were quantifiable in all biological replicates, amongst them 1130 proteins with the GO term “intrinsic to membrane”, thus representing putative BACE1 substrates. Figure 15 shows a scatter plot of all identified proteins and their corresponding fold changes.

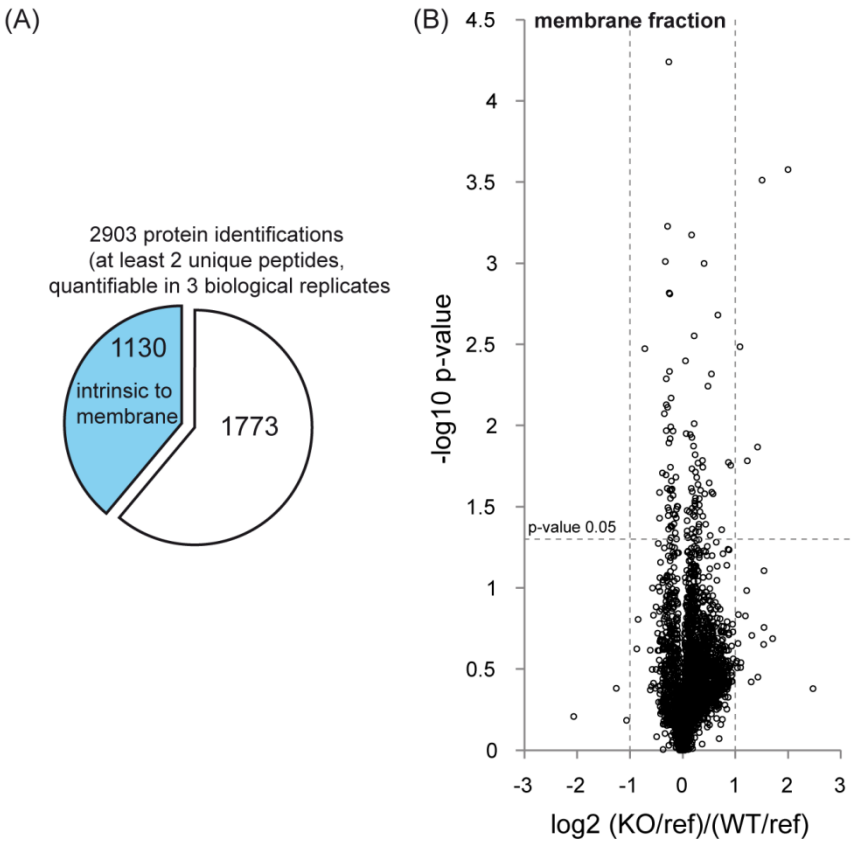

Figure 15. Accurate quantification of 2903 proteins in the BACE1-/- brain membrane fraction. A) Inclusion criteria for quantifiable proteins. Approximately 40% of the identified proteins were annotated as integral membrane proteins (GO term "intrinsic to membrane") **B)** Volcano plot: Each black circle represents an identified protein that was quantifiable in all three biological replicates. The illustrated changes represent the mean of all three biological replicates. The log2 fold change of the ratio of ratios is plotted against the -log10 of the p-value. The fold change of all proteins that are displayed above the horizontal dashed line is statistically significant (p-value 0.05 or below).

The observed changes in the membrane proteome in the absence of BACE could be attributed either to the accumulation of BACE1 substrates or to related secondary effects, due to enhanced or decreased activation of a signaling pathways. In order to focus more on the primary, shedding attributed effects, only proteins with the GO term "intrinsic to membrane" are visualized in the following figures. Figure 16 shows a scatter plot of these proteins and their fold changes in two biological replicates. The majority of proteins is unchanged, but the proteins that do change consistently in both biological replicates are increased in the membrane fraction of the BACE1-/- mice brains, which is the expected directional change for putative BACE1 substrates.

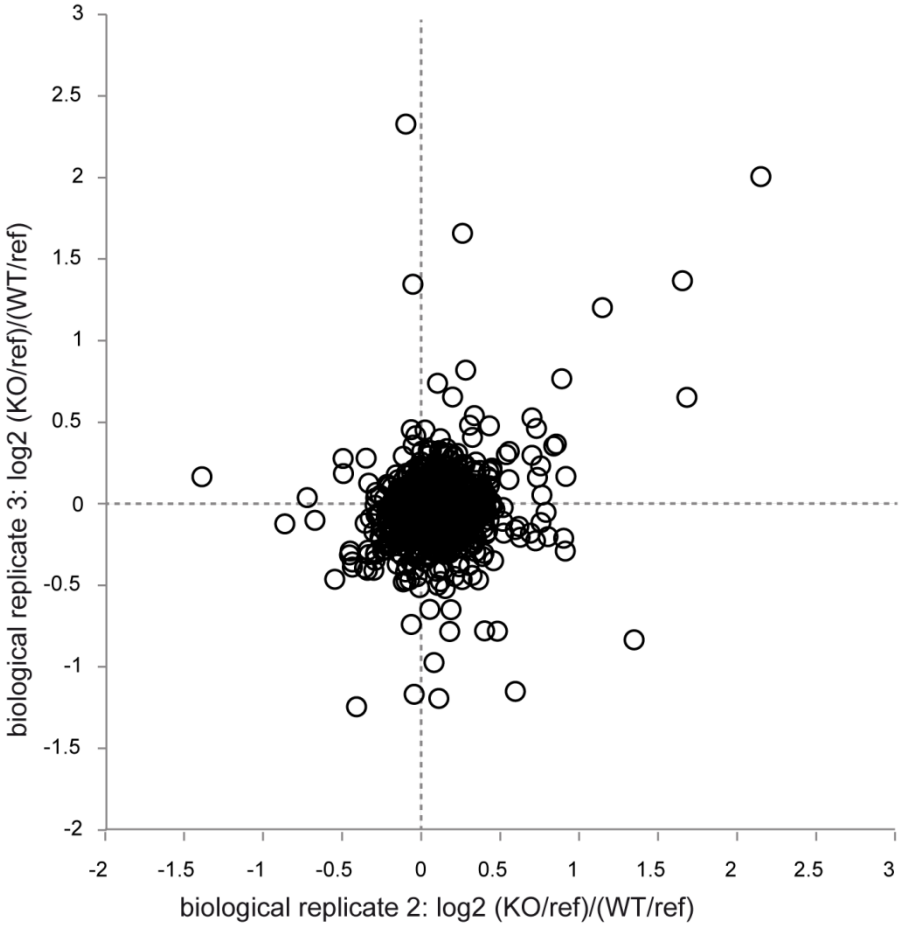

Figure 16. Integral membrane proteins accumulate in the membrane fraction of BACE1-/- mice. Each circle represents a protein annotated with the GO term "intrinsic to membrane". The ratio of ratios of the fold changes of two biological replicates are plotted against each other. Proteins that change consistently in both biological replicates are more likely to accumulate (right upper quadrant) than to be decreased (left lower quadrant) in BACE1-/- mice, consistent with their accumulation in the membrane in the absence of BACE1.

In order to display all three biological replicates and the statistical significance of the observed changes, the mean fold change of all biological replicates and their corresponding p-values are shown in Figure 17.

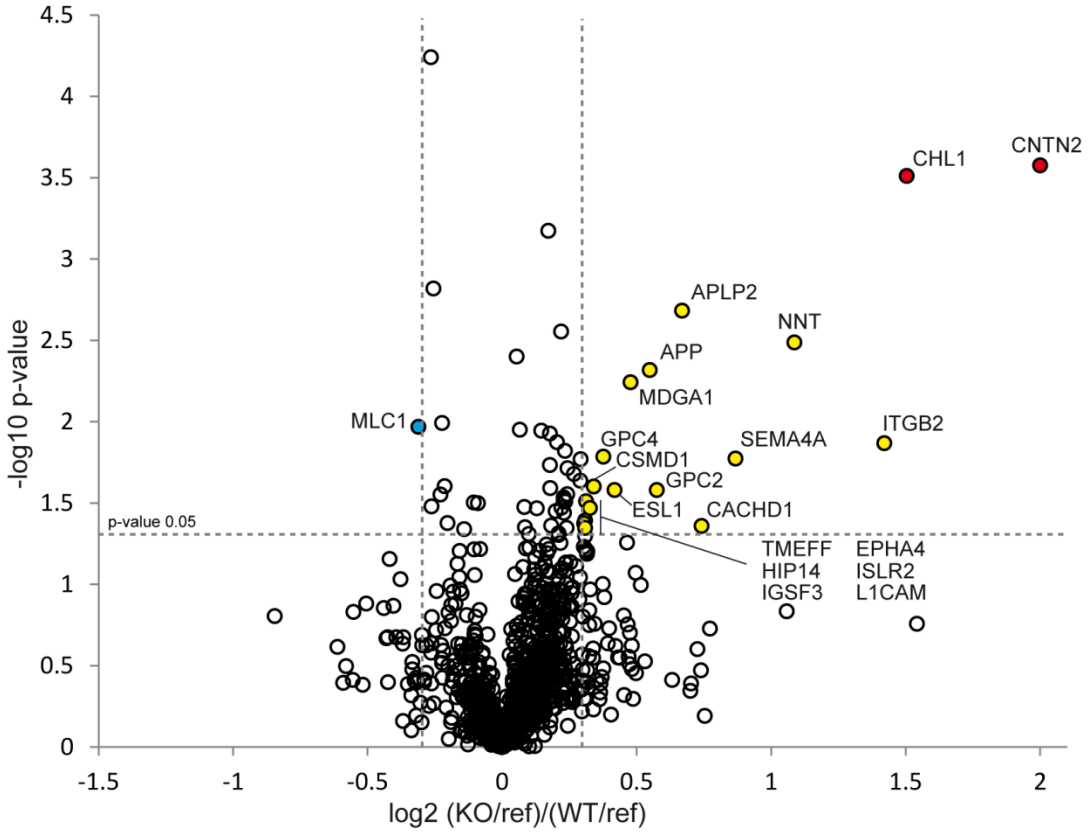

Figure 17. Identification and validation of putative BACE1 substrates in vivo. Each circle represents a protein annotated with the GO term "intrinsic to membrane" that was quantifiable in all biological replicates. The log2 fold change of the ratio of ratios is plotted against the –log10 of the p-value. The vertical bars mark a log2 fold change of at least 0.3. The horizontal bar shows the cutoff for statistical significance (p-value 0.05 or below). Proteins shown in red and yellow are regarded putative BACE1 substrates. The red circle indicates that these proteins remain significantly changed after a false discovery rate based multiple hypothesis testing. Only one protein (shown in blue) shows a significant log2 fold change of -0.3.

An arbitrary cutoff for the observed fold change was set at log2 0.3 (1.23-fold change). 19 proteins were found to be enriched in a statistically significant manner (without applying multiple hypothesis testing, see Figure 17) in the membrane proteome of BACE1-/- mice, whereas only one protein was downregulated significantly. Amongst the 19 upregulated proteins were the previously known BACE1 substrates APP and APLP2. Three of the identified proteins (CHL1, L1CAM, CACHD1) had been suggested by a previous study to be putatitive BACE substrates upon overexpression of the protease (Hemming et al., 2009). In addition, five of the identified proteins (CNTN2, SEMA4A, GPC2, GPC4, EPHA4) are close homologues to putative substrates that were identified in the aforementioned study. Except for 2 proteins (NNT and HIP14, multiple transmembrane domains, localized primarily to mitochondria and Golgi apparatus) all identified proteins were either type I transmembrane proteins (13 proteins) or GPI-anchored (4 proteins),

thus fulfilling the typical criteria for a BACE1 substrate. To conclude, ~50% of the identified proteins were previously known or putative BACE1 substrates, cross-validating the obtained dataset. Table 15 summarizes the identified novel and known BACE1 substrates and also lists the two proteins (NNT and HIP14) that are unlikely to be BACE1 substrates.

Gene Name	Protein Name	Topo - logy	log2 fold change	neg. log10 p-value	Function (general annotation from UniProt, unless stated otherwise)
CNTN2	Contactin-2	GPI	2.0	3.57	**May play a role in the initial growth and guidance of axons**. May be involved in cell adhesion.
CHL1	Cell adhesion molecule with homology to L1CAM	type I	1.5	3.51	Extracellular matrix and cell adhesion protein that plays a role in nervous system development and in synaptic plasticity. Both soluble and membranous forms promote neurite outgrowth of cerebellar and hippocampal neurons and suppress neuronal cell death.
ITGB2	Integrin beta-2	type I	1.4	1.86	Integrin alpha-L/beta-2 is a receptor for ICAM1, ICAM2, ICAM3 and ICAM4. ***ITGB1 (homologue to ITGB2) interacts with contactin, regulates CNS myelination (Laursen et al., 2009).***
NNT	Nicotinamide nucleotide transhydrogenase	Multi-pass	1.1	2.48	The transhydrogenation between NADH and NADP is coupled to respiration and ATP hydrolysis and functions as a proton pump across the membrane
SEMA4A	Semaphorin 4A	type I	0.9	1.77	Cell surface receptor for PLXNB1, PLXNB2, PLXNB3 and PLXND1 that plays an important role in cell-cell signaling. Promotes axon growth cone collapse. **Inhibits axonal extension by providing local signals to specify territories inaccessible for growing axons**.
CACHD1	VWFA and cache domain-containing protein 1	type I	0.7	1.35	May regulate voltage-dependent calcium channels
APLP2	Amyloid-like protein 2	type I	0.7	2.68	May play a role in the regulation of hemostasis. The soluble form may have inhibitory properties towards coagulation factors. May interact with cellular G-protein signaling pathways.
GPC2	Glypican-2	GPI	0.6	1.57	Cell surface proteoglycan that bears heparan sulfate. **May fulfill a function related to the motile behaviors of developing neurons**. ***GPC2 is expressed on developing axons and growth cones (Ivins et al., 1997).***
APP	Amyloid Precursor Protein	type I	0.5	2.31	Functions as a cell surface receptor and performs **physiological functions on the surface of neurons relevant to neurite growth, neuronal adhesion and axonogenesis**.
MDGA1	MAM domain-containing GPI anchor protein 1	GPI	0.5	2.24	**Required for radial migration of cortical neurons in the superficial layer of the neocortex**. ***Knockdown of MDGAs increases inhibitory synapse numbers in a neuroligin 2 dependent manner. Overexpression of MDGAs decreases inhibitory synapse density (Lee et al., 2013; Pettem et al., 2013).***
ESL1	E-selectin ligand 1	type I	0.4	1.57	Binds fibroblast growth factor. Binds E-selectin.
GPC4	Glypican-4	GPI	0.4	1.78	Cell surface proteoglycan that bears heparan sulfate. May be involved in the **development** of kidney tubules and **of the central nervous system. Astrocytic secreted GPC4** ***induces functional synapses in neurons, increases AMPA receptor surface levels and therefore functional connectivity. Defective synapse formation in GPC4 deficient mice (Allen et al., 2012).***
CSMD1	CUB and sushi domain-containing protein 1	type I	0.3	1.60	Function not annotated.
IGSF3	Immunoglobulin superfamily member 3	type I	0.3	1.46	Function not annotated.
TMEFF	Tomoregulin-1	type I	0.3	1.52	May inhibit NODAL and BMP signaling during **neural patterning**.

HIP14	Zinc finger DHHC domain-containing protein 17	Multi-pass	0.3	1.51	Palmitoyltransferase specific for a subset of neuronal proteins, including SNAP25, DLG4/PSD95, GAD2, SYT1 and HD.
L1CAM	Neural cell adhesion molecule L1	type I	0.3	1.34	Cell adhesion molecule with **an important role in the development of the nervous system. Involved in neuron-neuron adhesion, neurite fasciculation, outgrowth of neurites.**
EPHA4	Ephrin type-A receptor 4	type I	0.3	1.39	Plays an important role in the **development of the nervous system controlling different steps of axonal guidance** including the establishment of the corticospinal projections. Beside its role in axonal guidance plays a role in **synaptic plasticity**. ***Classical axon guidance molecule. Interacts with ephrins. Regulates repulsion and attraction of growth cones. Forward and reverse signaling, leads to cytoskeletal changes. Controls growth cone collapse (Klein, 2012).***
ISLR2	Immunoglobulin superfamily containing leucine-rich repeat protein 2	type I	0.3	1.37	Required for **axon extension during neural development**.

Table 15. Summary of BACE1 substrate candidates identified in the membrane fraction of BACE1-/- brains. BACE1 substrate candidates were selected if they were meeting the predefined cut-offs for observed fold changes and were significantly changed. They are ranked according to the observed log2 fold changes. A log2 fold change of 2 represents a 4-fold change, as the log2 of 4 equals 2 (log2 of 4=2, log2 of 2=1, log2 of 1=0, log2 of 1.23=0.3). “Function” column: Bold font emphasizes a physiological role in neuronal development, especially in neurite outgrowth, axonal guidance and synapse formation. Italic font is used if the presented information is taken from a source other than the UniProt database.

The function of the identified substrates points to a role of BACE1 in neurite ougrowth and synapse formation, as the identified putative substrates represent classical axon guidance molecules (EPHA4, SEMA4A, CHL1), regulate synaptic density (MDGA1), induce synapse formation (GPC4), neurite outgrowth (ISLR2, L1CAM) or have less clear defined roles in neurite development (CNTNC2, GPC2, APP). The BACE1 protease thus migth be a key player in establishing and maintaining structural and functional connectivity in the brain, by controlling the absoulte leves of these substrates and the release of proteolytic fragments with signalling function through RIP.

4.3.3 Validation of identified substrates in mouse brains by western blotting

The validation of the observed changes in the BACE1-/- membrane proteome was done using western blot analysis were antibodys where available and able to detect the endogenous proteins. An independent set of P3 mice was used for this analysis. The brains of wild type and BACE1-/- mice were fractionated using diethylamine extraction to obtain a soluble fraction (containing the shed ectodomains) and further processed by ultracentrifugation to enrich for the membrane fraction (containing the full length proteins). Two of the previously known BACE1 substrates and four of the novel putative BACE1 substrates were detectable upon western blot analysis. This included CNTN2 and CHL1, that showed a strong increase in the membrane fraction in the initial LC-MS/MS experiment (4-fold and 2.83-fold respectively) as well as APP, APLP2,

MDGA1 and EPHA4, that displayed only mild changes in the initial study (1.32-fold, 1.59-fold, 1.39-fold and 1.24-fold respectively). All proteins accumulated in the membrane fraction of the P3 BACE1-/- mice, and the observed fold changes closely correlated to the ones observed by mass spectrometry (Figure 18 A+B+C).

A concomitant decrease of the shed extracellular domains was observed for APLP2, CHL1 and EPHA4. The ectodomains of CNTN2 and MDGA1 were not detectable in the DEA fraction. No decrease was observed for APP in the DEA fraction, as the antibody detects the secreted ectodomains APPsβ and APPsα, with the latter one being upregulated upon knockdown/knockout of BACE1 and thus counteracting the effect on the total amount of secreted APP ectodomains (Colombo et al., 2012). Taken together, the western blot analyses validated the results of the LC-MS/MS data and demonstrated the processing of the new BACE substrates in vivo. In addition, the tight correlation of fold changes that were observed between immunoblot and quantitative proteomics demonstrates the accuracy of the SILAC approach.

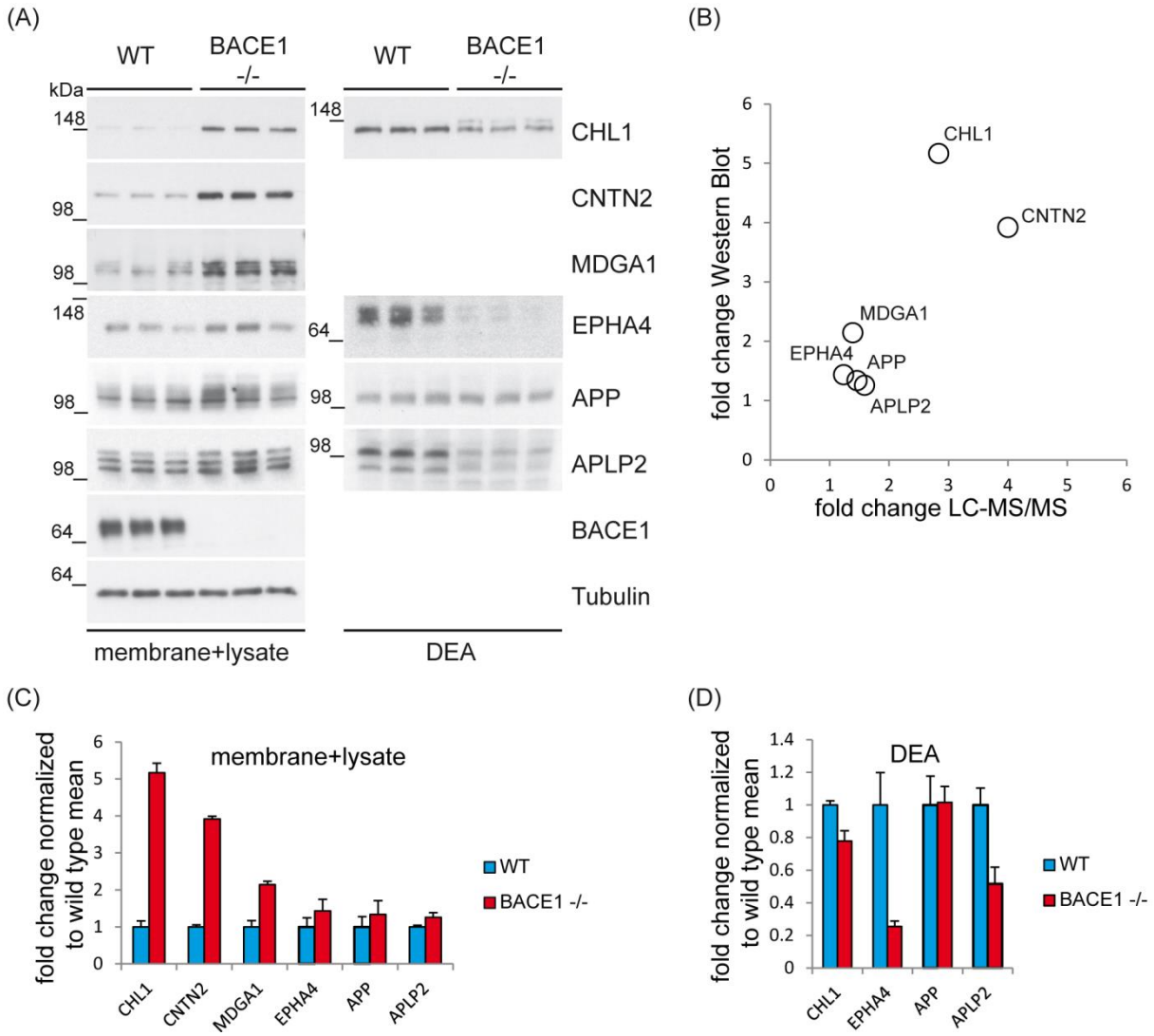

Figure 18. Validation of the identified BACE1 substrates by Western Blot analysis. A) The brains of three P3 wild type (WT) and three P3 BACE1-/- mice were fractionated into a soluble (DEA) and a membrane fraction using the DEA fractionation protocol, subjected to SDS-PAGE and analysed by western blotting. **B)** The observed fold changes (accumulation of BACE1 substrates in the membrane fraction) of the western blot analysis and the initial LC-MS/MS analysis are plotted against each other. **C)** Quantification of the western blot shown in A) for the membrane fraction. **D)** Quantifiaction of the western blot shown in A) for the soluble DEA fraction.

4.3.4 Processing of EPHA4 by BACE1 from embryogenesis through adulthood

EPHA4 (Ephrin type-A receptor 4) belongs to the Eph receptor family, which represents the largest group or receptor tyrosine kinases. The binding of membrane bound ephrin ligands to Eph receptors initiates a signaling cascade in the sending and receiving cell, which regulates a plethora of events during development, including axon repulsion and growth cone collapse in the case of EPHA4 (Bashaw and Klein, 2010; Klein, 2012). In addition, it was shown that EPHA4 is subjected

to RIP by matrix metalloproteinases and γ-secretase in response to synaptic activity. The resulting EPHA4 ICD is then able to regulate the number of dendritic spines via the RAC pathway (Inoue et al., 2009). Since EPHA4 was identified as a new BACE1 substrate in vivo, and its shedding was shown to be of physiological relevance, a more detailed analysis of its processing by BACE1 was performed. This included western blot analysis of P3, P7 and two month old (adult) BACE1-/- mice, as well as immunofluorescence analysis in primary cortical neurons (embryonic day 18). If this protein is also shed by BACE1 in adult mice, this could point to the physiological relevance of EPHA4 processing in the adult brain but also to possible adverse effects during therapeutic inhibition in humans. As demonstrated in Figure 18 A, the full length protein accumulated slightly in the membrane fraction of P3 BACE1-/- mice, whereas a strong decrease in the BACE1 shed EPHA4 ectodomain EPHA4β-NTF (N-terminal fragment) was observed in the soluble fraction. In addition, a shorter ectodomain (EPHA4α-NTF) that is generated by other protease activities, most likely matrix metalloproteinases, represented the major fraction of shed EPHA4 and had also been described in another study (Inoue et al., 2009). The increase in the full length proteins was no longer seen in P7 and the 2 month old BACE1-/- mice, despite the ongoing processing of EPHA4 by BACE1 that was observed in the soluble fraction. The levels of the ICD did not change between BACE1-/- and wild type mice for any of the age groups observed. Figure 19 A shows the results of the western blot analysis.

To investigate whether BACE1 also processes EPHA4 in neurons during the embryonic stages of brain development, primary cortical neurons were treated with the BACE1 inhibitor C3 or the broad spectrum metalloprotease inhibitor TAPI (Fig 19 B). EPHA4 was visualized via immunofluorescence after fixation and permeabilization of the cells using an antibody directed against the C-terminus of EPHA4. EPHA4 localized to the neuronal processes as well as to the soma and was seen at the cell surface and in vesicular structures within the neurons. Neurons that were treated with either C3 or TAPI showed an increase in EPHA4 staining, which supports the observation of BACE1 and metalloprotease dependent EPHA4 processing. In agreement with the observation from the brain lysates, the majority of EPHA4 shedding seems to be carried out by metalloproteases, as the increase in total EPHA4 in the neurons was stronger for TAPI than for C3.

In summary, BACE1 sheds EPHA4 from embryogenesis through adulthood. It acts as a minor sheddase next to a single or multiple sheddases of the metalloprotease family and its inhibition in mice leads to an increase in full length EPHA4 during embryogenesis and the first few days after birth.

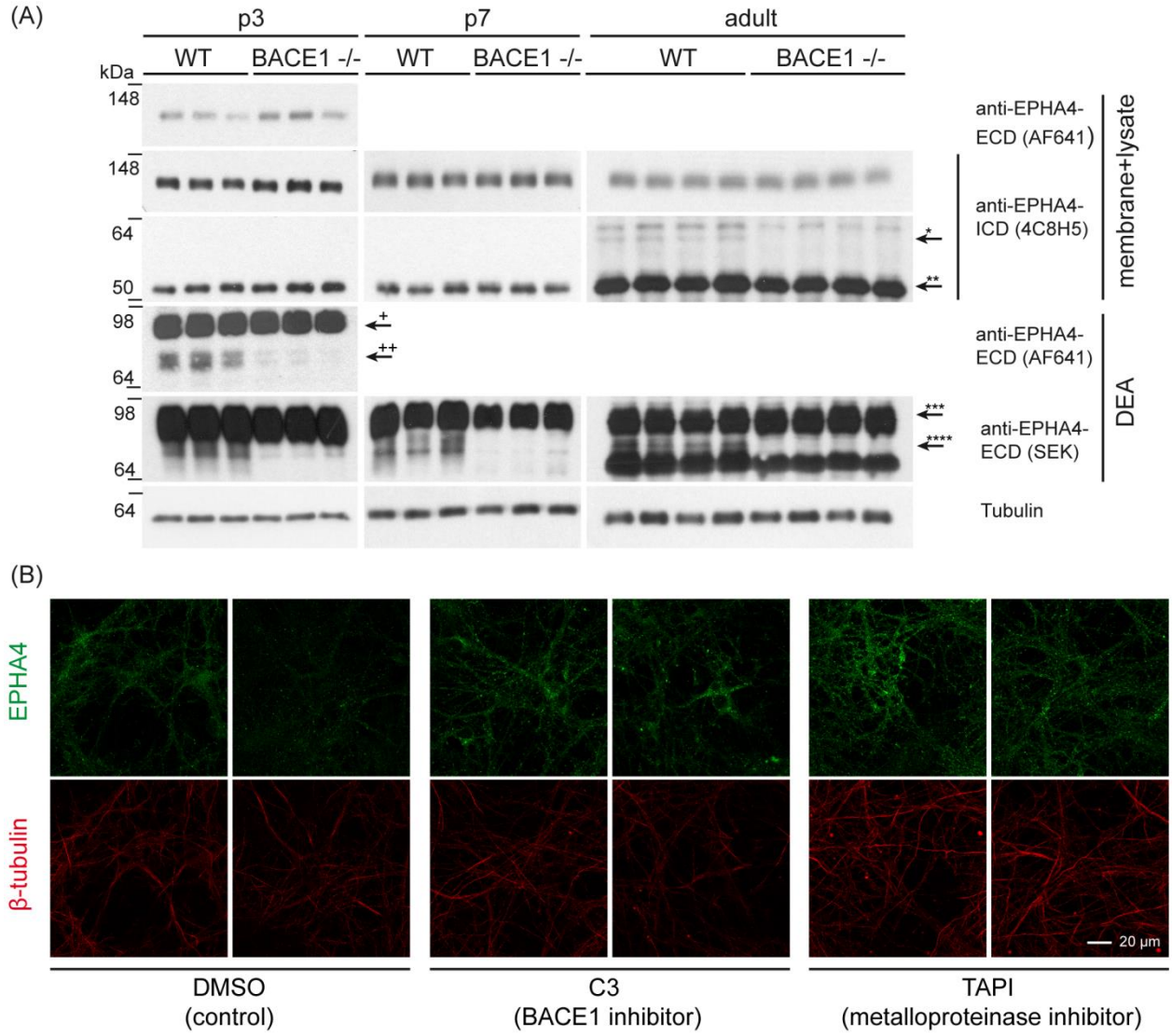

Figure 19. Processing of EPHA4 by BACE1 from embryogenesis through adulthood
A) Each lane represents the brain membrane or soluble (DEA) fraction of a P3, P7 or two month old (adult) BACE1-/- mouse or a wild type littermate. The antibodies AF641 and SEK have been raised against the extracellular domain (ECD) of EPHA4, whereas 4C8H5 has been raised against the intracellular domain (ICD). AF641 only recognized EPHA4 if the samples were processed under non-reducing conditions, which explains the difference in running behaviour of the EPHA4 ECDs when analzed by the SEK (reducing conditions) or AF641 (non-reducing conditions) antibody. Top panel: Full length EPHA4 recognized by AF641. Second panel: Full length EPHA4 recognized by 4C8H5. Third panel: ICD (**) recognized by 4C8H5. The band marked with * most likely represents the EPHA4β-CTF, as it is absent in the BACE1-/- brain. Fourth panel: EPHA4α-NTF (upper band, +) and EPHA4β-NTF (lower bands, ++) recognized by AF641. Fifth panel: EPHA4α-NTF (upper band, ***) and EPHA4β-NTF (lower band, ****) recognized by SEK. The lowest band (only seen in adult mice) is not detected in P3 and P7 mice and of unknown origin. The western blots carried out for P7 and adult mice under non-reducing conditions and probed with the AF641 antibody are not shown, as no distinct band pattern was obtained, due to a very low signal

to noise ratio (high background signal). Thus the reducing conditions and the corresponding SEK and 4C8H5 antibody were preferred for P7 and adult animals.
B) Immunofluorescence analysis of primary cortical neurons treated with the BACE1 inhibitor C3, the metalloprotease inhibitor TAPI or DMSO as control. Staining was carried out with antibodies against the C-terminus of EPHA4 and against β-tubulin in order to visualize the neuronal processes.

4.4 Analysis of the BACE1-/- brain soluble fraction reveals no major changes

In order to obtain a more comprehensive understanding of the changes related to the absence of BACE1 in the knockout mouse model but also during the putative long term treatment of AD patients with BACE1 inhibitors, the soluble fraction of the BACE1-/- brains was analyzed in parallel to the membrane fraction. The soluble fraction represents the high salt fraction without the membrane pellet, as described in Figure 6. LC-MS/MS and data analysis were carried out as described for the membrane fraction in 4.3.2. In total, 4537 proteins were quantified in all biological replicates, amongst them 543 proteins with the GO term “intrinsic to membrane”, which could be attributable to the detection of shed ectodomains in the soluble fraction. Only one protein (CNTN2) showed a significant 2-fold increase in the BACE1-/- brain, whereas all other proteins were more or less unchanged. The chronic absence of BACE1 does therefore not lead to major changes in the soluble fraction of the brain, which may indicate that adverse side effects upon therapeutic inhibition could be in an acceptable range. Figure 20 summarizes the data obtained from the analysis of the BACE1-/- soluble brain fraction.

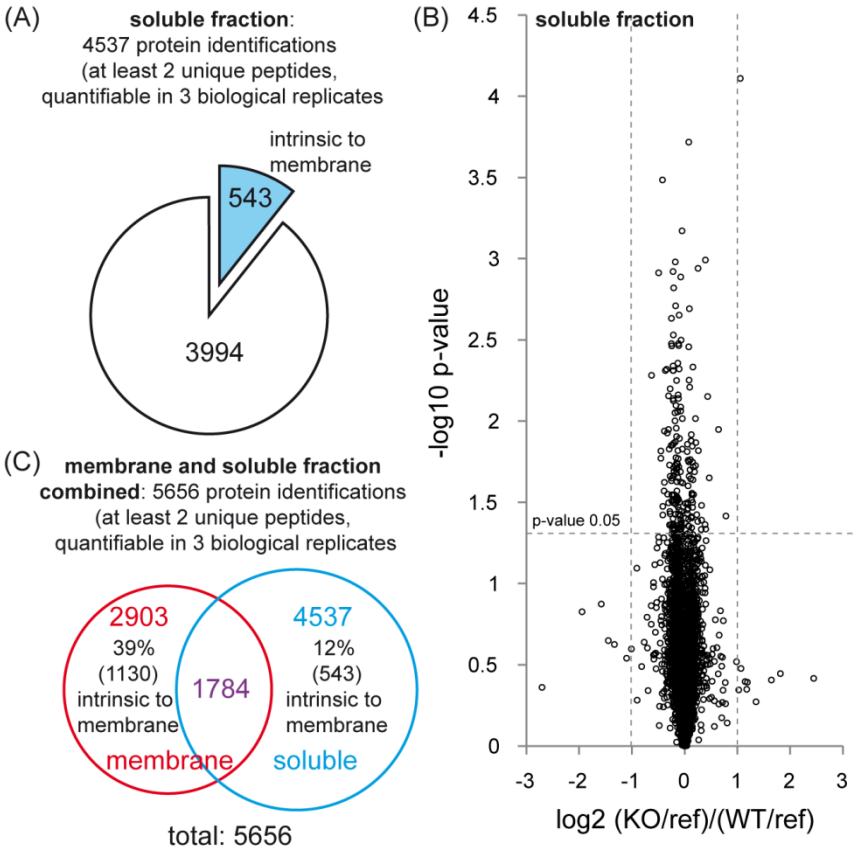

Figure 20. Accurate quantification of 4537 proteins in the BACE1-/- brain soluble fraction. A) Inclusion criteria for quantifiable proteins. 12% of the identified proteins were annotated as integral membrane proteins (GO term "intrinsic to membrane") **B)** Volcano plot: Each black circle represents an identified protein that was quantifiable in all biological replicates. The log 2 fold change of the ratio of ratios is plotted against the –log10 of the p-value. The fold change of all proteins that are displayed above the horizontal dashed line is statistically significant (p-value 0.05 or below). **C)** Summary of the identified proteins in the membrane and soluble fraction of BACE1-/- brains. A total of 5656 proteins were quantified, with 1784 of them in both fractions.

The soluble fraction contained 12% of proteins annotated with the GO term "intrinsic to membrane", which could be due to several reasons: First, some membrane proteins could have escaped from the membranous compartment during the high shear stress associated with sample preparation. Second, these protein fragments could be derived from RIP, being released into the extracellular space or liberated into the cytosol. Finally, they could represent membrane proteins that are in the process of being degraded via lysosomal/vacuolar or in some cases even proteasomal degradation (Bonifacino and Weissman, 1998). Figure 21 shows the quantitative changes observed for "intrinsic to membrane" proteins in the soluble fraction of BACE1-/- brains.

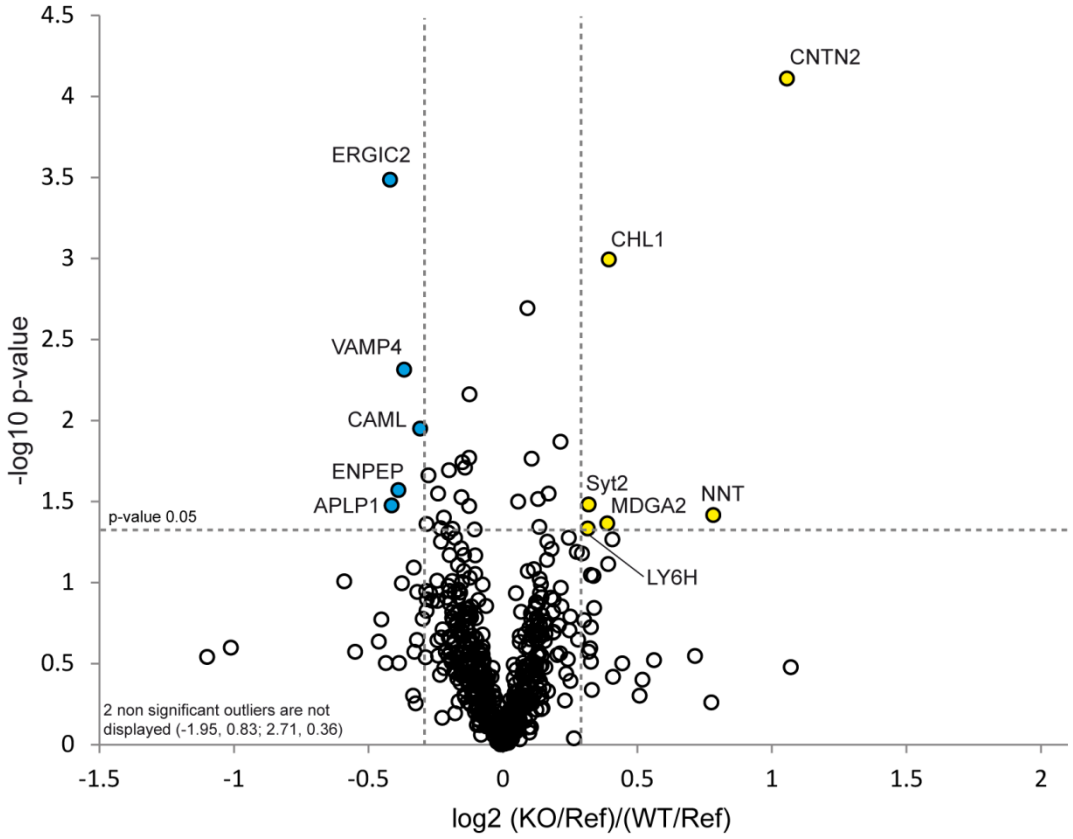

Figure 21. Quantitative changes of integral membrane proteins in the soluble fraction of BACE1-/- brains. Each circle represents a protein annotated with the GO term "intrinsic to membrane" that was quantifiable in all biological replicates. The log 2 fold change of the ratio of ratios is plotted against the –log10 of the p-value. The vertical bars mark a log2 fold change of at least 0.3, the same criteria that were used for the membrane fraction in figure 17. The horizontal bar shows the cutoff for statistical significance (p-value 0.05 or below). Proteins shown in yellow and blue have a log2 fold change of at least 0.3 or -0.3 respectively.

The top four upregulated proteins tagged with "intrinsic to membrane" were CNTN2, NNT, CHL1 and MDGA2. Three of these proteins were also amongst the top four proteins in the membrane fraction. CNTN2 is GPI-anchored, and was most likely released from the membrane due to shear stress in sample preparation or the presence of the high salt buffer. The same holds true for MDGA2, which is also GPI anchored and has also been increased in the membrane fraction (but not meeting the predefined criteria for statistical significance), together with its homologue MDGA1. The integral transmembrane proteins CHL1 and NNT also increased in the soluble and membrane fraction, pointing to the presence of some leftover membranous material in the high salt fraction. The expected decrease in shed ectodomains of a BACE1 substrate in the BACE1-/- brain was only observed for ALPL1, where two peptides mapping to the extracellular domain were decreased significantly.

Taken together, the analysis of the soluble fraction did not reveal major changes of the soluble proteome of BACE1-/- mice. The observed fold changes for the previously identified BACE1 substrates were most likely due to carry-over of some membrane proteins during sample preparation, as biochemical fractionation is not 100% efficient.

4.5 Analysis of mouse CSF by quantitative proteomics

The comprehensive analysis of the BACE1-/- mouse brains identified and validated several new BACE1 substrates. However, it is difficult to assess whether these substrates are also processed by BACE1 in humans, as it is difficult to obtain post mortem brain tissue of high quality. The collection and conservation of brain tissue shortly after death poses logistical and ethical challenges that are difficult to overcome. This however is required in order to avoid protein degradation and inhomogeneities in between samples. CSF in contrast can be obtained routinely in an inpatient or outpatient setting and also for multiple times in order to obtain longitudinal data. If the processing of BACE1 substrates can be monitored in this compartment, CSF of humans treated with BACE1 inhibitors should therefore partially answer the question of which of the BACE1 substrates are processed in man. In addition, these substrates could serve as biomarkers during drug development or therapy and serve as companion diagnostics in the clinical setting. As the number of individuals that had been treated with BACE1 inhibitors during clinical studies is scarce and the CSF sample are not available for the scientific community, a proof-of principle study in mouse CSF was performed. The study aimed to answer the following questions: 1. How many of the previously known BACE1 substrates can be identified in CSF? 2. Is it possible to quantify CSF proteins in an accurate manner, using only minute amounts of sample? 3. Does the presence or absence of BACE1 lead to an increase or decrease of BACE1 substrates in CSF?

4.5.1 Identification of more than 1200 proteins in the CSF of adult mice

The proteomic analysis of CSF proteins (protein concentration in CSF ~0.4 mg/ml) is usually done on human CSF samples and involves various protein concentration and fractionation steps as well as the depletion of highly abundant proteins, such as serum albumin. This allows the identification of several hundred up to 2600 proteins (Schutzer et al., 2010). However, as the yield of human CSF (several ml) is much higher than for mouse CSF (5-15 µl), sample processing and fractionation has to be kept to an absolute minimum in order to avoid sample loss when analyzing mouse CSF.

This is why a method was developed where the sample was neither concentrated nor prefractionated, but instead analyzed in only one run (referred to as “single-shot”). In order to maximize the number of protein identifications, ultra-long HPLC columns (50 cm) were used, as they are able to resolve more peptide species in the same amount of time due to increased separation performance (Eeltink et al., 2010). In addition, MS/MS was performed on a Q-Exactive mass spectrometer, that has a faster working cycle than the LTQ Velos Orbitrap instrument used

for the previous experiments, thus increasing the number of protein identifications by about 20% (Michalski et al., 2011). Initially, CSF samples were digested by FASP, subjected to clean up on C18 STAGE Tips, and analyzed on the Q-Exactive mass spectrometer using 50 cm columns and 4 h gradients. This resulted in the highest amount of identified proteins when compared to a parallel analysis performed with a 15 cm column setup on the Q-Exactive and Orbitrap Velos Pro mass spectrometers (Figure 22).

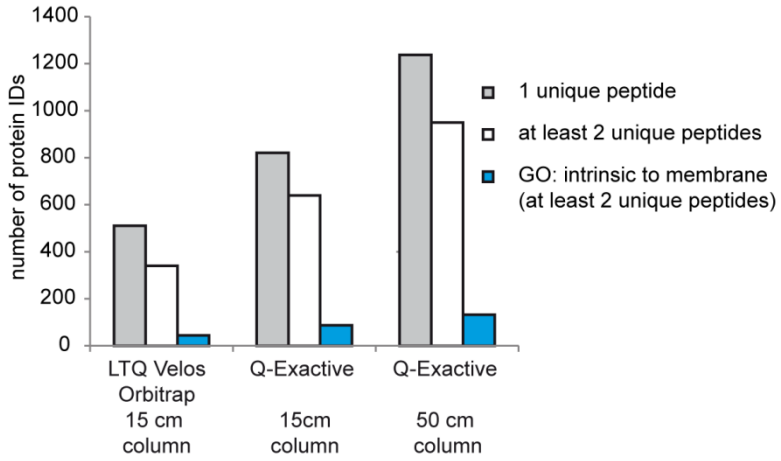

Figure 22. Single shot proteomics of murine CSF. 5 µl of tryptically digested CSF were analysed on two different mass spectrometrs using two different HPLC columns. The combination of the Q-Exactive mass spectrometer with a 50 cm column resulted in the highest number of protein identifications (IDs) and was thus chosen for the analysis of the BACE1-/- CSF.

The number of protein identifications was high using the FASP procedure (up to 1200 proteins were identified in a single run), but not reproducible in between different CFS samples. It was noted that the peptide recovery was inhomogeneous in between the individual FASP filter units and was independent of the samples tested. For this reason, a classical in-solution digest was compared to the FASP procedure. For low sample amounts, the in-solution digest resulted in a similar number of protein identifications and a far better reproducibility in between samples, which is why the in-solution digest was preferred for the following CSF measurements. In addition, subjecting more than 1.5 µg of total peptides to a single LC-MS/MS run resulted in clogging of the HPLC column. The input of peptides was therefore limited to 800 ng of peptides per run, in order to keep the column functional as long as possible.

In conclusions, FASP was efficient and reproducible when digesting membrane proteins and using 20-200 µg of total protein as input, but performed poorly for samples where the total amount of protein was low (0.8-4 µg), such as the CSF samples.

4.5.2 Analysis of the BACE1 -/- mouse CSF

After the proteomic workflow for the analysis of murine CSF was established, the BACE1-/- mouse model was used to obtain information about quantitative differences in the CSF composition in the absence of BACE1. The CSF of adult mice (on average 4 months old) from our BACE1-/- knockout colony was collected and stored at -80 °C until all samples were gathered. Adult mice were chosen for two reasons. On the one hand, the retrieval of CSF of newly born mice is extremely difficult and the sample amount is very low. On the other hand, adult mice reflect the chronic BACE1 inhibition in humans more closely. In order to avoid any additional steps in sample preparation and due to the absence of a suitable SILAC standard, a label-free quantitative proteomics approach was used. As mentioned in the introduction, label-free proteomics allow the accurate quantification by comparing the extracted ion chromatograms of peptides in between two different runs. The prerequisite for a successful label-free analysis is therefore a robust and highly reproducible chromatography, which ensures that the same peptide elutes at the same time in every run to be subjected to the final analysis. In general, label-free quantitation is not as sensitive as SILAC in detecting small changes. However, this kind of analysis focused on the soluble ectodomains rather than on the full length proteins in the membrane. It was therefore expected to observe stronger-fold changes, similar to what was seen in the conditioned media of the HEK-293E cells (Figure 12), that should be detectable by the label-free approach. Figure 23 illustrates the workflow for the comparative CSF analysis of BACE1-/- and their wild type littermates.

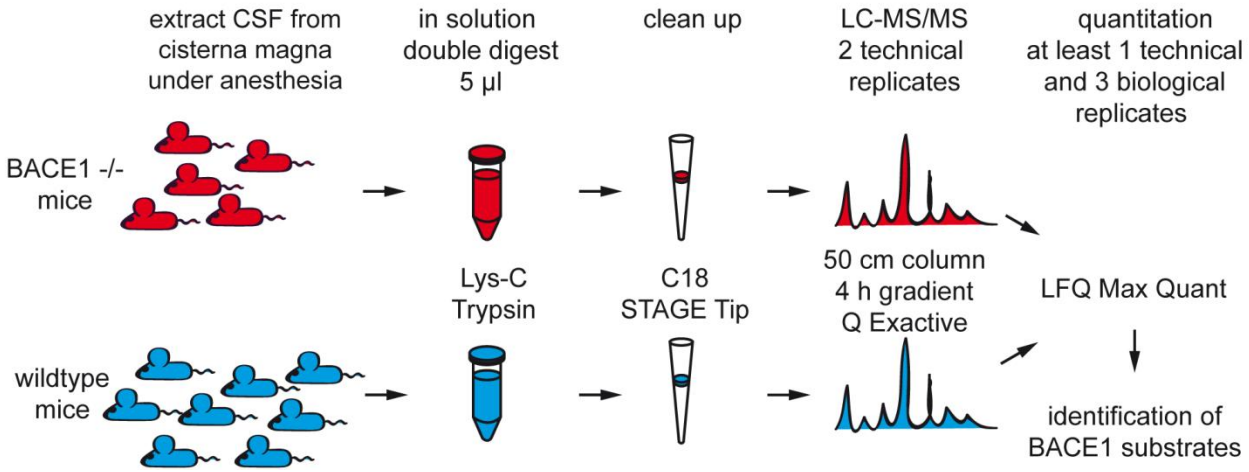

Figure 23. A label-free comparative CSF analysis of BACE1-/- mice. The CSF of BACE1-/- mice and wild type littermates was obtained from the cisterna magna. CSF was digested with Lys-C and trypsin in solution. Peptides were collected and purified on C18 STAGE Tips. Samples were measured on a 50 cm column using 4 h gradients in two technical replicates on the Q-Exactive mass spectrometer. The total ion chromatograms were than matched agains each other in order to adress any retention time shifts. Comparison of the extracted ion chromatogramms and normalization to the total peptide intensities result in the label free intensities (LFQ values, LFQ=Label Free Quantitation). LFQ values represent the relative intensities of a given peptide across the analyzed samples. Label free analysis was performed using the Max Quant algorithm.

The chromatography conditions were ideal, as only minor retention time shifts were observed in between technical and biological replicates. The overall composition of the total ion chromatograms, which represents the sum of the intensities of all measured masses across time, were highly reproducible in between the replicates, meeting the requirements for accurate label-free quantitation (Figure 24 A+B). In total 819 proteins were identified, and 525 proteins were quantifiable with at least two unique peptides each in at least three biological replicates. 74 of these proteins were annotated with the GO term “intrinsic to membrane” (Figure 24 C).

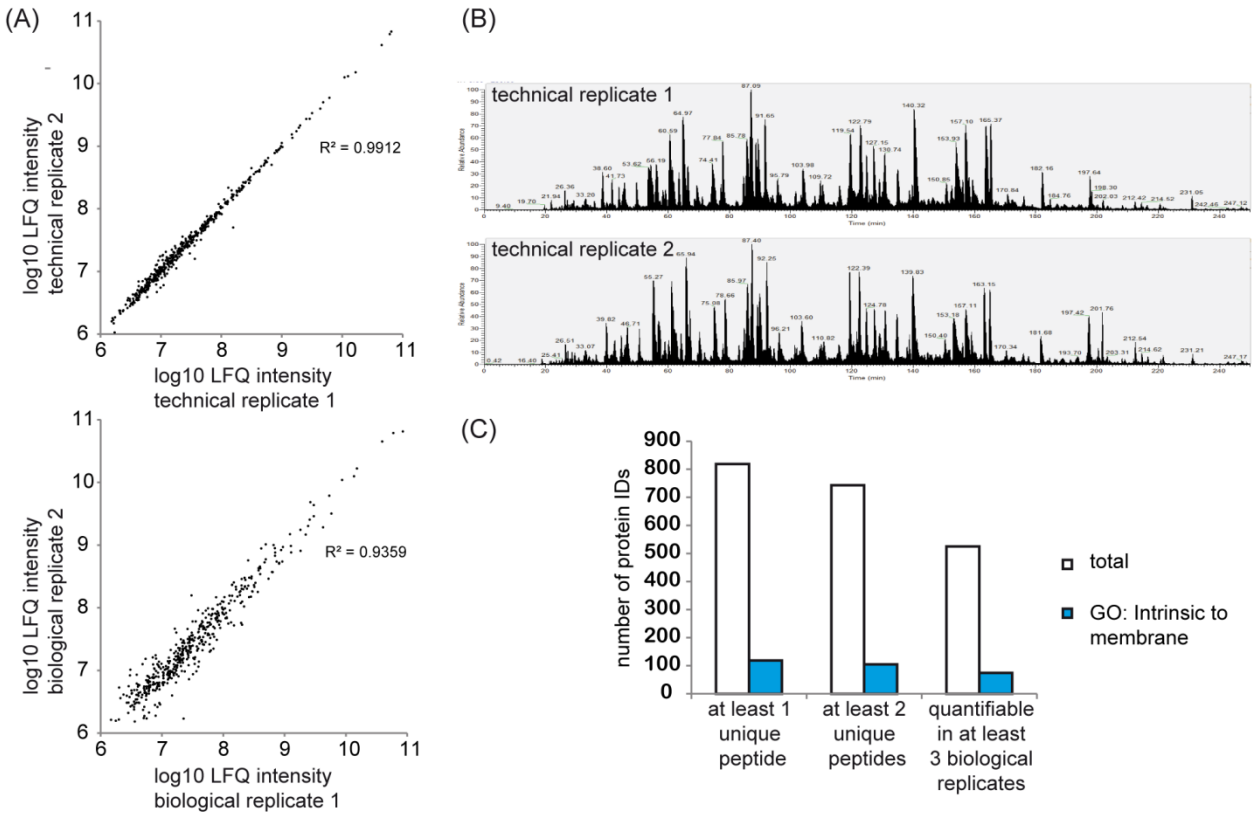

Figure 24. Quality control of the label-free comparative CSF analysis of BACE1-/- mice. A) Upper panel: The log10 LFQ intensities of two technical replicates are plotted against each other. Lower panel: The log10 LFQ intensities of two biological replicates are plotted against each other. Note the high correlation for both biological and technical replicates as indicated by the coefficient of determination being close to 1. **B)** Screenshot of the total ion chromatogram of two representative technical replicates. The total intensities and elution profiles over time are highly reproducible. **C)** Number of identified proteins that were detected by at least 1 unique peptide, at least 2 unique peptides and at least 2 unique peptides that were quantifiable in 3 or more biological replicates. LFQ: label free quantitation. ID: protein identification.

4.5.3 Accurate quantification of the BACE1-/- CSF allows the validation and identification of novel BACE1 substrates

Similar to the analysis of the BACE1-/- membrane and soluble brain proteome, the majority of the identified proteins was not altered. Only seven proteins showed a significant change of more than 2-fold, six of them being relatively enriched in the wild type, and one being downregulated in the wild type mice in comparison to the BACE1-/- mice (Figure 25). The term “relative enrichment” was chosen in order to illustrate the increase of BACE1 substrates in the soluble compartment in the presence of BACE1. However, in terms of absolute protein levels, it reflects the decrease of BACE1 substrates in the soluble compartment in the absence of BACE1 in the BACE1-/- mouse. The known BACE1 substrates APLP1 and APLP2 showed the strongest increase in the wild type mice (5.4- and 2.9-fold respectively) compared to the BACE1-/- mice, thus validating the outcome of the CSF analysis. In addition, CNTN2, APP and CHL1, in line with the results from the analysis of

the membrane proteome, were also significantly enriched, although to a milder extent (1.5-, 1.7-, 2-fold respectively). Five proteins remained significantly changed after a false discovery rate based multiple hypothesis testing was applied. These included the known BACE1 substrates APLP1 and APLP2 and the plexin domain-containing protein 2 (PLXDC2), which had been identified in a previous study as a putative BACE1 substrate (Hemming et al., 2009). In addition, two novel type I transmembrane proteins, the receptor-type tyrosine-protein phosphatase N2 (PTPRN2) and ectonucleotide pyrophosphatase/phosphodiesterase family member 5 (ENPP5) were identified, representing two putative novel BACE1 substrates that had not been identified in any previous approach (Figure 25).

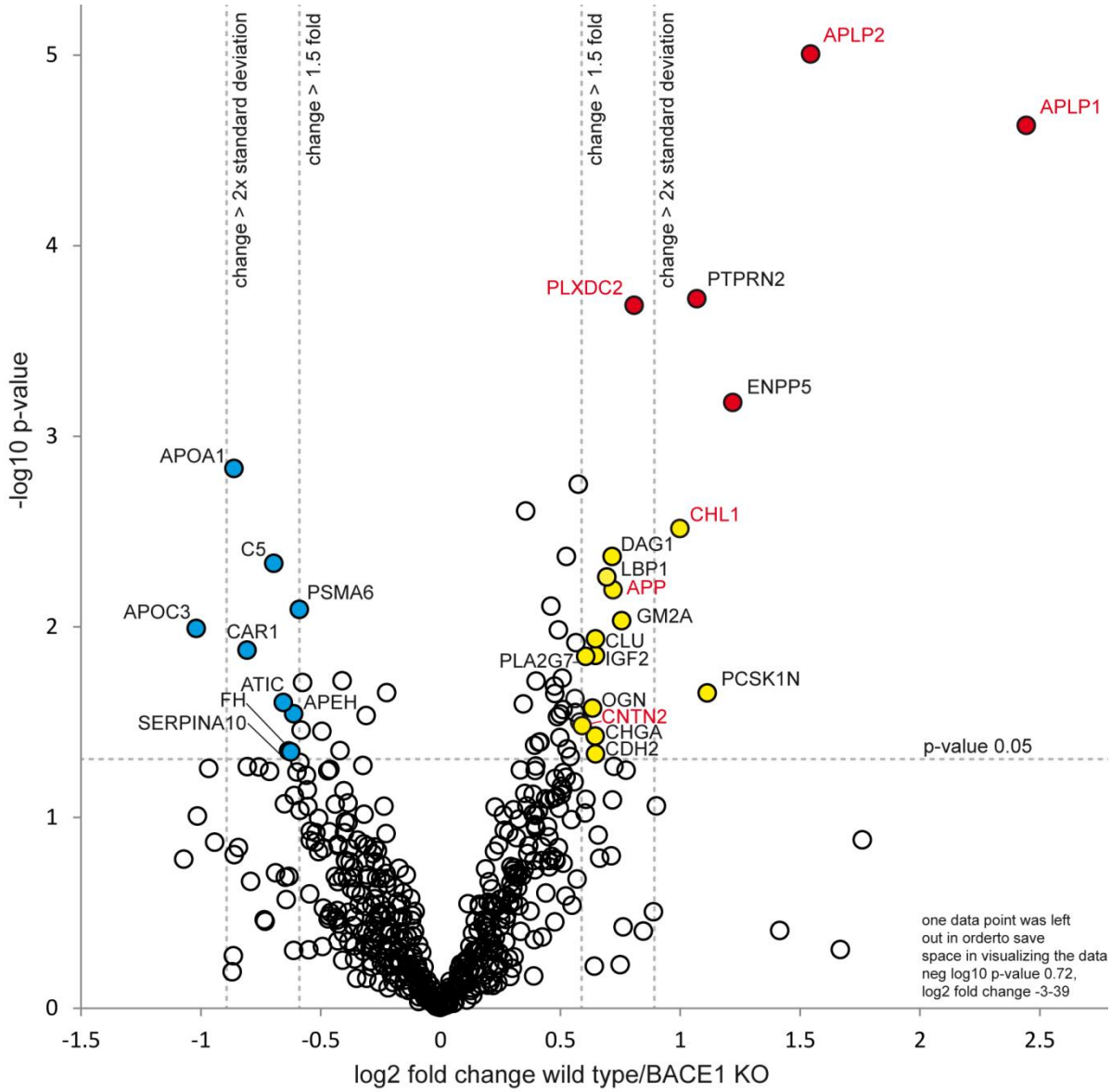

Figure 25. Identification and validation of putative BACE1 substrates in mouse CSF. Each circle represents a protein that was quantifiable in at least three biological replicates. The log2 fold change of the wild type:knockout ratio is plotted against the –log10 of the p-value. The vertical bars mark a fold change of at least 1.5 and greater than the 2-fold standard deviation. The horizontal bar shows the cutoff for statistical significance (p-value 0.05 or below). Proteins shown in red and yellow are regarded putative BACE1 substrates, as they are increased in the absence of BACE1. Gene names in "red" mark previously known BACE1 substrates. The red circle indicates that this proteins remain significantly changed after a false discovery rate based multiple hypothesis testing. The blue circle highlightes proteins that are signifcantly decreased in wild type compared to BACE1-/- mice.

Figure 26 shows the individual LFQ intensities measured in each biological replicate for the top 5 proteins identified in the CSF study and their relative abundance amongst all proteins identified in the CSF.

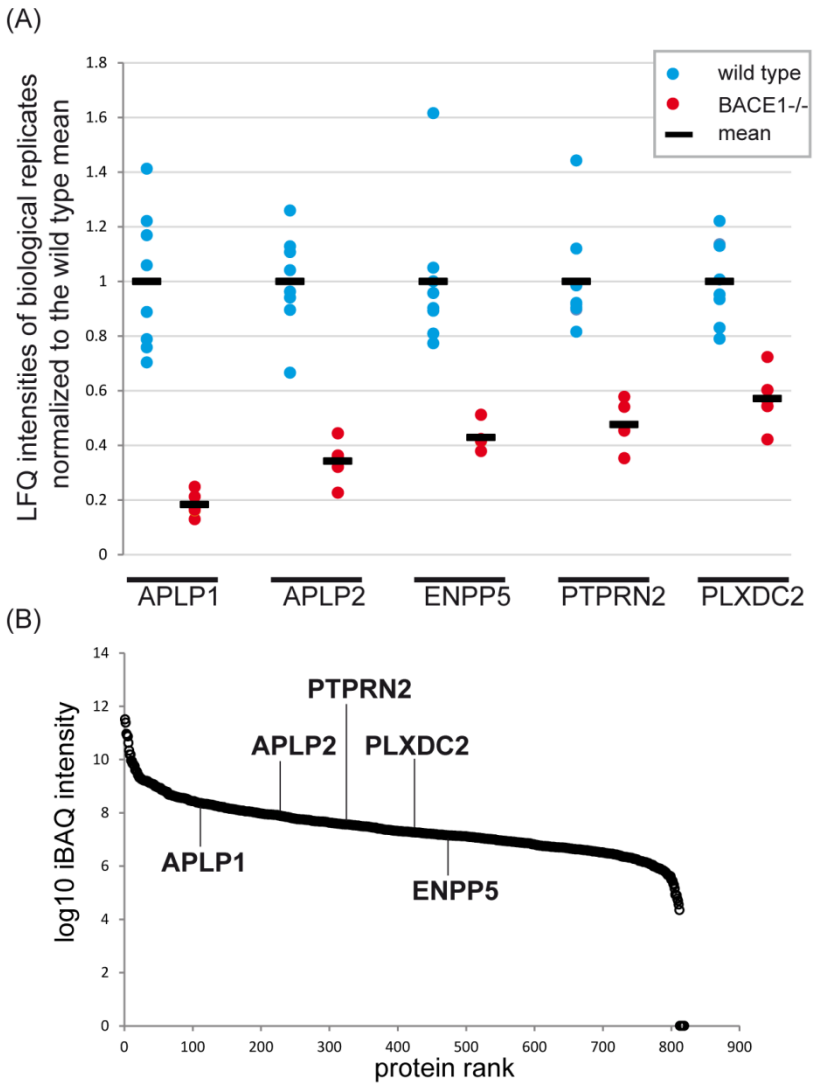

Figure 26. Top 5 proteins that are decreased in the BACE1-/- CSF. A) The LFQ values of the top 5 significantly regulated proteins are shown for each biological replicate. LFQ values are normalized to the wild type mean of all biological replicates (set to 1) for a given protein. **B)** Relative abundance of all observed proteins relative to each other as calculated by the IBAQ algorithm. Each protein identified in the CSF dataset is displayed as a black circle and ranked by its relative abundance in the CSF. The IBAQ (Intensity Based Absolute Quantification) score is calculated by dividing the total ion intensity of all observed peptides by the theoretical number of all observable peptides of a protein (Schwanhausser et al., 2011). The IBAQ score thus ranks the proteins in a dataset by their abundance, the proteins of highest abundance on top.

The total percentage of proteins annotated as “intrinsic to membrane” was only 14% in the entire dataset. However, 83% of the proteins that were enriched at least 2-fold and 56% of the proteins enriched at least 1.5 fold in the CSF of wild type mice in comparison to BACE1-/- mice were type I transmembrane or GPI anchored proteins, thus representing the expected protein topology of a BACE1 substrate. The remainder of the enriched proteins were found to be mainly secreted

proteins, including growth factors (Insulin-like growth factor II, IGF2), protease inhibitors (Proprotein convertase 1 inhibitor, PCSK1N), extracellular chaperones (Clusterin, CLU) as well as neuroendocrine secretory proteins (Chromogranin A, CHGA). Taken together, the analysis of adult BACE1-/- mouse CSF validated and identified BACE1 substrates, demonstrated the feasibility of label-free proteomics on minute amounts of CSF samples and provided insight into associated secondary changes due to the absence or presence of BACE1.

4.6 The QARIP webserver aids in the analysis of proteomic datasets targeted to RIP

The analysis of proteomic datasets is intrinsically tied to software algorithms that aid the researcher in coping with the huge amount of data obtained by modern mass spectrometry experiments. Thousands of proteins and tens of thousands of peptides are identified in a single LC-MS/MS run, which renders manual evaluation of the data impractical and extremely time consuming. In order to assist researchers with interest in proteomics and RIP in the evaluation of their proteomic datasets, a novel webserver termed QARIP (Quantitative Analysis of Regulated Intramembrane Proteolysis) was developed in collaboration with the bioinformatics group of Dmitrij Frishman (Technical University of Munich, Weihenstephan).

When investigating the RIP process by mass spectrometry, it is useful to know whether the identified peptides originate from the extracellular, intracellular or even transmembrane part of a protein. For example, if analyzing a whole cell lysate from control cells and from cells where a specific sheddase has been chemically inhibited, the amount of peptides arising from the extracellular region will be increased in the inhibitor treated cell lysate in comparison to the control, whereas the amount of peptides from the intracellular region may remain the same. By monitoring only the peptides originating from the extracellular region, the obtained ratios reflect the shedding event more accurately, as the unchanged intracellular peptides detected in both samples would reduce the overall fold change that is observed for the corresponding protein. In contrast, when examining the conditioned media of these samples, only peptides from the extracellular region are expected to decrease in the inhibitor treated cells. Contaminating cytosolic peptides in the conditioned media that are present in inhibitor treated and control cells, e.g. by exocytosis, apoptosis or mechanical disruption of the cells during sample preparation, will decrease the actual effect.

The QARIP server aids the researcher by assigning all detected peptides automatically to the extracellular, intracellular, or transmembrane part of a protein and allows the differential quantitation of these peptides. It uses the general and sequence annotation features of the UniProt database to assign the detected peptides. In addition, it predicts the protein topology of each protein using the PHOBIUS algorithm, if the topology annotation in UniProt is faulty or

missing. The server is publicly available at webclu.bio.wzw.tum.de/qarip and requires the user to upload the data in tab-delimited text format. The input file consist of four columns, that contain the UniProt ID, the peptide sequence, the observed LFQ intensities in case of label free datasets or the observed “heavy” to “light” ratio of SILAC based datasets for each peptide. After a processing time of up to 30 minutes, depending on the size of the dataset, the server returns the processed data and displays it online in an interactive table. It displays the UniProt ID, Protein Name, Gene Name, Gene Ontology information, protein topology, protein length, number of transmembrane domains, number of peptides identified, overall peptide ratio, extracellular peptide ratio and the intracellular peptide ratio for each protein. In addition, a schematic of each protein is shown, that shows the distribution of the different topological regions and the identified peptides within the according protein. The table can be filtered directly online, which allows the quick categorization of the identified proteins into type I, type II and multi-pass transmembrane proteins and to sort the proteins by the number of peptides identified. Each protein can be investigated in detail by clicking on it, in order to display the peptide sequences and the number of protein isoforms that are explainable by the detected peptides. Finally, the user is able to download the data as text, for further processing in a spreadsheet software, such as Microsoft Excel. Figure 27 shows the general appearance of the webserver and uses two examples to illustrate its usefulness in the proteomics based analysis of RIP.

(A)

Gene name	Topology	TM phobius	TM uniprot	Number of peptides	GO	rE	rC	r	Protein	Number of isoforms	TM topology predicted by Phobius	Protein length
Sez6l2	I	1	1	7	C:0005789	1		1	Q4V9Z5	1		910
Aplp2	I	1		11	C:0016021	1		1	Q61482	1		763
Ptprn2	I	1	1	9	C:0016021	1		1	P80560	1		1001
Cntn2	Out	0		13	C:0031225	1		1	Q61330	1		1040
Enpp5	I	1	1	3	C:0005576	1		1	Q9EQG7	1		477
Plxdc2	I	1		3	C:0016021	1		1	B1AY84	1		530
Chl1	I	1	1	12	C:0045177	1		1	A2RRK1	1		1209
Pam	I	1	1	15	C:0005829	1		1	P97467	1		979
App	I	1	1	19	C:0045177	1		1	P12023	1		770

(B)

Representative isoform	Accession code	Gene name	Topology	TM phobius	TM uniprot	Number of peptides	GO	rE	rC	r	Protein	Number of isoforms	TM topology predicted by Phobius	Protein length
APLP2_HUMAN	Q06481	APLP2	I	1	1	9	C:0016021	7.64		7.64	Q06481	94		763
A4_HUMAN	P05067	APP	I	1	1	8	C:0045177	5.83		5.83	P05067	523		770
CAHD1_HUMAN	Q5VU97	CACHD1	I	1	1	9	C:0016021	2.6		2.6	Q5VU97	59		1274
DSG2_HUMAN	Q14126	DSG2	I	1	1	5	C:0005911	1.7		1.7	Q14126	61		1118
MPRI_HUMAN	P11717	IGF2R	I	1	1	16	C:0009986	4.09	0.28	3.85	P11717	160		2491
PLXB2_HUMAN	O15031	PLXNB2	I	1	1	4	C:0005887	1.72	0.98	1.35	O15031	55		1838
CALX_HUMAN	P27824	CANX	I	1	1	2	C:0030424	0.86	2.09	1.47	P27824	85		592

Figure 27. Layout and functionality of the QARIP webserver. The server returns the uploaded data after up to 30 minutes of processing in the format seen in A) and B). The table can be filtered by each column. TM: number of transmembrane domains as predicted by UniProt or PHOEBIUS. GO: Gene Ontology identifier. rE: ratio of extracellular peptides. rC: ratio of cytosolic peptides. r: overall peptide ratio. Protein: UniProt ID. The scheme on the right of the table shows the primary structure of each protein, with the different topological regions marked in different colors. Pink: signal peptide. Blue: extracellular domain. Yellow: transmembrane domain. Green: Intracellular domain. Black: Peptides identified in the original dataset. **A)** The peptide sequences of novel or previously identified BACE1 substrate that were decreased in the CSF of BACE1-/- (Figure 25) were uploaded to the QARIP server. The individual schemes for each protein on the right immediately show that all detected peptides (black bars) originate from the extracellular part of the identified proteins. This indicates that the detected peptides are in deed reduced in the BACE1-/- CSF due to a decrease in ectodomain shedding. It also indicates that no contaminating cytosolic peptides were present in CSF. The corresponding LFQ intensities were not uploaded to the server, the ratios were arbitrarily set to “1”. **B)** The dataset obtained from the analysis of the conditioned media of HEK293 cells overexpressing BACE1 compared to cells expressing the empty control vector (Figure 12) was uploade to the QARIP server. The ectodomains of BACE1 substrates are expected to increase in the conditioned media of the BACE1 overexpressing cells. Green box: Peptides detected for APP, APLP2, CACHD1 and DSG2 all originated from the ectodomain of these proteins, their overall ratio thus equals the ratio of extracellular peptides and accurately reflects the increased cleavage by BACE1. Yellow

box: For IGFR2 and PLXNB2, peptides originating from the extracellular domain as well as contaminating intrallelular peptides were detected. This decreased the overall ratio in comparison to the ratio for the extracellular peptides. The effect of contaminating cytosolic peptides is especially strong for IGFR2, as the amount of these peptides was unequal in between the two conditions. Red box: The overall ratio observed for Calnexin also suggest that this protein is shed by BACE1. However, the analysis by QARIP shos that the ratio for the extracellular peptides is close to 1 (= no change), and that the unequal distribution of contaminating cytosolic peptides leads to the false positive overall ratio of this protein.

RIP involves more than 30 proteases and an estimated number of 1000 proteins. This is why system level approaches are needed to understand this general biological process in its entire complexity. The QARIP webserver is the first freely available webserver that supports the needs of an increasing community of proteomic researchers investigating the processes of ectodomain shedding and intramembrane proteolysis using modern quantitative mass spectrometry. It allows the rapid identification of putative RIP substrates, aids in the detection of false positive shedding events and allows the accurate monitoring of the RIP process.

5 Discussion

5.1 BACE1 and its therapeutic potential

The recent interest in BACE1 and its substrates is mainly due to two reasons. First, the robust reduction of Aβ upon inhibition of this protease in preclinical and clinical settings. Second, the discovery of the complex phenotype of BACE1-/- mice, which raises concerns about mechanism-based side effects upon therapeutic inhibition. These animals suffer from emotional and cognitive deficits, epileptic seizures, reduced myelination in the central and peripheral nervous system, hyperactive behavior, schizophrenia like phenotypes, alterations in synaptic plasticity and function as well as defects in axonal guidance and outgrowth (Cao et al., 2012; Harrison et al., 2003; Hitt et al., 2012; Hu et al., 2006; Hu et al., 2010; Savonenko et al., 2008; Willem et al., 2006). Proof of principle studies demonstrate the efficient reduction of Aβ using orally available BACE1 inhibitors in non-human primates and humans, thus illustrating the therapeutic benefit of BACE1 inhibition (Fukumoto et al., 2010; May et al., 2011; Sankaranarayanan et al., 2009; Stockley and O'Neill, 2008). Thus, BACE1 inhibition is currently considered to be one of the preferred strategies to treat AD patients, besides the active or passive immunization against the Aβ peptide itself. This makes the need to understand and discover mechanism-based adverse effects of therapeutic inhibition of this protease more important than ever before.

5.2 Different approaches increase the number of BACE1 substrates

Before the work described here was carried out, only one study using an unbiased approach towards the identification of new BACE substrates had been performed in the year 2009 (Hemming et al., 2009). In the meantime, four additional studies were published in 2012 and 2013 (Hogl et al., 2013; Kuhn et al., 2012; Stutzer et al., 2013; Zhou et al., 2012). All of them used discovery-based mass spectrometry, but with different methodological and biological approaches. Therefore, a total of six different discovery based studies (including this work) contribute to the BACE1 substratome and are confirming each other at least partially. This is encouraging, especially due to the heterogeneity of the applied methods and cell lines or tissues that were used. Two studies were relying on the overexpression of the protease, while others used pharmaceutical inhibition, shRNA mediated knockdown or tissue isolated from BACE1 knockout animals. Three studies monitored the change in shed ectodomains observed in the conditioned media of peripheral immortalized cell lines, primary cortical neurons or pancreatic islets, while one of them monitored the quantitative changes in the whole brain lysate of BACE1-/- zebrafish.

In the work presented here, a total of 22 proteins were identified as BACE1 substrate candidates in vivo. The term “substrate candidates” is used, as the increase of full length protein levels in the membrane compartment could be due to effects that are indirectly related to ectodomain

shedding by BACE1, for example the co-stabilization of a protein that interacts with the full length form of a BACE1 substrate. 12 of these substrate candidates were also found in at least one of the other studies. For three additional substrates presented in this work, close homologs of the identified proteins were found. There are primarily three reasons why the overlap in between the studies is only partial. First and foremost, the proteome coverage varies drastically between the different approaches, from a few hundred up to several thousands of identified proteins, due to differences in sample complexity, sensitivity of the used mass spectrometers and performance of the liquid chromatography systems. Second, not all BACE1 substrates are expressed ubiquitously or at the same expression level in different cell types, rendering them inaccessible for mass spectrometry. Third, proteins identified upon overexpression of BACE1 may not be cleaved under endogenous conditions in vitro or in vivo. A summary of the dataset derived from the proteomic profiling of the BACE1-/- mouse in this work and its overlap with other studies is illustrated in Table 16.

Gene Name	Protein Name	Accumulates in BACE1 KO membrane fraction	Decreases in BACE1 KO soluble fraction	Decreases in CSF of BACE1 KO	Identified by others as BACE1 substrate	Additional validation
APLP2	Amyloid-like protein 2	Yes	Not significantly changed	Yes	(Li and Sudhof, 2004)	Validated by western blot in brain membrane prep of BACE1 KO
APLP1	Amyloid-like protein 1	Not detected	Yes	Yes	(Li and Sudhof, 2004)	
APP	Amyloid Precursor Protein	Yes	unchanged	Yes	(Vassar et al., 1999)	Validated by western blot in brain membrane prep of BACE1 KO
CACHD1	VWFA and cache domain-containing protein 1	Yes	Not significantly changed	Not detected	(Hemming et al., 2009; Kuhn et al., 2012)	
CHL1	Semaphorin 4A	Yes	Increases	Yes	(Kuhn et al., 2012; Zhou et al., 2012)	Validated by western blot in brain membrane prep of BACE1 KO
CNTN2	Contactin-2	Yes	Increases	Yes	(Kuhn et al., 2012; Zhou et al., 2012)	Validated by western blot in brain membrane prep of BACE1 KO
CSMD1	CUB and sushi domain-containing protein 1	Yes	Not detected	Not detected	Not previously identified	
ENPP5	Ectonucleotide pyrophosphatase/phosphodiesterase family member 5	Not significantly changed	Not significantly changed	Yes	Not previously identified	
EPHA4	Ephrin type-A receptor 4	Yes	Not significantly changed	Not detected	(Hemming et al., 2009)	Validated by western blot in brain membrane prep of BACE1 KO
ESL1	E-selectin ligand 1	Yes	Not significantly changed	Not detected	(Hemming et al., 2009; Kuhn et al., 2012; Zhou et al., 2012)	
GPC2	Glypican-2	Yes	Not detected	Not detected	Not previously identified	Homolog increased in zebrafish BACE1 KO brains (Hogl et al., 2013)
GPC4	Glypican-4	Yes	Not significantly changed	Not detected	Not previously identified	Homolog GPC1-like increased in zebrafish BACE1 KO brains (Hogl et al., 2013)

IGSF3	Immunoglobulin superfamily member 3	Yes	Not significantly changed	Not detected	Not previously identified	
ISLR2	Immunoglobulin superfamily containing leucine-rich repeat prot. 2	Yes	Not significantly changed	Not detected	(Zhou et al., 2012)	
ITGB2	Integrin beta-2	Yes	Not detected	Not detected	Not previously identified	
L1CAM	Neural cell adhesion molecule L1	Yes	Not significantly changed	Not detected	(Hemming et al., 2009; Kuhn et al., 2012; Zhou et al., 2012)	
MDGA1	MAM domain-containing GPI anchor protein 1	Yes	Not detected	Not detected	Not previously identified	Validated by western blot in brain membrane prep of BACE1 KO
PLXDC2	Plexin domain-containing protein 2	Not detected	Not detected	Yes	(Hemming et al., 2009; Kuhn et al., 2012; Zhou et al., 2012)	
PTPRN2	Receptor-type tyrosine-protein phosphatase N2	Not significantly changed	Not significantly changed	Yes	(Stutzer et al., 2013)	Homolog PTPRN also found to be increased In BACE1 KO pancreatic islets (Stutzer et al., 2013)
SEMA4A	Semaphorin 4A	Yes	Not detected	Not detected	Not previously identified	Homologs found to be processed by BACE1 (Hemming et al., 2009; Kuhn et al., 2012)
TMEFF	Tomoregulin-1	Yes	Not significantly changed	Not detected	Not previously identified	

Table 16. Summary of BACE1 substrate candidates identified in this work. BACE1 substrate candidates were selected if they were meeting the predefined cutoffs for observed fold changes and were significantly changed. They are presented in alphabetical order.

5.3 The physiological role of BACE1: lessons from the BACE1-/- mouse model and the BACE1 substratome

5.3.1 Defects in axonal guidance and outgrowth

As pointed out in table 15, the majority of the identified BACE1 substrates play a role in the development of the central nervous system, especially in the outgrowth and guidance of axons, pointing to a role of BACE1 in establishing and maintaining correct neuronal wiring in the brain. In accordance with this observation, two independent studies observed the mistargeting of olfactory sensory neurons in the BACE1-/- mouse, leading to malformed glomeruli in the olfactory bulb (Cao et al., 2012; Rajapaksha et al., 2011). An additional study reported shortened infrapyramidal bundle axons in the hippocampus of BACE1-/- mice, phenocopying CHL1-/- mice (Heyden et al., 2008; Hitt et al., 2012). BACE1 localizes to the presynaptic membrane and could therefore regulate the levels of full length proteins involved in axonal guidance and the secretion of their functional ectodomains. CHL1 and EPHA4, represent classical axon guidance molecules, and their disturbed processing in the absence of BACE1 could explain the mistargeting of axons. Both proteins have been shown to be processed by BACE1 in vivo in this work. As the secreted CHL1 ectodomain acts as a stimulator of neurite outgrowth in vitro, reduced shedding of CHL1 by

BACE1 could mimic the knockout of CHL1 (Naus et al., 2004). This is in accordance with the previously mentioned study, where BACE1 was found to be co-localized with CHL1 in the presynaptic compartment of hippocampal neurons (Hitt et al., 2012).

The authors also investigated the processing of EPHA4, but did not observe any evidence for the in vivo cleavage of EPHA4 by BACE1. This is in contrast to the results of this work, where EPHA4 was shown to be processed in the mouse brain from embryogenesis to adulthood. Although the levels in full length EPHA4 changed only during embryogenesis and the first few days after birth upon the knockout of BACE1, the EPHA4β-NTF was reduced in P3, P7 and adult mice. The authors were only able to detect the full length protein, which does not change at the investigated age. They were unable to detect the EPHA4β-NTF, most likely due to a different protocol in generating the brain homogenate and the use of reducing conditions in their sample buffer prior to SDS Page. The AF641 antibody however detects the EPHA4β-NTF only in non-reducing conditions. As EPHA4 is the receptor for EphrinB3, which induces the growth cone collapse of axons, the disturbed processing of its cognate receptor could be partially responsible for the observed phenotype in BACE1-/- mice (Kullander et al., 2001). Whether the resulting decrease in EPHA4β-NTF or the increase in the full length protein is responsible for this phenotype is currently unknown. It was demonstrated in Figure 19 that the EPHA4β-NTF represents only the minor shedding product of EPHA4, as the majority of EPHA4 is shed by alternative protease activities. This explains the relatively mild increase in the full length protein, but does not implicate that BACE1 cleavage is of a minor importance. First, as EPHA4 is expressed both on the pre-and the postsynaptic compartment, the presynaptic pool could be majorly shed by the presynaptically localized BACE1, whereas ADAM and matrix metalloproteases could be responsible for the postsynaptic processing, resulting in the compartment specific ectodomain shedding of this receptor. Second, EPHA4β-NTF and EPHA4α-NTF could inherit different functional properties, as it has been shown for example for APPsα and APPsβ (Lichtenthaler and Haass, 2004).

Taken together, EPHA4 and CHL1 have been identified and validated as BACE substrates in vivo and their impaired processing explains at least partially the observed defects in axonal guidance in the BACE1-/- mouse. The new BACE1 substrate candidates GPC2, SEMA4 and ISLR2 and L1CAM have been assigned various roles in neurite outgrowth and axonal guidance and may all contribute to the misguiding of axons in the absence of BACE1.

5.3.2 Synaptic Plasticity

The newly identified GPI–anchored BACE1 substrate candidates GPC4 and MDGA1 play a role in the development of functional synapses. Secreted GPC4 induces the development of functional excitatory synapses in neurons (Allen et al., 2012). It is currently unclear how GPC4 is released, but its accumulation in the membrane proteome of BACE1-/- suggests BACE1 dependent processing, resulting in the functional active form of GPC4. MDGA1 has recently been shown by two independent research groups to regulate the amount of inhibitory synapses in a neuroligin 2

dependent manner. Full length MDGA1 interacts with neuregulin 2, thus preventing the synapse promoting interaction between neuregulin 2 and neurexin. Knockdown of MDGA1 results in an increase of inhibitory synapse formation, whereas the overexpression of MDGA1 leads to a decrease in inhibitory synapse formation (Lee et al., 2013; Pettem et al., 2013). As BACE1 regulates the full length levels of MDGA1, there could be a MDGA1 dependent effect of BACE1 on the amount of inhibitory synapses, with an expected decrease in inhibitory synapses in the absence of BACE1, due to the accumulation of the full length protein. The impaired processing of these substrates could thus be attributable to the deficits in synaptic plasticity and activity in BACE1-/- mice, which have been linked to the altered emotional and cognitive performance of these animals (Wang et al., 2008; Wang et al., 2010).

5.3.3 Reduced myelination

Amongst all substrates that were accumulating in the membrane fraction of BACE1-/-, CNTN2 showed the strongest accumulation (4-fold in comparison to wild type littermates). The GPI-anchored protein belongs to the L1 and immunoglobulin family and has diverse roles in neurogenesis, axonal outgrowth and myelination (Denaxa et al., 2001; Ma et al., 2008; Wolman et al., 2008). CNTN2 is strongly expressed in the olfactory bulb and hippocampus in adult mice, regions of the nervous system that feature continuous neurogenesis even during adulthood (Wolfer et al., 1998). The impaired CNTN2 processing could therefore be responsible for a variety of the BACE1-/- mouse phenotypes, including impaired axon outgrowth and reduced myelination. Interestingly, the identified BACE2 substrates L1CAM and CHL1 also contribute to myelination. Thus the reduced myelination in BACE1-/- mice could not only dependent on the improper processing of type III NRG1, but depend on the impaired processing of at least four proteins (Hu et al., 2006; Willem et al., 2006; Zhang et al., 2008).

5.4 The quantitative analysis of murine CSF leads to the discovery of biomarkers

CSF represents an information rich compartment of the brain that is accessible on a routine basis in humans. This compartment consists of interstitial fluid that is in continuous exchange with the brain and the blood system, and extends from the inner and outer parts of the brain into the spinal cord. It is in direct contact with brain tissue, and thus contains secreted proteins whose changes are directly related to changes in brain tissue. The liquid nature and the accessibility from the periphery render it a perfect compartment for the study of neurological processes in health and disease with biochemical and molecular biology based methods (Romeo et al., 2005).

The protein concentration in the CSF is around 100 times lower than in the blood, but features the same dynamic range of protein abundances, with some high abundance proteins such as albumin and immunoglobulins being present in the micromolar range, contributing around 2/3rd

of the total protein content of CSF. This can be an issue when studying proteins of low abundance such as chemokines by mass spectrometry. As the dynamic range between the peptides of interest and the high abundance proteins spans several orders of magnitude, the achievable proteomic depth is limited, because peptides of lower abundance are masked by those of higher abundance (Kroksveen et al., 2011; van Gool and Hendrickson, 2012). For this reason, the sample preparation of CSF for subsequent analysis by LC-MS/MS usually involves the depletion of highly abundant proteins using immunoaffinity columns or hexapeptide libraries and further fractionating the remaining sample in order to reduce its complexity (Fratantoni et al., 2010; Mouton-Barbosa et al., 2010). This is feasible if working with larger amounts of CSF, such as human, dog, or non-human primate CSF and allows the identification of up to 2500 proteins (Schutzer et al., 2010). The laboratory mouse however is the most commonly used preclinical animal model and yields only 5-15µl of CSF, depending on whether serial CSF collection is desired or not (Liu and Duff, 2008). Efficient depletion of highly abundant proteins is not feasible in such small sample amounts, as the sample will be lost due to various handling steps and exposure to large surface areas of beads, columns, etc. For this reason, a simple and straightforward sample preparation for murine CSF was developed, that keeps sample handling to a minimum. In addition, label-free proteomics were chosen over label-dependent proteomics, as a satisfactory SILAC spike-in standard is not available and chemical labeling would introduce additional steps in sample preparation, with the above mentioned disadvantages for low sample amounts. In order to make the most out of the complex and dynamic (in terms of protein abundances) sample, ultra-long columns were used for HPLC in conjunction with a mass spectrometers using fast scan speed while maintaining a high resolution. This setup proofed to be feasible of detecting more than 1200 proteins in a single run, and allowed the accurate quantification of CSF proteins. This workflow is of use for the study of CSF in murine models of neurological diseases and for the discovery of novel biomarkers in those models.

The proof of principle for the usefulness of this workflow was shown by the comparative analysis of CSF from adult BACE1-/- mice and their wild type littermates. The analysis showed the significant reduction of shed ectodomains for 7 previously identified BACE1 substrate candidates including APP in the BACE1-/- mouse, thus partially confirming the results from the analysis of the membrane proteome and studies on BACE1 substrates performed by others. In addition, PTPRN2 and ENPP5 were for the first time described as BACE1 substrates in the brain. Up to 17 peptides per substrate were identified, and the analysis by QARIP revealed that all peptides matched to the extracellular domain of these proteins, thus confirming that is indeed the ectodomains of proteins that are found and regulated in the CSF by BACE1. These results are in concordance with a study that compared the peptidome and the proteome in CSF using a 10 kDa cut off filter to distinguish peptides from intact proteins. The authors came to the conclusion that the majority of membrane proteins present in CSF are derived from ectodomain shedding, as the cleavage sites of ectodomain sheddases could be determined from the peptide fraction (Zougman et al.,

2008). This is in contrast to the urinary proteome, where also full length proteins are found, most likely derived from secretion via exosomes (Adachi et al., 2006).

In conclusion, ectodomain shedding can be accurately monitored in the CSF. The panel of BACE1 substrates may now be used for as biomarkers in drug development, for prognosis and treatment, as they allow the relative specificity of BACE1 inhibitors towards APP to be measured. The extension of this analysis to non-human primates and humans treated with a BACE1 inhibitor will give meaningful insights to the extent changes and related adverse effects and allow the discovery of BACE1 substrates in man.

5.5 Outlook

Taking into account all recent studies on BACE1, this protease cleaves more than 40 substrates, however not all of the have been validated in vivo. The complex phenotype of the knockout mouse is partially understood, with the recent discovery that many BACE substrates are involved in axonal guidance and outgrowth, matching the corresponding axonal pathologies in the hippocampus and olfactory bulb of these mice (Cao et al., 2012; Hitt et al., 2012; Rajapaksha et al., 2011). BACE1 seems to play a major role in the development of the nervous system, controlling myelination, synaptic plasticity and neural wiring.

However, these processes may also have implications in adults, as myelination is involved during nerve injury and the hippocampus and olfactory bulb maintain their plasticity neurogenesis in mammals throughout life (Ming and Song, 2011). Thus mechanism-based side effects affecting the brain and peripheral nervous system have to be taken into account upon therapeutic inhibition. In addition, the analysis of mouse CSF however showed that not all BACE1 substrates may be processed to the same extent in adult animals. CNTN2 and APP for example show only mild changes in the absence of their ectodomains, due to the processing by other sheddases or unknown mechanisms. This may also be reflected in the observation that the analysis of the soluble brain proteome of BACE1 mice revealed no major changes, arguing against strong secondary effects. This could be a benefit in the therapeutically setting and weaken some of the current concerns about mechanism-based side effects in the BACE1 community.

Major pharmaceutical companies such as Merck, Roche, Genentech and Eli Lilly are involved in clinical trials of BACE1 inhibitors and have been partially moved on to phase II, as a robust reduction of Aβ in CSF, Plasma and brain tissue was observed (Wang et al., 2013). The BACE1 substrates identified and validated in this work and their observed change in the CSF in the absence of BACE1 will be of benefit for clinical researchers performing these studies to anticipate the specific effectiveness of an inhibitor towards APP (sparing other BACE1 targets) and to foresee possible side effects. Beyond that, the detailed analysis of those substrates and the functional consequences of their ectodomain shedding will give more insight into the biological and

pathophysiological role of BACE1 and RIP in general. Last but not least, the established workflow for the validation of sheddases in vivo and for the accurate quantification of the CSF proteome can be extended to other animal models.

6 Summary

BACE1 is the rate limiting enzyme of Aβ generation and its inhibition or knockout abolishes the generation of this neurotoxic peptide. It is for this reason that BACE1 inhibition is regarded one of the main targets for the treatment of AD, which is still incurable despite the cloning of the APP gene more than 25 years ago (Kang et al., 1987). The recent discovery of complex behavioral and cognitive deficits, an increased lethality and structural changes of the peripheral and central nervous system in the BACE1-/- mouse have raised concerns about the safety and possible adverse effects of chronic BACE1 inhibition in humans (Dominguez et al., 2005; Hitt et al., 2012; Hu et al., 2006; Hu et al., 2010; Savonenko et al., 2008; Willem et al., 2006). In order to understand the physiological role of BACE1 and the associated mechanism based side effects upon therapeutic inhibition, a detailed analyses of the BACE1-/- brain proteome was performed. As the function of a protease is defined by its substrates, the identification of novel and the validation of previously known BACE1 substrates in vivo had the highest priority.

1. A SILAC based quantitative proteomics workflow led to the identification of 17 BACE1 substrate candidates in the membrane fraction of BACE1-/- mice, amongst them the previously known BACE1 substrates APP and APLP2. Several of these substrates could be validated by antibody based techniques in an independent set of animals, including the proteins that showed the strongest fold change, CNTN2 and CHL1. The functional annotation of the identified BACE1 substrate candidates suggests a role of BACE1 protease in the establishment and maintenance of neuronal connectivity, as the majority of identified proteins are involved in neuronal outgrowth, axonal guidance and synapse formation.

2. The analysis of the soluble fraction of the BACE1-/- mouse brain allowed the accurate quantification of more than 4500 proteins, but did not reveal major changes. Only 2 proteins were significantly changed, one was found to be upregulated, while the other was downregulated. This suggests that the missing processing of BACE1 substrates does not have strong secondary effects on associated signaling pathways or interaction partners. These results fit to the viability of the knockout mouse and point to the alternative processing of BACE substrates in the chronic absence of BACE1 in order to compensate for the missing cleavage.

3. A novel workflow was established that allowed the accurate identification of up to 1200 proteins in minute amounts of murine CSF. The workflow proved to be robust and reproducible enough to accurately quantify more than 500 proteins in the BACE1-/- mouse. The previously known BACE1 substrates APP, APLP1 and APLP2 decreased as expected, along with CHL1 and CNTN2, that were identified as BACE1 substrates in the membrane proteome of the BACE1-/- mouse. In addition, PTPRN2 and ENPP5 identified as novel BACE1 substrate candidates.

Taken together, this work established a global proteomic profile of the BACE1-/- mouse brain, identified and validated a total of 22 proteins as BACE1 substrates in vivo and demonstrated the

feasibility of label-free quantitative proteomics in murine CSF. The identified substrates enhance the knowledge of the physiological function of BACE1 and may serve as diagnostic and prognostic biomarkers in AD patients and during the establishment of novel therapeutic strategies in clinical and preclinical studies.

7 Abbreviations

AD	Alzheimer's disease
ADAM	A disintegrin and metalloproteinase
AICD	APP intracellular domain
APLP1/2	Amyloid-like protein
APLP2	Amyloid-like protein 2
APP	Amyloid precursor protein
APPs	soluble APP ectodomain
Aβ	Aβ-peptide
BACE1	β-site APP cleaving enzyme 1
CACHD1	VWFA and cache domain-containing protein 1
CHGA	Chromogranin A
CHL1	Cell adhesion molecule with homology to L1CAM
CLU	Clusterin
CNTN2	Contactin-2
CSF	cerebrospinal fluid
CSMD1	CUB and sushi domain-containing protein 1
CTF	C-terminal fragment
Da	Dalton (atomic mass unit)
ECD	extracellular domain
EGF	epidermal growth factor
ENPP5	Ectonucleotide pyrophosphatase/phosphodiesterase family member 5
EPHA4	Ephrin type-A receptor 4
ESL1	E-selectin ligand 1
FASP	filter aided sample preparation
GO	Gene ontology
GPC2	Glypican 2
GPC4	Glypican 4
GPI	glycophosphatidylinositol
HEK-293E	Human embryonic kidney cells 293 EBNA
HIP14	Zinc finger DHHC domain-containing protein 17
HPLC	high performance liquid chromatography
ICD	intracellular domain
ID	protein identification
IGF2	Insulin-like growth factor II
IGF2R	Cation-independent mannose-6-phosphate receptor
IGSF3	Immunoglobulin superfamily member 3
ISLR2	Immunoglobulin superfamily containing leucine-rich repeat protein 2
ITGB2	Integrin beta-2
L1CAM	Neural cell adhesion molecule L1
LC	liquid chromatography
LC-MS/MS	liquid chromatography coupled to tandem mass spectrometry

LFQ	label free quantitation
MDGA1	MAM domain-containing GPI anchor protein 1
MS	mass spectrometry
MS/MS or MS2	tandem mass spectrometry
NMWCO	nominal molecular weight cut off
NNT	Nicotinamide nucleotide transhydrogenase
NRG1	Neuregulin 1
NTF	N-terminal fragment
P	postnatal, e.g. P7 = seven days after birth
PCSK1N	Proprotein convertase 1 inhibitor
PLXDC2	Plexin domain-containing protein 2
PTPRN2	Receptor-type tyrosine-protein phosphatase N2
QARIP	quantitative analysis of regulated intramembrane proteolysis
RIP	regulated intramembrane proteolysis
SAX	strong anion exchange chromatography
SEMA4A	Semaphorin 4A
SILAC	stable isotope labeling with amino acids in cell culture
STAGE Tip	Stop and go extraction Tip
TMEFF	Tomoregulin-1
TNF	tumor necrosis factor
VGSC	voltage-gated sodium channel

8 Index

Adachi, J., Kumar, C., Zhang, Y., Olsen, J.V., and Mann, M. (2006). The human urinary proteome contains more than 1500 proteins, including a large proportion of membrane proteins. Genome biology *7*, R80.

Ahrens, C.H., Brunner, E., Qeli, E., Basler, K., and Aebersold, R. (2010). Generating and navigating proteome maps using mass spectrometry. Nature reviews Molecular cell biology *11*, 789-801.

Allen, N.J., Bennett, M.L., Foo, L.C., Wang, G.X., Chakraborty, C., Smith, S.J., and Barres, B.A. (2012). Astrocyte glypicans 4 and 6 promote formation of excitatory synapses via GluA1 AMPA receptors. Nature *486*, 410-414.

Altmeppen, H.C., Prox, J., Puig, B., Kluth, M.A., Bernreuther, C., Thurm, D., Jorissen, E., Petrowitz, B., Bartsch, U., De Strooper, B.*, et al.* (2011). Lack of a-disintegrin-and-metalloproteinase ADAM10 leads to intracellular accumulation and loss of shedding of the cellular prion protein in vivo. Molecular neurodegeneration *6*, 36.

Alzheimer, A. (1907). Über eine eigenartige Erkrankung der Hirnrinde. Allgemeine Zeitschrift fur Psychiatrie und Psychisch-gerichtliche Medizin *64*, 3.

Alzheimer, A., Stelzmann, R.A., Schnitzlein, H.N., and Murtagh, F.R. (1995). An English translation of Alzheimer's 1907 paper, "Uber eine eigenartige Erkankung der Hirnrinde". Clinical anatomy *8*, 429-431.

Babu, M., Vlasblom, J., Pu, S., Guo, X., Graham, C., Bean, B.D., Burston, H.E., Vizeacoumar, F.J., Snider, J., Phanse, S.*, et al.* (2012). Interaction landscape of membrane-protein complexes in Saccharomyces cerevisiae. Nature *489*, 585-589.

Bashaw, G.J., and Klein, R. (2010). Signaling from axon guidance receptors. Cold Spring Harbor perspectives in biology *2*, a001941.

Benjannet, S., Cromlish, J.A., Diallo, K., Chretien, M., and Seidah, N.G. (2004). The metabolism of beta-amyloid converting enzyme and beta-amyloid precursor protein processing. Biochemical and biophysical research communications *325*, 235-242.

Benjannet, S., Elagoz, A., Wickham, L., Mamarbachi, M., Munzer, J.S., Basak, A., Lazure, C., Cromlish, J.A., Sisodia, S., Checler, F.*, et al.* (2001). Post-translational processing of beta-secretase (beta-amyloid-converting enzyme) and its ectodomain shedding. The pro- and transmembrane/cytosolic domains affect its cellular activity and amyloid-beta production. The Journal of biological chemistry *276*, 10879-10887.

Bennett, B.D., Denis, P., Haniu, M., Teplow, D.B., Kahn, S., Louis, J.C., Citron, M., and Vassar, R. (2000). A furin-like convertase mediates propeptide cleavage of BACE, the Alzheimer's beta - secretase. The Journal of biological chemistry *275*, 37712-37717.

Bertram, L., and Tanzi, R.E. (2005). The genetic epidemiology of neurodegenerative disease. The Journal of clinical investigation *115*, 1449-1457.

Bonifacino, J.S., and Weissman, A.M. (1998). Ubiquitin and the control of protein fate in the secretory and endocytic pathways. Annual review of cell and developmental biology *14*, 19-57.

Bozkulak, E.C., and Weinmaster, G. (2009). Selective use of ADAM10 and ADAM17 in activation of Notch1 signaling. Molecular and cellular biology *29*, 5679-5695.

Brown, M.S., Ye, J., Rawson, R.B., and Goldstein, J.L. (2000). Regulated intramembrane proteolysis: a control mechanism conserved from bacteria to humans. Cell *100*, 391-398.

Cai, H., Wang, Y., McCarthy, D., Wen, H., Borchelt, D.R., Price, D.L., and Wong, P.C. (2001). BACE1 is the major beta-secretase for generation of Abeta peptides by neurons. Nature neuroscience *4*, 233-234.
Cao, L., Rickenbacher, G.T., Rodriguez, S., Moulia, T.W., and Albers, M.W. (2012). The precision of axon targeting of mouse olfactory sensory neurons requires the BACE1 protease. Scientific reports *2*, 231.
Capell, A., Steiner, H., Willem, M., Kaiser, H., Meyer, C., Walter, J., Lammich, S., Multhaup, G., and Haass, C. (2000). Maturation and pro-peptide cleavage of beta-secretase. The Journal of biological chemistry *275*, 30849-30854.
Citron, M. (2010). Alzheimer's disease: strategies for disease modification. Nature reviews Drug discovery *9*, 387-398.
Colombo, A., Wang, H., Kuhn, P.H., Page, R., Kremmer, E., Dempsey, P.J., Crawford, H.C., and Lichtenthaler, S.F. (2012). Constitutive alpha- and beta-secretase cleavages of the amyloid precursor protein are partially coupled in neurons, but not in frequently used cell lines. Neurobiology of disease *49C*, 137-147.
Cox, J., and Mann, M. (2011). Quantitative, high-resolution proteomics for data-driven systems biology. Annual review of biochemistry *80*, 273-299.
De Strooper, B., Vassar, R., and Golde, T. (2010). The secretases: enzymes with therapeutic potential in Alzheimer disease. Nature reviews Neurology *6*, 99-107.
DeMattos, R.B., Bales, K.R., Parsadanian, M., O'Dell, M.A., Foss, E.M., Paul, S.M., and Holtzman, D.M. (2002). Plaque-associated disruption of CSF and plasma amyloid-beta (Abeta) equilibrium in a mouse model of Alzheimer's disease. Journal of neurochemistry *81*, 229-236.
Denaxa, M., Chan, C.H., Schachner, M., Parnavelas, J.G., and Karagogeos, D. (2001). The adhesion molecule TAG-1 mediates the migration of cortical interneurons from the ganglionic eminence along the corticofugal fiber system. Development *128*, 4635-4644.
Dislich, B., and Lichtenthaler, S.F. (2012). The Membrane-Bound Aspartyl Protease BACE1: Molecular and Functional Properties in Alzheimer's Disease and Beyond. Frontiers in physiology *3*, 8.
Dominguez, D., Tournoy, J., Hartmann, D., Huth, T., Cryns, K., Deforce, S., Serneels, L., Camacho, I.E., Marjaux, E., Craessaerts, K.*, et al.* (2005). Phenotypic and biochemical analyses of BACE1- and BACE2-deficient mice. The Journal of biological chemistry *280*, 30797-30806.
Eeltink, S., Dolman, S., Detobel, F., Swart, R., Ursem, M., and Schoenmakers, P.J. (2010). High-efficiency liquid chromatography-mass spectrometry separations with 50 mm, 250 mm, and 1 m long polymer-based monolithic capillary columns for the characterization of complex proteolytic digests. Journal of chromatography A *1217*, 6610-6615.
Esch, F.S., Keim, P.S., Beattie, E.C., Blacher, R.W., Culwell, A.R., Oltersdorf, T., McClure, D., and Ward, P.J. (1990). Cleavage of amyloid beta peptide during constitutive processing of its precursor. Science *248*, 1122-1124.
Ferri, C.P., Prince, M., Brayne, C., Brodaty, H., Fratiglioni, L., Ganguli, M., Hall, K., Hasegawa, K., Hendrie, H., Huang, Y.*, et al.* (2005). Global prevalence of dementia: a Delphi consensus study. Lancet *366*, 2112-2117.
Fleck, D., Garratt, A.N., Haass, C., and Willem, M. (2012). BACE1 dependent neuregulin processing: review. Current Alzheimer research *9*, 178-183.

Fleck, D., van Bebber, F., Colombo, A., Galante, C., Schwenk, B.M., Rabe, L., Hampel, H., Novak, B., Kremmer, E., Tahirovic, S.*, et al.* (2013). Dual Cleavage of Neuregulin 1 Type III by BACE1 and ADAM17 Liberates Its EGF-Like Domain and Allows Paracrine Signaling. The Journal of neuroscience : the official journal of the Society for Neuroscience *33*, 7856-7869.
Fluhrer, R., Grammer, G., Israel, L., Condron, M.M., Haffner, C., Friedmann, E., Bohland, C., Imhof, A., Martoglio, B., Teplow, D.B.*, et al.* (2006). A gamma-secretase-like intramembrane cleavage of TNFalpha by the GxGD aspartyl protease SPPL2b. Nature cell biology *8*, 894-896.
Fratantoni, S.A., Piersma, S.R., and Jimenez, C.R. (2010). Comparison of the performance of two affinity depletion spin filters for quantitative proteomics of CSF: Evaluation of sensitivity and reproducibility of CSF analysis using GeLC-MS/MS and spectral counting. Proteomics Clinical applications *4*, 613-617.
Friedmann, E., Hauben, E., Maylandt, K., Schleeger, S., Vreugde, S., Lichtenthaler, S.F., Kuhn, P.H., Stauffer, D., Rovelli, G., and Martoglio, B. (2006). SPPL2a and SPPL2b promote intramembrane proteolysis of TNFalpha in activated dendritic cells to trigger IL-12 production. Nature cell biology *8*, 843-848.
Fukumoto, H., Takahashi, H., Tarui, N., Matsui, J., Tomita, T., Hirode, M., Sagayama, M., Maeda, R., Kawamoto, M., Hirai, K.*, et al.* (2010). A noncompetitive BACE1 inhibitor TAK-070 ameliorates Abeta pathology and behavioral deficits in a mouse model of Alzheimer's disease. The Journal of neuroscience : the official journal of the Society for Neuroscience *30*, 11157-11166.
Geiger, T., Wisniewski, J.R., Cox, J., Zanivan, S., Kruger, M., Ishihama, Y., and Mann, M. (2011). Use of stable isotope labeling by amino acids in cell culture as a spike-in standard in quantitative proteomics. Nature protocols *6*, 147-157.
Ghosh, A.K., Bilcer, G., Harwood, C., Kawahama, R., Shin, D., Hussain, K.A., Hong, L., Loy, J.A., Nguyen, C., Koelsch, G.*, et al.* (2001). Structure-based design: potent inhibitors of human brain memapsin 2 (beta-secretase). Journal of medicinal chemistry *44*, 2865-2868.
Gilmore, J.M., and Washburn, M.P. (2010). Advances in shotgun proteomics and the analysis of membrane proteomes. Journal of proteomics *73*, 2078-2091.
Glish, G.L., and Vachet, R.W. (2003). The basics of mass spectrometry in the twenty-first century. Nature reviews Drug discovery *2*, 140-150.
Gruninger-Leitch, F., Schlatter, D., Kung, E., Nelbock, P., and Dobeli, H. (2002). Substrate and inhibitor profile of BACE (beta-secretase) and comparison with other mammalian aspartic proteases. The Journal of biological chemistry *277*, 4687-4693.
Guruharsha, K.G., Kankel, M.W., and Artavanis-Tsakonas, S. (2012). The Notch signalling system: recent insights into the complexity of a conserved pathway. Nature reviews Genetics *13*, 654-666.
Haass, C., Hung, A.Y., Schlossmacher, M.G., Oltersdorf, T., Teplow, D.B., and Selkoe, D.J. (1993). Normal cellular processing of the beta-amyloid precursor protein results in the secretion of the amyloid beta peptide and related molecules. Annals of the New York Academy of Sciences *695*, 109-116.
Haass, C., and Selkoe, D.J. (2007). Soluble protein oligomers in neurodegeneration: lessons from the Alzheimer's amyloid beta-peptide. Nature reviews Molecular cell biology *8*, 101-112.
Harada, H., Tamaoka, A., Ishii, K., Shoji, S., Kametaka, S., Kametani, F., Saito, Y., and Murayama, S. (2006). Beta-site APP cleaving enzyme 1 (BACE1) is increased in remaining neurons in Alzheimer's disease brains. Neuroscience research *54*, 24-29.

Harrison, S.M., Harper, A.J., Hawkins, J., Duddy, G., Grau, E., Pugh, P.L., Winter, P.H., Shilliam, C.S., Hughes, Z.A., Dawson, L.A.*, et al.* (2003). BACE1 (beta-secretase) transgenic and knockout mice: identification of neurochemical deficits and behavioral changes. Molecular and cellular neurosciences *24*, 646-655.
Hartmann, D., de Strooper, B., Serneels, L., Craessaerts, K., Herreman, A., Annaert, W., Umans, L., Lübke, T., Lena Illert, A., von Figura, K.*, et al.* (2002). The disintegrin/metalloprotease ADAM 10 is essential for Notch signalling but not for α-secretase activity in fibroblasts. Human molecular genetics *11*, 2615-2624.
Hayashida, K., Bartlett, A.H., Chen, Y., and Park, P.W. (2010). Molecular and cellular mechanisms of ectodomain shedding. Anatomical record *293*, 925-937.
Hemming, M.L., Elias, J.E., Gygi, S.P., and Selkoe, D.J. (2009). Identification of beta-secretase (BACE1) substrates using quantitative proteomics. PloS one *4*, e8477.
Heyden, A., Angenstein, F., Sallaz, M., Seidenbecher, C., and Montag, D. (2008). Abnormal axonal guidance and brain anatomy in mouse mutants for the cell recognition molecules close homolog of L1 and NgCAM-related cell adhesion molecule. Neuroscience *155*, 221-233.
Hitt, B., Riordan, S.M., Kukreja, L., Eimer, W.A., Rajapaksha, T.W., and Vassar, R. (2012). beta-Site amyloid precursor protein (APP)-cleaving enzyme 1 (BACE1)-deficient mice exhibit a close homolog of L1 (CHL1) loss-of-function phenotype involving axon guidance defects. The Journal of biological chemistry *287*, 38408-38425.
Hogl, S., van Bebber, F., Dislich, B., Kuhn, P.H., Haass, C., Schmid, B., and Lichtenthaler, S.F. (2013). Label-free quantitative analysis of the membrane proteome of Bace1 protease knock-out zebrafish brains. PROTEOMICS *13*, 1519-1527.
Hong, L., Koelsch, G., Lin, X., Wu, S., Terzyan, S., Ghosh, A.K., Zhang, X.C., and Tang, J. (2000). Structure of the protease domain of memapsin 2 (beta-secretase) complexed with inhibitor. Science *290*, 150-153.
Horiuchi, K., Kimura, T., Miyamoto, T., Takaishi, H., Okada, Y., Toyama, Y., and Blobel, C.P. (2007). Cutting edge: TNF-alpha-converting enzyme (TACE/ADAM17) inactivation in mouse myeloid cells prevents lethality from endotoxin shock. Journal of immunology *179*, 2686-2689.
Hu, X., Hicks, C.W., He, W., Wong, P., Macklin, W.B., Trapp, B.D., and Yan, R. (2006). Bace1 modulates myelination in the central and peripheral nervous system. Nature neuroscience *9*, 1520-1525.
Hu, X., Zhou, X., He, W., Yang, J., Xiong, W., Wong, P., Wilson, C.G., and Yan, R. (2010). BACE1 deficiency causes altered neuronal activity and neurodegeneration. The Journal of neuroscience : the official journal of the Society for Neuroscience *30*, 8819-8829.
Huse, J.T., Pijak, D.S., Leslie, G.J., Lee, V.M., and Doms, R.W. (2000). Maturation and endosomal targeting of beta-site amyloid precursor protein-cleaving enzyme. The Alzheimer's disease beta-secretase. The Journal of biological chemistry *275*, 33729-33737.
Hussain, I., Powell, D., Howlett, D.R., Tew, D.G., Meek, T.D., Chapman, C., Gloger, I.S., Murphy, K.E., Southan, C.D., Ryan, D.M.*, et al.* (1999). Identification of a novel aspartic protease (Asp 2) as beta-secretase. Molecular and cellular neurosciences *14*, 419-427.
Inoue, E., Deguchi-Tawarada, M., Togawa, A., Matsui, C., Arita, K., Katahira-Tayama, S., Sato, T., Yamauchi, E., Oda, Y., and Takai, Y. (2009). Synaptic activity prompts gamma-secretase-mediated cleavage of EphA4 and dendritic spine formation. The Journal of cell biology *185*, 551-564.

Irizarry, M.C., Locascio, J.J., and Hyman, B.T. (2001). beta-site APP cleaving enzyme mRNA expression in APP transgenic mice: anatomical overlap with transgene expression and static levels with aging. The American journal of pathology *158*, 173-177.
Ittner, L.M., Ke, Y.D., Delerue, F., Bi, M., Gladbach, A., van Eersel, J., Wolfing, H., Chieng, B.C., Christie, M.J., Napier, I.A.*, et al.* (2010). Dendritic function of tau mediates amyloid-beta toxicity in Alzheimer's disease mouse models. Cell *142*, 387-397.
Ivins, J.K., Litwack, E.D., Kumbasar, A., Stipp, C.S., and Lander, A.D. (1997). Cerebroglycan, a developmentally regulated cell-surface heparan sulfate proteoglycan, is expressed on developing axons and growth cones. Developmental biology *184*, 320-332.
Jonsson, T., Atwal, J.K., Steinberg, S., Snaedal, J., Jonsson, P.V., Bjornsson, S., Stefansson, H., Sulem, P., Gudbjartsson, D., Maloney, J.*, et al.* (2012). A mutation in APP protects against Alzheimer's disease and age-related cognitive decline. Nature *488*, 96-99.
Kang, E.L., Cameron, A.N., Piazza, F., Walker, K.R., and Tesco, G. (2010). Ubiquitin regulates GGA3-mediated degradation of BACE1. The Journal of biological chemistry *285*, 24108-24119.
Kang, J., Lemaire, H.G., Unterbeck, A., Salbaum, J.M., Masters, C.L., Grzeschik, K.H., Multhaup, G., Beyreuther, K., and Muller-Hill, B. (1987). The precursor of Alzheimer's disease amyloid A4 protein resembles a cell-surface receptor. Nature *325*, 733-736.
Kim, D.Y., Carey, B.W., Wang, H., Ingano, L.A., Binshtok, A.M., Wertz, M.H., Pettingell, W.H., He, P., Lee, V.M., Woolf, C.J.*, et al.* (2007). BACE1 regulates voltage-gated sodium channels and neuronal activity. Nature cell biology *9*, 755-764.
Kim, D.Y., Gersbacher, M.T., Inquimbert, P., and Kovacs, D.M. (2011). Reduced sodium channel Na(v)1.1 levels in BACE1-null mice. The Journal of biological chemistry *286*, 8106-8116.
Klaver, D.W., Wilce, M.C., Cui, H., Hung, A.C., Gasperini, R., Foa, L., and Small, D.H. (2010). Is BACE1 a suitable therapeutic target for the treatment of Alzheimer's disease? Current strategies and future directions. Biological chemistry *391*, 849-859.
Klein, R. (2012). Eph/ephrin signalling during development. Development *139*, 4105-4109.
Kovacs, D.M., Gersbacher, M.T., and Kim, D.Y. (2010). Alzheimer's secretases regulate voltage-gated sodium channels. Neuroscience letters *486*, 68-72.
Kroksveen, A.C., Opsahl, J.A., Aye, T.T., Ulvik, R.J., and Berven, F.S. (2011). Proteomics of human cerebrospinal fluid: discovery and verification of biomarker candidates in neurodegenerative diseases using quantitative proteomics. Journal of proteomics *74*, 371-388.
Kruger, M., Moser, M., Ussar, S., Thievessen, I., Luber, C.A., Forner, F., Schmidt, S., Zanivan, S., Fassler, R., and Mann, M. (2008). SILAC mouse for quantitative proteomics uncovers kindlin-3 as an essential factor for red blood cell function. Cell *134*, 353-364.
Kuhn, P.H., Koroniak, K., Hogl, S., Colombo, A., Zeitschel, U., Willem, M., Volbracht, C., Schepers, U., Imhof, A., Hoffmeister, A.*, et al.* (2012). Secretome protein enrichment identifies physiological BACE1 protease substrates in neurons. The EMBO journal *31*, 3157-3168.
Kuhn, P.H., Wang, H., Dislich, B., Colombo, A., Zeitschel, U., Ellwart, J.W., Kremmer, E., Rossner, S., and Lichtenthaler, S.F. (2010). ADAM10 is the physiologically relevant, constitutive alpha-secretase of the amyloid precursor protein in primary neurons. The EMBO journal *29*, 3020-3032.
Kullander, K., Croll, S.D., Zimmer, M., Pan, L., McClain, J., Hughes, V., Zabski, S., DeChiara, T.M., Klein, R., Yancopoulos, G.D.*, et al.* (2001). Ephrin-B3 is the midline barrier that prevents corticospinal tract axons from recrossing, allowing for unilateral motor control. Genes & development *15*, 877-888.

Laird, F.M., Cai, H., Savonenko, A.V., Farah, M.H., He, K., Melnikova, T., Wen, H., Chiang, H.C., Xu, G., Koliatsos, V.E.*, et al.* (2005). BACE1, a major determinant of selective vulnerability of the brain to amyloid-beta amyloidogenesis, is essential for cognitive, emotional, and synaptic functions. The Journal of neuroscience : the official journal of the Society for Neuroscience *25*, 11693-11709.
Lal, M., and Caplan, M. (2011). Regulated intramembrane proteolysis: signaling pathways and biological functions. Physiology *26*, 34-44.
Lammich, S., Kojro, E., Postina, R., Gilbert, S., Pfeiffer, R., Jasionowski, M., Haass, C., and Fahrenholz, F. (1999). Constitutive and regulated alpha-secretase cleavage of Alzheimer's amyloid precursor protein by a disintegrin metalloprotease. Proceedings of the National Academy of Sciences of the United States of America *96*, 3922-3927.
Lang, A.E. (2010). Clinical trials of disease-modifying therapies for neurodegenerative diseases: the challenges and the future. Nature medicine *16*, 1223-1226.
Larance, M., Bailly, A.P., Pourkarimi, E., Hay, R.T., Buchanan, G., Coulthurst, S., Xirodimas, D.P., Gartner, A., and Lamond, A.I. (2011). Stable-isotope labeling with amino acids in nematodes. Nature methods *8*, 849-851.
Laursen, L.S., Chan, C.W., and ffrench-Constant, C. (2009). An integrin-contactin complex regulates CNS myelination by differential Fyn phosphorylation. The Journal of neuroscience : the official journal of the Society for Neuroscience *29*, 9174-9185.
Lazarov, O., Lee, M., Peterson, D.A., and Sisodia, S.S. (2002). Evidence that synaptically released beta-amyloid accumulates as extracellular deposits in the hippocampus of transgenic mice. The Journal of neuroscience : the official journal of the Society for Neuroscience *22*, 9785-9793.
Lazarov, V.K., Fraering, P.C., Ye, W., Wolfe, M.S., Selkoe, D.J., and Li, H. (2006). Electron microscopic structure of purified, active gamma-secretase reveals an aqueous intramembrane chamber and two pores. Proceedings of the National Academy of Sciences of the United States of America *103*, 6889-6894.
Lee, K., Kim, Y., Lee, S.J., Qiang, Y., Lee, D., Lee, H.W., Kim, H., Je, H.S., Sudhof, T.C., and Ko, J. (2013). MDGAs interact selectively with neuroligin-2 but not other neuroligins to regulate inhibitory synapse development. Proceedings of the National Academy of Sciences of the United States of America *110*, 336-341.
Li, Q., and Sudhof, T.C. (2004). Cleavage of amyloid-beta precursor protein and amyloid-beta precursor-like protein by BACE 1. The Journal of biological chemistry *279*, 10542-10550.
Li, X., Dang, S., Yan, C., Gong, X., Wang, J., and Shi, Y. (2013). Structure of a presenilin family intramembrane aspartate protease. Nature *493*, 56-61.
Liao, L., McClatchy, D.B., and Yates, J.R. (2009). Shotgun proteomics in neuroscience. Neuron *63*, 12-26.
Lichtenthaler, S.F., and Haass, C. (2004). Amyloid at the cutting edge: activation of alpha-secretase prevents amyloidogenesis in an Alzheimer disease mouse model. The Journal of clinical investigation *113*, 1384-1387.
Lichtenthaler, S.F., Haass, C., and Steiner, H. (2011). Regulated intramembrane proteolysis--lessons from amyloid precursor protein processing. Journal of neurochemistry *117*, 779-796.
Lichtenthaler, S.F., and Steiner, H. (2007). Sheddases and intramembrane-cleaving proteases: RIPpers of the membrane. Symposium on regulated intramembrane proteolysis. EMBO reports *8*, 537-541.

Lin, X., Koelsch, G., Wu, S., Downs, D., Dashti, A., and Tang, J. (2000). Human aspartic protease memapsin 2 cleaves the beta-secretase site of beta-amyloid precursor protein. Proceedings of the National Academy of Sciences of the United States of America *97*, 1456-1460.
Liu, L., and Duff, K. (2008). A technique for serial collection of cerebrospinal fluid from the cisterna magna in mouse. Journal of visualized experiments : JoVE.
Luber, C.A., Cox, J., Lauterbach, H., Fancke, B., Selbach, M., Tschopp, J., Akira, S., Wiegand, M., Hochrein, H., O'Keeffe, M.*, et al.* (2010). Quantitative proteomics reveals subset-specific viral recognition in dendritic cells. Immunity *32*, 279-289.
Luo, Y., Bolon, B., Kahn, S., Bennett, B.D., Babu-Khan, S., Denis, P., Fan, W., Kha, H., Zhang, J., Gong, Y.*, et al.* (2001). Mice deficient in BACE1, the Alzheimer's beta-secretase, have normal phenotype and abolished beta-amyloid generation. Nature neuroscience *4*, 231-232.
Ma, Q.H., Futagawa, T., Yang, W.L., Jiang, X.D., Zeng, L., Takeda, Y., Xu, R.X., Bagnard, D., Schachner, M., Furley, A.J.*, et al.* (2008). A TAG1-APP signalling pathway through Fe65 negatively modulates neurogenesis. Nature cell biology *10*, 283-294.
Makarov, A. (2000). Electrostatic axially harmonic orbital trapping: a high-performance technique of mass analysis. Analytical chemistry *72*, 1156-1162.
Mann, M. (2006). Functional and quantitative proteomics using SILAC. Nature reviews Molecular cell biology *7*, 952-958.
Mann, M., Kulak, N.A., Nagaraj, N., and Cox, J. (2013). The coming age of complete, accurate, and ubiquitous proteomes. Molecular cell *49*, 583-590.
May, P.C., Dean, R.A., Lowe, S.L., Martenyi, F., Sheehan, S.M., Boggs, L.N., Monk, S.A., Mathes, B.M., Mergott, D.J., Watson, B.M.*, et al.* (2011). Robust central reduction of amyloid-beta in humans with an orally available, non-peptidic beta-secretase inhibitor. The Journal of neuroscience : the official journal of the Society for Neuroscience *31*, 16507-16516.
Mei, L., and Xiong, W.C. (2008). Neuregulin 1 in neural development, synaptic plasticity and schizophrenia. Nature reviews Neuroscience *9*, 437-452.
Merl, J., Ueffing, M., Hauck, S.M., and von Toerne, C. (2012). Direct comparison of MS-based label-free and SILAC quantitative proteome profiling strategies in primary retinal Müller cells. PROTEOMICS *12*, 1902-1911.
Michalski, A., Damoc, E., Hauschild, J.P., Lange, O., Wieghaus, A., Makarov, A., Nagaraj, N., Cox, J., Mann, M., and Horning, S. (2011). Mass spectrometry-based proteomics using Q Exactive, a high-performance benchtop quadrupole Orbitrap mass spectrometer. Molecular & cellular proteomics : MCP *10*, M111 011015.
Ming, G.L., and Song, H. (2011). Adult neurogenesis in the mammalian brain: significant answers and significant questions. Neuron *70*, 687-702.
Mouton-Barbosa, E., Roux-Dalvai, F., Bouyssie, D., Berger, F., Schmidt, E., Righetti, P.G., Guerrier, L., Boschetti, E., Burlet-Schiltz, O., Monsarrat, B.*, et al.* (2010). In-depth exploration of cerebrospinal fluid by combining peptide ligand library treatment and label-free protein quantification. Molecular & cellular proteomics : MCP *9*, 1006-1021.
Murphy, G., Murthy, A., and Khokha, R. (2008). Clipping, shedding and RIPping keep immunity on cue. Trends in immunology *29*, 75-82.
Naus, S., Richter, M., Wildeboer, D., Moss, M., Schachner, M., and Bartsch, J.W. (2004). Ectodomain shedding of the neural recognition molecule CHL1 by the metalloprotease-disintegrin

ADAM8 promotes neurite outgrowth and suppresses neuronal cell death. The Journal of biological chemistry *279*, 16083-16090.
Nielsen, P.A., Olsen, J.V., Podtelejnikov, A.V., Andersen, J.R., Mann, M., and Wisniewski, J.R. (2005). Proteomic mapping of brain plasma membrane proteins. Molecular & cellular proteomics : MCP *4*, 402-408.
O'Brien, R.J., and Wong, P.C. (2011). Amyloid precursor protein processing and Alzheimer's disease. Annual review of neuroscience *34*, 185-204.
Ong, S.-E., Blagoev, B., Kratchmarova, I., Kristensen, D.B., Steen, H., Pandey, A., and Mann, M. (2002). Stable Isotope Labeling by Amino Acids in Cell Culture, SILAC, as a Simple and Accurate Approach to Expression Proteomics. Molecular & Cellular Proteomics *1*, 376-386.
Ong, S.E., and Mann, M. (2006). A practical recipe for stable isotope labeling by amino acids in cell culture (SILAC). Nature protocols *1*, 2650-2660.
Ostermann, N., Eder, J., Eidhoff, U., Zink, F., Hassiepen, U., Worpenberg, S., Maibaum, J., Simic, O., Hommel, U., and Gerhartz, B. (2006). Crystal structure of human BACE2 in complex with a hydroxyethylamine transition-state inhibitor. Journal of molecular biology *355*, 249-261.
Perry, R.H., Cooks, R.G., and Noll, R.J. (2008). Orbitrap mass spectrometry: instrumentation, ion motion and applications. Mass spectrometry reviews *27*, 661-699.
Pettem, K.L., Yokomaku, D., Takahashi, H., Ge, Y., and Craig, A.M. (2013). Interaction between autism-linked MDGAs and neuroligins suppresses inhibitory synapse development. The Journal of cell biology *200*, 321-336.
Postina, R., Schroeder, A., Dewachter, I., Bohl, J., Schmitt, U., Kojro, E., Prinzen, C., Endres, K., Hiemke, C., Blessing, M.*, et al.* (2004). A disintegrin-metalloproteinase prevents amyloid plaque formation and hippocampal defects in an Alzheimer disease mouse model. The Journal of clinical investigation *113*, 1456-1464.
Querfurth, H.W., and LaFerla, F.M. (2010). Alzheimer's disease. The New England journal of medicine *362*, 329-344.
Rajapaksha, T.W., Eimer, W.A., Bozza, T.C., and Vassar, R. (2011). The Alzheimer's beta-secretase enzyme BACE1 is required for accurate axon guidance of olfactory sensory neurons and normal glomerulus formation in the olfactory bulb. Molecular neurodegeneration *6*, 88.
Rapoport, M., Dawson, H.N., Binder, L.I., Vitek, M.P., and Ferreira, A. (2002). Tau is essential to beta -amyloid-induced neurotoxicity. Proceedings of the National Academy of Sciences of the United States of America *99*, 6364-6369.
Rappsilber, J., Mann, M., and Ishihama, Y. (2007). Protocol for micro-purification, enrichment, pre-fractionation and storage of peptides for proteomics using StageTips. Nature protocols *2*, 1896-1906.
Reiss, K., and Saftig, P. (2009). The "a disintegrin and metalloprotease" (ADAM) family of sheddases: physiological and cellular functions. Seminars in cell & developmental biology *20*, 126-137.
Roberds, S.L., Anderson, J., Basi, G., Bienkowski, M.J., Branstetter, D.G., Chen, K.S., Freedman, S.B., Frigon, N.L., Games, D., Hu, K.*, et al.* (2001). BACE knockout mice are healthy despite lacking the primary beta-secretase activity in brain: implications for Alzheimer's disease therapeutics. Human molecular genetics *10*, 1317-1324.

Romeo, M.J., Espina, V., Lowenthal, M., Espina, B.H., Petricoin, E.F., 3rd, and Liotta, L.A. (2005). CSF proteome: a protein repository for potential biomarker identification. Expert review of proteomics *2*, 57-70.
Sabido, E., Selevsek, N., and Aebersold, R. (2012). Mass spectrometry-based proteomics for systems biology. Current opinion in biotechnology *23*, 591-597.
Saftig, P., and Reiss, K. (2011). The "A Disintegrin And Metalloproteases" ADAM10 and ADAM17: novel drug targets with therapeutic potential? European journal of cell biology *90*, 527-535.
Sagare, A.P., Bell, R.D., and Zlokovic, B.V. (2012). Neurovascular dysfunction and faulty amyloid beta-peptide clearance in Alzheimer disease. Cold Spring Harbor perspectives in medicine *2*.
Sankaranarayanan, S., Holahan, M.A., Colussi, D., Crouthamel, M.C., Devanarayan, V., Ellis, J., Espeseth, A., Gates, A.T., Graham, S.L., Gregro, A.R.*, et al.* (2009). First demonstration of cerebrospinal fluid and plasma A beta lowering with oral administration of a beta-site amyloid precursor protein-cleaving enzyme 1 inhibitor in nonhuman primates. The Journal of pharmacology and experimental therapeutics *328*, 131-140.
Sannerud, R., Declerck, I., Peric, A., Raemaekers, T., Menendez, G., Zhou, L., Veerle, B., Coen, K., Munck, S., De Strooper, B.*, et al.* (2011). ADP ribosylation factor 6 (ARF6) controls amyloid precursor protein (APP) processing by mediating the endosomal sorting of BACE1. Proceedings of the National Academy of Sciences of the United States of America *108*, E559-568.
Savonenko, A.V., Melnikova, T., Laird, F.M., Stewart, K.A., Price, D.L., and Wong, P.C. (2008). Alteration of BACE1-dependent NRG1/ErbB4 signaling and schizophrenia-like phenotypes in BACE1-null mice. Proceedings of the National Academy of Sciences of the United States of America *105*, 5585-5590.
Schmechel, A., Strauss, M., Schlicksupp, A., Pipkorn, R., Haass, C., Bayer, T.A., and Multhaup, G. (2004). Human BACE forms dimers and colocalizes with APP. The Journal of biological chemistry *279*, 39710-39717.
Schutzer, S.E., Liu, T., Natelson, B.H., Angel, T.E., Schepmoes, A.A., Purvine, S.O., Hixson, K.K., Lipton, M.S., Camp, D.G., Coyle, P.K.*, et al.* (2010). Establishing the proteome of normal human cerebrospinal fluid. PloS one *5*, e10980.
Schwanhausser, B., Busse, D., Li, N., Dittmar, G., Schuchhardt, J., Wolf, J., Chen, W., and Selbach, M. (2011). Global quantification of mammalian gene expression control. Nature *473*, 337-342.
Selkoe, D.J. (2011). Alzheimer's disease. Cold Spring Harbor perspectives in biology *3*.
Sheng, J.G., Price, D.L., and Koliatsos, V.E. (2003). The beta-amyloid-related proteins presenilin 1 and BACE1 are axonally transported to nerve terminals in the brain. Experimental neurology *184*, 1053-1057.
Sinha, S., Anderson, J.P., Barbour, R., Basi, G.S., Caccavello, R., Davis, D., Doan, M., Dovey, H.F., Frigon, N., Hong, J.*, et al.* (1999). Purification and cloning of amyloid precursor protein beta-secretase from human brain. Nature *402*, 537-540.
Sjödin, M.O.D., Wetterhall, M., Kultima, K., and Artemenko, K. (2013). Comparative study of label and label-free techniques using shotgun proteomics for relative protein quantification. Journal of Chromatography B *928*, 83-92.
Stachel, S.J., Coburn, C.A., Steele, T.G., Jones, K.G., Loutzenhiser, E.F., Gregro, A.R., Rajapakse, H.A., Lai, M.T., Crouthamel, M.C., Xu, M.*, et al.* (2004). Structure-based design of potent and selective cell-permeable inhibitors of human beta-secretase (BACE-1). Journal of medicinal chemistry *47*, 6447-6450.

Steen, H., and Mann, M. (2004). The ABC's (and XYZ's) of peptide sequencing. Nature reviews Molecular cell biology *5*, 699-711.
Steiner, H., Fluhrer, R., and Haass, C. (2008). Intramembrane proteolysis by gamma-secretase. The Journal of biological chemistry *283*, 29627-29631.
Stockley, J.H., and O'Neill, C. (2008). Understanding BACE1: essential protease for amyloid-beta production in Alzheimer's disease. Cellular and molecular life sciences : CMLS *65*, 3265-3289.
Stutzer, I., Selevsek, N., Esterhazy, D., Schmidt, A., Aebersold, R., and Stoffel, M. (2013). Systematic Proteomic Analysis Identifies beta-Site Amyloid Precursor Protein Cleaving Enzyme 2 and 1 (BACE2 and BACE1) Substrates in Pancreatic beta-Cells. The Journal of biological chemistry *288*, 10536-10547.
Sury, M.D., Chen, J.X., and Selbach, M. (2010). The SILAC fly allows for accurate protein quantification in vivo. Molecular & cellular proteomics : MCP *9*, 2173-2183.
Turner, R.T., 3rd, Hong, L., Koelsch, G., Ghosh, A.K., and Tang, J. (2005). Structural locations and functional roles of new subsites S5, S6, and S7 in memapsin 2 (beta-secretase). Biochemistry *44*, 105-112.
Urban, S., and Freeman, M. (2002). Intramembrane proteolysis controls diverse signalling pathways throughout evolution. Current opinion in genetics & development *12*, 512-518.
van Gool, A.J., and Hendrickson, R.C. (2012). The proteomic toolbox for studying cerebrospinal fluid. Expert review of proteomics *9*, 165-179.
Vassar, R., Bennett, B.D., Babu-Khan, S., Kahn, S., Mendiaz, E.A., Denis, P., Teplow, D.B., Ross, S., Amarante, P., Loeloff, R.*, et al.* (1999). Beta-secretase cleavage of Alzheimer's amyloid precursor protein by the transmembrane aspartic protease BACE. Science *286*, 735-741.
Vassar, R., and Kandalepas, P. (2011). The beta-secretase enzyme BACE1 as a therapeutic target for Alzheimer's disease. Alzheimer's Research & Therapy *3*, 20.
Wahle, T., Prager, K., Raffler, N., Haass, C., Famulok, M., and Walter, J. (2005). GGA proteins regulate retrograde transport of BACE1 from endosomes to the trans-Golgi network. Molecular and cellular neurosciences *29*, 453-461.
Walter, J., Fluhrer, R., Hartung, B., Willem, M., Kaether, C., Capell, A., Lammich, S., Multhaup, G., and Haass, C. (2001). Phosphorylation regulates intracellular trafficking of beta-secretase. The Journal of biological chemistry *276*, 14634-14641.
Wang, H., Li, R., and Shen, Y. (2013). beta-Secretase: its biology as a therapeutic target in diseases. Trends in pharmacological sciences *34*, 215-225.
Wang, H., Song, L., Laird, F., Wong, P.C., and Lee, H.K. (2008). BACE1 knock-outs display deficits in activity-dependent potentiation of synaptic transmission at mossy fiber to CA3 synapses in the hippocampus. The Journal of neuroscience : the official journal of the Society for Neuroscience *28*, 8677-8681.
Wang, H., Song, L., Lee, A., Laird, F., Wong, P.C., and Lee, H.K. (2010). Mossy fiber long-term potentiation deficits in BACE1 knock-outs can be rescued by activation of alpha7 nicotinic acetylcholine receptors. The Journal of neuroscience : the official journal of the Society for Neuroscience *30*, 13808-13813.
Washburn, M.P., Wolters, D., and Yates, J.R., 3rd (2001). Large-scale analysis of the yeast proteome by multidimensional protein identification technology. Nature biotechnology *19*, 242-247.

Willem, M., Garratt, A.N., Novak, B., Citron, M., Kaufmann, S., Rittger, A., DeStrooper, B., Saftig, P., Birchmeier, C., and Haass, C. (2006). Control of peripheral nerve myelination by the beta-secretase BACE1. Science *314*, 664-666.
Wisniewski, J.R., Zougman, A., and Mann, M. (2009a). Combination of FASP and StageTip-based fractionation allows in-depth analysis of the hippocampal membrane proteome. Journal of proteome research *8*, 5674-5678.
Wisniewski, J.R., Zougman, A., Nagaraj, N., and Mann, M. (2009b). Universal sample preparation method for proteome analysis. Nature methods *6*, 359-362.
Wolfer, D.P., Giger, R.J., Stagliar, M., Sonderegger, P., and Lipp, H.P. (1998). Expression of the axon growth-related neural adhesion molecule TAG-1/axonin-1 in the adult mouse brain. Anatomy and embryology *197*, 177-185.
Wolman, M.A., Sittaramane, V.K., Essner, J.J., Yost, H.J., Chandrasekhar, A., and Halloran, M.C. (2008). Transient axonal glycoprotein-1 (TAG-1) and laminin-alpha1 regulate dynamic growth cone behaviors and initial axon direction in vivo. Neural development *3*, 6.
Wong, H.K., Sakurai, T., Oyama, F., Kaneko, K., Wada, K., Miyazaki, H., Kurosawa, M., De Strooper, B., Saftig, P., and Nukina, N. (2005). beta Subunits of voltage-gated sodium channels are novel substrates of beta-site amyloid precursor protein-cleaving enzyme (BACE1) and gamma-secretase. The Journal of biological chemistry *280*, 23009-23017.
Wu, Z., Yan, N., Feng, L., Oberstein, A., Yan, H., Baker, R.P., Gu, L., Jeffrey, P.D., Urban, S., and Shi, Y. (2006). Structural analysis of a rhomboid family intramembrane protease reveals a gating mechanism for substrate entry. Nature structural & molecular biology *13*, 1084-1091.
Wyss-Coray, T. (2006). Inflammation in Alzheimer disease: driving force, bystander or beneficial response? Nature medicine *12*, 1005-1015.
Yan, R., Bienkowski, M.J., Shuck, M.E., Miao, H., Tory, M.C., Pauley, A.M., Brashier, J.R., Stratman, N.C., Mathews, W.R., Buhl, A.E*., et al.* (1999). Membrane-anchored aspartyl protease with Alzheimer's disease beta-secretase activity. Nature *402*, 533-537.
Yan, R., Han, P., Miao, H., Greengard, P., and Xu, H. (2001). The transmembrane domain of the Alzheimer's beta-secretase (BACE1) determines its late Golgi localization and access to beta -amyloid precursor protein (APP) substrate. The Journal of biological chemistry *276*, 36788-36796.
Zanivan, S., Krueger, M., and Mann, M. (2012). In Vivo Quantitative Proteomics: The SILAC Mouse. In Integrin and Cell Adhesion Molecules, M. Shimaoka, ed. (Humana Press), pp. 435-450.
Zhang, Y., Yeh, J., Richardson, P.M., and Bo, X. (2008). Cell adhesion molecules of the immunoglobulin superfamily in axonal regeneration and neural repair. Restorative neurology and neuroscience *26*, 81-96.
Zhao, J., Fu, Y., Yasvoina, M., Shao, P., Hitt, B., O'Connor, T., Logan, S., Maus, E., Citron, M., Berry, R*., et al.* (2007). Beta-site amyloid precursor protein cleaving enzyme 1 levels become elevated in neurons around amyloid plaques: implications for Alzheimer's disease pathogenesis. The Journal of neuroscience : the official journal of the Society for Neuroscience *27*, 3639-3649.
Zhou, L., Barao, S., Laga, M., Bockstael, K., Borgers, M., Gijsen, H., Annaert, W., Moechars, D., Mercken, M., Gevaert, K*., et al.* (2012). The neural cell adhesion molecules L1 and CHL1 are cleaved by BACE1 protease in vivo. The Journal of biological chemistry *287*, 25927-25940.
Zougman, A., Pilch, B., Podtelejnikov, A., Kiehntopf, M., Schnabel, C., Kumar, C., and Mann, M. (2008). Integrated analysis of the cerebrospinal fluid peptidome and proteome. Journal of proteome research *7*, 386-399.

Zubarev, R.A., and Makarov, A. (2013). Orbitrap Mass Spectrometry. Analytical chemistry.

9 Publication list

A minor part of the presented data has been already published in the following manuscripts:

QARIP: a web server for quantitative proteomic analysis of regulated intramembrane proteolysis.

Ivankov DN, Bogatyreva NS, Hönigschmid P, **Dislich B**, Hogl S, Kuhn PH, Frishman D, Lichtenthaler SF.

Nucleic Acids Res. 2013 May 31.

Label-free quantitative analysis of the membrane proteome of Bace1 protease knock-out zebrafish brains.

Hogl S, van Bebber F, **Dislich B**, Kuhn PH, Haass C, Schmid B, Lichtenthaler SF.

Proteomics. 2013 May;13(9):1519-27. doi: 10.1002/pmic.201200582. Epub 2013 Apr 2.

The Membrane-Bound Aspartyl Protease BACE1: Molecular and Functional Properties in Alzheimer's Disease and Beyond.

Dislich B, Lichtenthaler SF.

Front Physiol. 2012;3:8. doi: 10.3389/fphys.2012.00008. Epub 2012 Feb 17.